Universidade do Minho
Escola de Medicina

Rui Miguel Fernandes Duarte

BIOLIF: Biologic Lumbar Interbody Fusion - an instrumentation-free approach

dezembro de 2021

BIOLIF: Biologic Lumbar Interbody Fusion - an instrumentation-free approach
Rui Miguel Fernandes Duarte
UMinho | 2021

Universidade do Minho
Escola de Medicina

Rui Miguel Fernandes Duarte

BIOLIF: Biologic Lumbar Interbody Fusion - an instrumentation-free approach

Tese de Doutoramento em Medicina

Trabalho efetuado sob a orientação do
Professor Doutor Jorge Manuel Nunes Correia Pinto
e da
Professora Doutora Ana Rita Cruz Duarte

dezembro de 2021

Acknowledgments

At the end of this important learning stage, I want to express my enormous gratitude to all those who contributed to the development of this work and sponsored this path. I am also a reflection of all those who accompanied me on this ambitious journey.

First, I thank my beloved wife and my dear children. To Cristina for her unconditional support, continuous encouragement, and selfless help. To Luís and Sofia for the contagious energy.

To the School of Medicine of the University of Minho and the Institute of Life and Health Sciences, in the person of my supervisor and friend, Professor Jorge Correia Pinto. A leading figure of the School of Medicine, he built a legacy on postgraduate training with the development of the most robust program at the national level of practical training in the surgical sciences. Much of the recognition of the Medical School as a high-quality institution is due to the work and commitment of Professor Jorge Correia-Pinto. He taught and proved that it is worth doing well and doing it differently. To the 3B's Research Group, in the person of my co-advisor and friend, Professor Ana Rita Cruz Duarte, one of the greatest Portuguese scientists. Her excitement and multifaceted pursuit for innovation is inevitably contagious to those who work with her. With Professor Ana Rita Duarte, I found beauty in doubt, curiosity in the raw idea and the fluidity that transports us from an idea to a product. I learned what to do with an idea. To the Portuguese Foundation for Science and Technology (FCT), I acknowledge the financial support provided through the projects UIDB/50026/2020 and UIDP/50026/2020.

I am grateful to Hospital de Braga, a secular institution, a safe haven for everyone who needs it. There is no membrane thick enough to separate research from care, which unite and sustain each other in an endless cycle. Many thanks to all my patients, who in their most fragile moments shared their fears and placed their hopes with confidence. I also leave my thanks to the Orthopedics department at the Hospital de Braga, cradle of my surgical training and extension of my family. To Dr. Manuel Vieira da Silva for his vision of progress and ability to fight for change. To all colleagues in the department, thank you for all your support. They were the best in the world to have by my side. I hope I have also helped. To all my friends who, in addition to their care and constant availability, have marked my personal, professional and academic path in their own way. To Nuno Ferreira, for the maximum example of challenging the *status quo* and pursuit of new solutions. To Bruno Santos for his constant reinforcement and inexhaustible dedication. To Nuno Sevivas for the example of serenity based on solid knowledge. To Pedro Varanda, the master and mentor in spinal surgery. In each of my surgeries I seek to carry my master's rigor.

There is still so much to learn, so much to do. I await the future with the enthusiasm and curiosity that characterizes me.

Statement of integrity

I hereby declare having conducted this academic work with integrity. I confirm that I have not used plagiarism or any form of undue use of information or falsification of results along the process leading to its elaboration.

I further declare that I have fully acknowledged the Code of Ethical Conduct of the University of Minho.

BIOLIF: Biologic Lumbar Interbody Fusion - an instrumentation-free approach

Abstract

Spinal fusion (SF) is a surgical procedure conducted to promote bone growth in-between spinal segments, supported by fixation hardware, and complemented by bone graft or bone substitute. There are recognized risks and complications associated with instrumentation, such as damage to surrounding tissues, neurological deficits, material failure or migration and non-union. In this thesis, a novel approach is proposed based on the development of an adhesive, biodegradable and injectable foam, with the purpose to avoid instrumentation in SF. Carbon dioxide foaming was explored as processing methodology to generate, within physiologically compatible conditions, polycaprolactone (PCL) foams with morphological characteristics equivalent to those found in trabecular bone. A three-dimensional, mechanically stable and bioactive composite of PCL+βTCP+Dexamethasone was foamed at 45°C and 5 MPa. This optimized PCL processing opened the possibility for creating a porous foam, delivered directly into the intervertebral space through a surgical tool designed and built for this purpose. The adhesive properties of PCL were further improved through modification with polydopamine (pDA) and polymethacrylic acid (pMAA). After tensile testing, PCL pDA pMAA material–bone interface remained intact at both ends (adhesivity significantly superior to non-modified PCL, $p<0.05$). Further *in vitro* assays confirmed the formulation as non-cytotoxic and bioactive (calcium phosphate (CaP) layer formation). Lastly, the surgical feasibility of PCL pDA pMAA foaming and its biological performance for non-instrumented spinal fusion were assessed in a 6-month survival study using an interbody fusion porcine model. Segmental instrumented arthrodesis was used as control group. Minimally invasive *in situ* foaming of PCL pDA pMAA (BIOLIF) was technically achieved, leading to reduced surgical time ($p<0.05$) as compared to instrumentation. Animals in BIOLIF approach demonstrated no surgical complications and a higher mobility ($p<0.05$) at immediate post-op. Spinal fusion was determined by a set of assessments including: i) bone volume/ tissue volume percentage (BV/TV), superior in BIOLIF group ($p<0.05$); ii) reduced range of motion and increased stiffness of the treated spinal segment, equivalent in both groups; and iii) a relatively well-organized newly formed osseous structure identified by histological analysis at BIOLIF samples. As conclusion, the results obtained in this work could open a new perspective for lumbar instrumentation-free spinal fusion using biologic solutions.

Keywords: *in situ* foaming, non-instrumented, polycaprolactone, spinal fusion

BIOLIF: Artrodese lombar intersomática - abordagem não instrumentada

Resumo

A artrodese da coluna vertebral é um procedimento cirúrgico que visa a indução de crescimento ósseo entre segmentos vertebrais, utilizando sistemas de fixação e suplementação com enxerto ósseo ou substituto sintético. São reconhecidos riscos e complicações associados à instrumentação, incluindo, danos nos tecidos circundantes, compromisso neurológico, risco de mobilização ou migração do material e pseudartrose. Nesta tese, é proposta uma nova abordagem, baseada no desenvolvimento de uma espuma adesiva, biodegradável e injetável, de forma de realizar artrodese intersomática lombar sem recurso a instrumentação. A tecnologia supercrítica/subcrítica foi explorada para a produção de uma espuma de policaprolactona (PCL), em condições fisiologicamente compatíveis, com características morfológicas equivalentes às encontradas no osso trabecular. Foi possível obter a 45°C e 5 MPa, uma estrutura tridimensional de PCL+βTCP+Dexametasona mecanicamente estável e com propriedades bioativas. Estas condições tornaram possível a extrusão da espuma diretamente no espaço intersomático, através de um instrumento cirúrgico desenvolvido para esse efeito. As propriedades adesivas do PCL foram otimizadas através da modificação do polímero com polidopamina (pDA) e ácido polimetacrílico (pMAA), que se demonstrou significativamente mais adesivo do que o PCL $p<0,05$ em ensaios mecânicos de tração. As propriedades citocompatíveis e bioativas da formulação foram confirmadas em ensaios *in vitro*. Por fim, a exequibilidade cirúrgica da extrusão da espuma de PCL pDA pMAA, e o seu desempenho biológico, foram avaliados num estudo de sobrevida de 6 meses usando o porco doméstico como modelo animal. Como grupo de controlo foi realizada artrodese intersomática instrumentada. Foi tecnicamente possível efetuar extrusão *in situ* de PCL pDA pMAA (BIOLIF) por via minimamente invasiva, sendo o tempo de procedimento cirúrgico significativamente inferior ($p<0,05$) ao grupo da instrumentação. Os animais do grupo BIOLIF não demonstraram complicações cirúrgicas e apresentaram uma maior mobilidade ($p<0,05$) no pós-operatório imediato. A qualidade da artrodese foi avaliada por um conjunto de parâmetros: i) a relação volume ósseo/ volume total (BV/TV), superior no grupo BIOLIF ($p<0,05$); ii) a redução da amplitude de movimento e o aumento da rigidez do segmento vertebral intervencionado, equivalente em ambos os grupos; e iii) uma estrutura óssea recém-formada relativamente bem-organizada no grupo BIOLIF, identificada por análise histológica. Em conclusão, os resultados obtidos neste trabalho podem abrir uma nova perspectiva para a utilização de soluções biológicas como forma de realizar artrodese intersomática lombar sem recurso a instrumentação.

Palavras-chave: artrodese intersomática, libertação *in situ*, não-instrumentado, policaprolactona

Table of Contents

List of Abbreviations

A

aCaSO4	a-calcium sulfate
ABG	Autologous bone graft
AEC	Amnion-derived epithelial cell
AT-MSC	Adipose tissue-derived mesenchymal stem cell
ACIF	Anterior cervical interbody fusion
ALIF	Anterior lumbar interbody fusion
A/B	Antibiotic / Antimycotic
ANOVA	ANalysis Of Variance
AR	Axial Rotation

B

b-TCP	beta Tricalcium Phosphate
BCP	Biphasic calcium phosphate
BMA	Bone Marrow Aspirate
BMP-2	Bone Morphogenic Protein-2
BM-MSC	Bone marrow mesenchymal stem cell
BMSC	Bone Marrow Stem Cell
BV	Bone Volume
BV/TV	Bone Volume per Tissue Volume

C

$CaCO_3$	Calcium carbonate
$CaHPO_4$	Dicalcium phosphate
CaP	Calcium phosphate
cm	centimeter
CO_2	Carbon Dioxide
Col	Collagen
COMP-Ang1	Cartilage oligomeric matrix protein- angiopoietin-1

D

°	Degree (angle)
°C	Degree Celsius
DA	Dalton
DBM	Demineralized bone matrix
Dex	Dexamethasone
DMEM	Dulbecco's Modified Eagle Medium
DOPA	3,4-dihydroxy-L- phenylalanine

E

eV	electronvolt
EDC	N-(3-dimethylaminopropyl)-N'-ethylcarbodiimide polymer-bound
EDS	Energy-dispersive X-ray spectroscope

F

FBS	Fetal Bovine Serum
FDA	United States Food and Drug Administration
FDM	Fused deposition modeling
FE	Flexion-Extension
FTIR	Fourier transformed infrared

G

g	gram
g/cm^3	gram per cubic centimetre
GE cells	Genetically modified cells
GF	Growth Factor
GPa	Giga Pascal

H

h	hour
HA	Hydroxyapatite
HCl	Hydrochloric acid

I

ICBG	Iliac crest bone graft
IF	Interbody Fusion
IM	Intramuscular
IRC	Instrumentation-related complications
IV	Intravenous
IVD	Intervertebral disc

K

KCl	Potassium chloride
$K_2HPO_4.3H_2O$	Dipotassium hydrogen phosphate trihydrate
kN	Kilonewton
KeV	Kilo-electronvolts

L

LB	lateral Bending
L929	Immortalized mouse lung fibroblasts cell line

M

M	Molar
µCT	micro Computed Tomography
µA	microampere
µg/mL	microgram per milliliter
µL	microliter
µm	micrometer
mA	milliampere
mg	milligram
mg/kg	milligram per kilogram
mg/kg/h	milligram per kilogram per hour
mg/mL	milligram per milliliter
microCT	micro Computed Tomography
min	minute
MISS	Minimally Invasive Spine Surgery
mL	milliliter
mm	millimeter
mm/min	millimeter per minute
mm^2	square millimeter
Mn	Number average molecular weight
MPa	Mega Pascal
MPa/min	Mega Pascal per minute
MSC	Mesenchymal Stem Cell
mol%	Mole percent
MTS	3-(4,5-dimethylthiazol-2-yl)-5(3-carboxymethoxyphenyl)-2(4-sulfofenyl)-2H-tetrazolium
$MgCl_2.6H_2O$	Magnesium chloride hexahydrate

N

n	total number of data points
N	Newton
N/cm^2	Newtons per square centimetre
Nm	Newton-meter (moment)
$NaHCO_3$	Sodium bicarbonate
Na_2SO_4	Sodium sulfate
NaCl	Sodium chloride
NELL-1	Nel-like protein-1
nHA	nano-hydroxyapatite
NHS	*N*-hydroxysuccinimide
nm	nanometer

O

Oxy	Oxysterol

P

%	Percentage
p	probability value
P	Pressure
Pc	Critical pressure
Pin	Initial pressure
PBS	Phosphate Buffer Saline
PCL	Poly(ε-caprolactone)
pDA	Polydopamine
PEG	Poly(ethylene glycol)
PEC	Polyelectrolyte complex
PEEK	Polyether ether ketone
PETA	Pentaerythritol triacrylate-co-trimethylolpropane
PLA	Polylactic acid
PLSF	Posterolateral spinal fusion
PLCL	Poly(lactic-co-ε-caprolactone)
PLGA	Poly(lactic-co-glycolic acid)
pMAA	Polymethacrylic acid
pMMA	Poly(methyl methacrylate)
Post-op	Postoperative
PRP	Platelet-rich plasma
PSC	Perivascular stem cells

R

rhBMP-2	Recombinant human bone morphogenetic protein 2
ROI	Region of interest
ROM	Range of Motion

S

SBF	Simulated Body Fluid
SEM	Scanning Electron Microscopy
SF	Spinal Fusion
SiCaP	Silicate calcium phosphate
SVF	Stromal Vascular Fraction

T

T	Temperature
Tc	Critical temperature
TCP	Tricalcium phosphate

V

VEGF	Vascular endothelial growth factor

W

wt	Weight
wt %	Weight percent

X

XPS	X-ray photoelectron spectroscopy

List of Figures

List of Tables

Thesis planning

The present thesis is divided in 3 sections and 7 chapters. The **first section** is composed of a comprehensive overview of the state of play on what regards the biological performance of new biomaterials and diverse bioactive agents on the enhancement of Spinal Fusion (SF). The **second section** details the experimental work performed within the scope of this thesis, on the development and *in vivo* performance evaluation of a new biomaterial and surgical device. The **third section** provides a general discussion and compiles the main conclusions attained by the work developed in this thesis. A concise description of each section to follow:

Section 1.

Chapter I refers to a comprehensive review of the most innovative biological solutions developed to overcome the limited fusion outcomes currently witnessed in clinical practice. Results were collected from peer-reviewed articles published during 2010-2016, on the *in vivo* testing of i) new biomaterials that pursue adequate physical and chemical aptitudes; ii) growth factors (GF) to accelerate new bone formation; and/or iii) cells to improve functional bone development. Sophisticated platforms for delivery of these agents were highlighted alongside their application, and an overview of the diverse animal models used, fusion location and anatomical level, as well as the surgical approach used for *in vivo* spinal fusion studies is presented.

Chapter II describes the objectives of this thesis.

Section 2.

Chapter III presents the development of an innovative procedure to produce three-dimensional foams made of polycaprolactone (PCL), compatible with physiological conditions, for the purpose of delivering such foam into the intervertebral disc space for spinal fusion. In this work, subcritical carbon dioxide foaming conditions were achieved, alongside incorporation of bioactive agents such as β-tricalcium phosphate and dexamethasone.

Chapter IV describes advancements of the technology developed in the previous study: for PCL foaming, the benchtop reactor was replaced by a custom-built portable reactor, designed to be used as surgical tool for *in situ* foaming and hardening at the intervertebral disc space. The PCL foam composition was further improved to achieve superior adhesive and bioactive properties, by the addition of polydopamine (pDA) and polymethacrylic acid (pMAA).

Chapter V reports on the *in vivo* surgical feasibility of the BIOLIF approach, using the porcine model, to reproduce to scale, the *in situ* delivery of the BIOLIF foam, using the developed surgical tool. This 6-month survival study further allowed a performance assessment of the BIOLIF foam for fusion of the treated vertebral segment.

Chapter VI presents the findings of previous chapters as a novel system, susceptible of industrial application, where the developed injectable and expandable compositions, devices, kits and methods are described for the *in situ* foaming of polymers for bone or tissue defects.

Section 3.

Chapter VII provides a general discussion of the main findings and challenges of this work; outlines the author's personal considerations and future perspectives in the field of spinal fusion and delivers the main conclusions and progress beyond state-of-the-art achieved with this thesis.

SECTION 1.

CHAPTER I

Biomaterials and Bioactive Agents in Spinal Fusion

This chapter is based on the following publication: **Duarte RM**, Varanda P, Reis. RL, Duarte ARC and Correia-Pinto J, *Biomaterials and Bioactive Agents in Spinal Fusion;* Tissue Engineering: Part B (2017) 23:6. DOI: 10.1089/ten.teb.2017.0072.

TISSUE ENGINEERING: Part B
Volume 23, Number 6, 2017

DOI: 10.1089/ten.teb.2017.0072

termis
Tissue Engineering
& Regenerative Medicine
International Society

REVIEW ARTICLE

Biomaterials and Bioactive Agents in Spinal Fusion

Rui M. Duarte, MD,[1–4] Pedro Varanda, MD,[2–4] Rui L. Reis, PhD,[3,5]
Ana Rita C. Duarte, PhD,[3,5] and Jorge Correia-Pinto, MD, PhD[1–3,6]

Management of degenerative spine pathologies frequently leads to the need for spinal fusion (SF), where bone growth is induced toward stabilization of the interventioned spine. Autologous bone graft (ABG) remains the gold-standard inducer, whereas new bone graft substitutes attempt to achieve effective *de novo* bone formation and solid fusion. Limited fusion outcomes have driven motivation for more sophisticated and multidisciplinary solutions, involving new biomaterials and/or biologics, through innovative delivery platforms. The present review will analyze the most recent body of literature that is focused on new approaches for consistent bone fusion of spinal vertebrae, including the development of new biomaterials that pursue physical and chemical aptitudes; the delivery of growth factors (GF) to accelerate new bone formation; and the use of cells to improve functional bone development. Bone graft substitutes currently in clinical practice, such as demineralized bone matrix and ceramics, are still used as a starting point for the study of new bioactive agents. Polyesters such as polycaprolactone and polylactic acid arise as platforms for the development of composites, where a mineral element and cell/GF constitute the delivery system. Exciting fusion outcomes were obtained in several small and large animal models with these. On what regards bioactive agents, mesenchymal stem cells, preferentially derived from the bone marrow or adipose tissue, were studied in this context. Autologous and allogeneic approaches, as well as osteogenically differentiated cells, have been tested. These cell sources have further been genetically engineered for specific GF expression. Nevertheless, results on fusion efficacy with cells have been inconsistent. On the other hand, the delivery of GF (most commonly bone morphogenetic protein-2 [BMP-2]) has provided favorable outcomes. Complications related to burst release and dosing are still the target of research through the development of controlled release systems or alternative GF such as Nel-like molecule-1 (NELL-1), Oxysterols, or COMP-Ang1. Promising solutions with new biomaterial and GF compositions are becoming closer to the human patient, as these evidence high-fusion performance, while offering cost and safety advantages. The use of cells has not yet proved solid benefits, whereas a further understanding of cell behavior remains a challenge.

Keywords: adult stem cells, growth factors, polymeric scaffolds, spinal fusion

Introduction

Spinal fusion (SF) remains the gold-standard indication for surgical treatment of diverse spine ailments that are caused by degeneration, deformity, trauma, or infection,[1–4] where removal of the damaged anatomical structure is required (commonly the intervertebral disk or vertebral lamina). Removal of such tissue results in mechanical instability of the spine, whereas the main goal of SF is to fuse two or more vertebras, by inducing bone growth in-between such segments, ultimately resulting in stabilization of the interventioned spine.[1] The current surgical techniques include fixation systems[5,6] such as screws, rods, plates, and cages, complemented by bone graft or bone graft substitute,[7] to achieve adequate bone healing and solid fusion. Despite development efforts on bone substitutes (both structural and

[1]School of Medicine, University of Minho, Braga, Portugal.
[2]Life and Health Sciences Research Institute (ICVS), School of Medicine, University of Minho, Braga, Portugal.
[3]ICVS/3B's—PT Government Associate Laboratory, Braga/Guimarães, Portugal.
[4]Orthopedic Surgery Department, Hospital de Braga, Braga, Portugal.
[5]3B's Research Group—Biomaterials, Biodegradables and Biomimetics, University of Minho, Headquarters of the European Institute of Excellence on Tissue Engineering and Regenerative Medicine, Barco, Portugal.
[6]Pediatric Surgery Department, Hospital de Braga, Braga, Portugal.

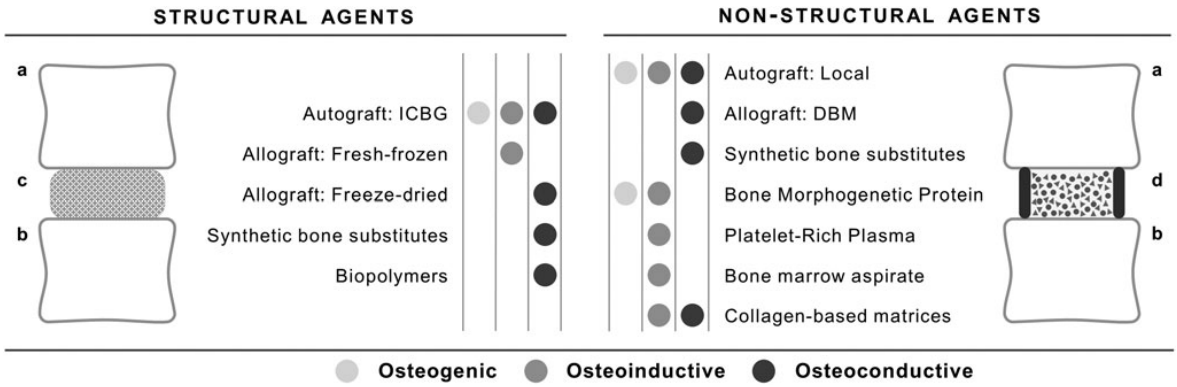

FIG. 1. Structural and non-structural agents currently in clinical practice for spinal fusion. Representative illustration of: **(a)** top vertebra; **(b)** bottom vertebra; **(c)** intervertebral space containing a structural biomaterial; **(d)** intervertebral space containing a cage filled with non-structural agents. DBM, demineralized bone matrix; ICBG, iliac crest bone graft.

non-structural, Fig. 1), autograft bone remains the optimum standard in orthopedic surgery in general,[8,9] as well as in SF procedures,[10] majorly due to its inherent fusion properties: osteogenic potential, osteoinductivity, and osteoconductivity.[8,9,11] Another recognized advantage is the low cost and the absence risk for disease transmission.[11] However, some limitations subside, such as increased surgical time, comorbidity associated with the donor site, and the lack of available bone, particularly in revision surgery.[9,11] To avoid these particular limitations, bone allografts (derived from cadavers or living patients undergoing total joint replacement) are regularly used in some spinal centers. These grafts maintain the osteoconductive and osteoinductive characteristics, yet they lose osteogenic properties and mechanical strength[12–14] due to the sterilization process. Compared with autograft, allograft incorporation in native bone is slower and less complete, which is highly related to lack of vascularization.[12,14]

The need for alternative solutions to overcome limitations of bone grafts has led to the development and commercialization of several bone substitutes and bone enhancers. Ceramic-based substitutes such as hydroxyapatite (HA), tricalcium phosphate (TCP), and calcium sulfate have played a fundamental role in replacing bone grafts, mostly due to their chemical similarity with the inorganic phase of bone, and consequently, their osteo-friendly characteristics: biocompatibility, osteoconductivity, and strong mechanical properties.[8,12] Further advantages include unlimited supply, low risk of disease transmission or immunogenicity, and easy sterilization and storage, and their properties can be tailored to increase bone ingrowth such as pore size and distribution, scaffold shape, and size.[11,12,15,16] Degradation rates are not yet optimal, whereas calcium sulfate is reabsorbed within weeks; TCP requires several months as compared with HA, which is absorbed along several years.[11,17] Ceramic-based substitutes also lack osteogenic properties; however, recent research has studied the effectiveness of these as carriers and scaffolds to deliver cells or growth factors (GF) to the fusion site in several animal models. Such studies are detailed in Table 1 and thoroughly discussed in the respective sections.

Demineralized bone matrix (DBM) was introduced in 1991 as an alternative or even supplement to autologous bone grafts (ABGs). A mild acid-extraction process, initially developed by Urist in 1965,[18] removes the mineralized component of bone, resulting in a composite of collagen, noncollagenous proteins, and GF.[19,20] This provides DBM extraordinary osteoconductive and osteoinductive properties, which yield improved bone formation. DBM is provided in putty formulations, is easily molded to the target lesion, and becomes very surgeon friendly.[19,21] There are several commercially available solutions that differ mostly in their osteoinductive activity, which is a consequence of specific allograft processing methods.[19,20] Murphy *et al.* scrutinized several of these commercial matrices, by evaluating cell adhesion/retention and osteogenesis by gene expression. Collagen-containing substitutes solubilized and lost structure, whereas bone-based and inorganic substrates supported significantly more cell retention.[22] Clinical outcomes of the use of DBM in SF were recently reviewed by Tilkeridis *et al.*[20] and Aghdasi *et al.*[21] Despite the evidence of efficacy comparable with autologous grafts, both authors highlighted the need for additional studies to better define the specific target indications and patient populations to benefit from DBM. At a research stage, DBM has been considerably used as a structure to deliver cells and/or GF to the spine, to study efficacy of these bioactive agents in SF (Table 1). To improve scaffolding properties of DBM, some authors have performed enrichments of the matrix: Ye *et al.*[23] coated DBM with poly-L-lysine, aiming at increased retention of bone marrow cells and consequent improved bone formation,[23] whereas Lee *et al.*[24] and Li *et al.*[25] used DBM supplemented with TCP in their studies with NEL-like protein-1 (NELL-1).

Despite satisfactory outcomes on what regards *de novo* bone formation within these biomaterials,[26,27] their poor compressive and shear strength, as well as suboptimal osteogenic and osteoinduction properties, have led to the exploration of new solutions (Fig. 2) by following a multidisciplinary approach, including:

(i) development of new biomaterials that pursue physical and chemical aptitudes
(ii) delivery of GF to accelerate new bone formation
(iii) use of cells to improve functional bone development.

Table 1. Combinatorial Approaches of Biomaterials, Cells, and Growth Factors Tested *In Vivo* for Spinal Fusion (2010–2016)

Cells	*BM-MSC*				*AT-MSC*		*PSC*		*Fibroblasts*	*AEC*	*BMA*		*Osteo MSC*	*None*						
Growth factors	*BMP-2*	*Oxy*	*GE cells*	*None*	*GE cells*	*None*	*NELL-1*	*None*	*GE cells*	*None*	*BMP-2*	*None*	*None*	*BMP-2*	*PRP*	*NELL-1*	*Oxy*	*COMP-Ang1*	*WNT3A*	*None*
DBM				56				57					58			59,60				61,62
DBM/TCP							24									25				
DBM/poly-L-lysine				23																
HA				63									64	65	66					
TCP			67											68,69,a						70
HA/TCP				71–75,b						75		76	77	78						
PCL/TCP (+alginate)	79			40									41	40,42						43
PCL/CaP														46						
PCL/HA																				47
PETA/HA																				47
PLGA				52																
PLCL						44,45														
PLA/TCP (/PEG)												50		51						48
PLA or PLGA/HA/collagen				80		49								53						81
$CaHPO_4$/CaP																				54
$CaCO_3$/HA															82					
$\alpha CaSO_4$/βTCP																				55
SiCaP												83								
PEC (/heparin+alginate)														84–86						
ABM/P-15																				87
Collagen (/TCP/HA)		88	89		90						91		92	93–97	98		99	100		
Gelatin (/TCP)			101										102		103					
Fibrin	104		105		106															
Silk fibroin				107																
ABG																			108	
None									109											

[a]*Escherichia coli* rhBMP-2.
[b]Allogeneic MSC.

$\alpha CaSO_4$, α-calcium sulfate; ABG, autologous bone graft; ABM/P-15, anorganic bovine-derived hydroxyapatite matrix+synthetic 15 amino acid residue; AECs, amnion-derived epithelial cell; AT-MSC, adipose tissue-derived mesenchymal stem cell; BMA, bone marrow aspirate; BM-MSC, bone marrow mesenchymal stem cell; BMP-2, bone morphogenetic protein 2; $CaCO_3$, calcium carbonate; $CaHPO_4$, dicalcium phosphate; CaP, calcium phosphate; COMP-Ang1, cartilage oligomeric matrix protein-angiopoietin-1; DBM, dimineralized bone matrix; GE cells, genetically engineered cells; HA, hydroxyapatite; NELL-1, NEL-like protein-1; Osteo MSC, osteogenic differentiated mesenchymal stem cells; Oxy, oxysterol; PCL, poly(ε-caprolactone); PEC, polyelectrolyte complex; PETA, pentaerythritol triacrylate-co-trimethylolpropane; PLA, polylactic acid; PLCL, poly(lactide-co-ε-caprolactone); PLGA, poly(lactic-co-glycolic acid); PRP, platelet-rich plasma; PSC, perivascular stem cells; rhBMP-2, recombinant human bone morphogenetic protein 2; SiCaP, silicate calcium phosphate; TCP, tricalcium phosphate.

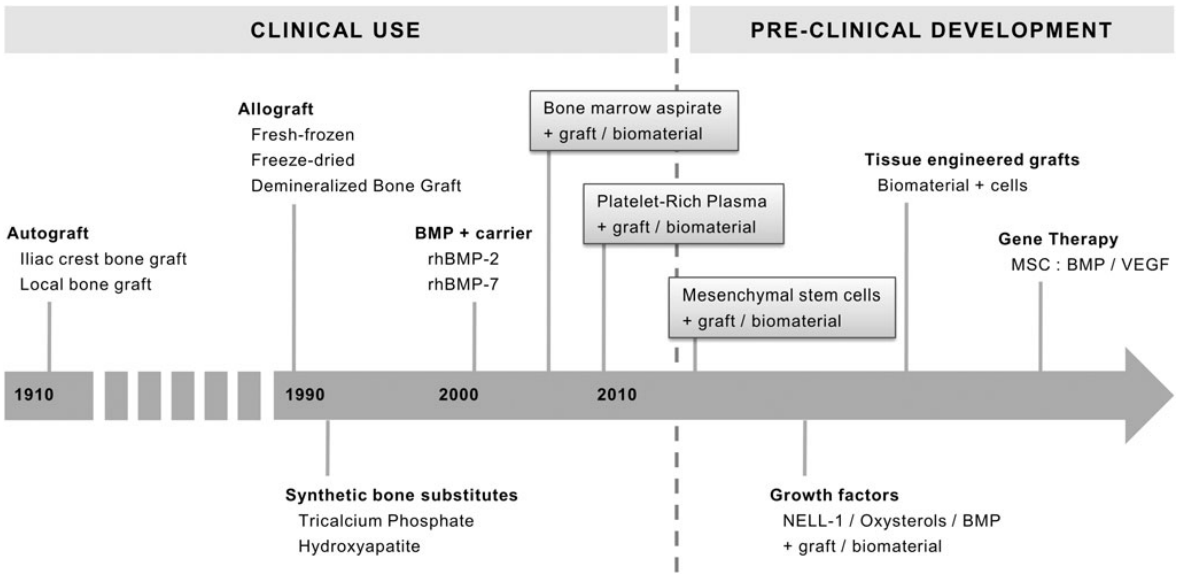

FIG. 2. Temporal progression of biomaterials and bioactive agents used for spinal fusion. MSC, mesenchymal stem cell; NELL-1, NEL-like protein-1; rhBMP, recombinant human bone morphogenetic protein; VEGF, vascular endothelial growth factor.

Under the scope of this review, experimental SF studies published between 2010 and 2016 were analyzed, comprehensively discussed, and presented as a bird view in Table 1.

Biomaterials

Remarkable advancements in the field of biomaterials have occurred to meet the increasing demands of tissue repair; whereas nowadays, a plethora of solutions, more or less sophisticated, are proposed for bone tissue regeneration. Common characteristics of these biomaterials include: biocompatibility; surface chemistry and stiffness[28,29] that favor cell migration, attachment, and osteogenic matrix deposition[29,30]; porosity suitable for cell migration, nutrient diffusion,[31,32] and development of a vascular network[33,34]; as well as a degradation rate that is simultaneous to new bone formation.[32] In addition to this demanding list, a scaffold suitable for spine fusion must gather specific mechanical characteristics: a modulus comparable to its surrounding trabecular bone, while withstanding differential load and dynamics occurring between new bone formation and scaffold structure.[35,36]

To fine-tune the challenging biochemical and structural requirements for bone formation, alternative biomaterials have been the target of extensive research. As observed in Table 1, new scaffolding materials are polyester based, including poly(ε-caprolactone) (PCL), poly(lactide-co-ε-caprolactone) (PLCL), polylactic acid (PLA), and poly(lactic-co-glycolic acid) (PLGA). Polyesters act as biologically inert materials, with tunable physical and mechanical properties that are suitable for scaffolding purposes and/or drug delivery.[37,38] Such polyesters are easily modified to tackle issues such as cell adhesion, hydrophobicity, and inflammatory side effects. Aliphatic polyesters are mostly hydrophobic biodegradable polymers. Mechanical performance and degradation behaviors are characteristics that distinguish the different polyesters.[37,38]

PCL has attracted attention for its biocompatibility, bioabsorbability, and mechanical properties. A significant body of literature has used PCL in SF studies; however, reinforcement with a mineral component seems fundamental to achieve effective fusion (Table 1). Abbah *et al.* have contributed with significant *in vivo* data,[39–41] where PCL combined with TCP (PCL/TCP) was explored as a bioactive and bioresorbable scaffold to deliver either bone morphogenetic protein-2 (BMP-2) or bone marrow mesenchymal stem cells (BM-MSC) in an anterior lumbar interbody fusion (ALIF) porcine model.[39–41] Although the scaffold *per se* did not improve bone fusion as compared with autograft after 9 months of implantation,[41] the synergistic effect of BMP or BM-MSC with this scaffold seems very promising for SF.[39–41] Abbah *et al.* also tested a controlled release system for BMP-2 by loading surface functionalized microbeads (based on heparin and strontium alginate) into the pores of PCL/TCP scaffolds.[42] The evidence of well-contained newly formed bone was important in this study, as opposed to collagen sponge carriers of BMP-2.[42] Later, in 2014, Li *et al.* reported successful bone fusion by PCL/TCP scaffold alone, yet at a longer time-point (12 months), where fusion was comparable to autograft treatment.[43] Work developed by Vergroesen and Kroeze[44,45] demonstrated bone fusion by PLCL alone, within a polyetheretherketone (PEEK) cage in a lumbar interbody fusion (IF) goat model. Further efforts have been made to improve bone fusion outcomes with PCL. Yong et al.[46] tested calcium phosphate (CaP)-coated PCL scaffolds in a sheep thoracic IF model, where CaP was aimed at promoting bone ingrowth and regeneration. These CaP-PCL scaffolds were further functionalized with recombinant human bone morphogenetic protein 2 (rhBMP-2), which outperformed scaffold alone, as well as autograft.[46]

Although the chemical nature of biomaterials is fundamental in directing cell osteogenesis as well as in providing strong mechanical properties, the physical form by which these are used at the lesion site also impacts fusion efficacy. Evidences of such are provided by Chen *et al*.,[47] who compared a new formulation based on a blend of pentaerythritol triacrylate-co-trimethylolpropane (PETA) and HA (80:20) with PCL/HA (80:20). Although solid PCL/HA shows higher mechanical properties than PETA/HA, when these are produced as a foam, PETA/HA proved higher mechanical properties as well as osteogenesis than PLC/HA.[47]

PLA has been explored in SF studies, *per se*,[48,49] or in combination with cells or BMP-2.[50,51] As described earlier for PLC, reinforcement with a mineral component such as HA or TCP is consistent, providing optimistic bone fusion outcomes. PLGA copolymer was used by Niu *et al.*[52] and Jakus *et al.*,[53] also within a composite system further composed of HA or biphasic calcium phosphate (BCP) ceramics. Niu *et al.* loaded and implanted MSC in a posterolateral spinal fusion (PLSF) rabbit model for 10 weeks. Increased bone formation was obtained with the PLGA/BCP composite than with PLGA/HA, highlighting the importance of scaffold composition toward effective fusion.[52] Jakus *et al.* proposed a hyperelastic ''bone'' based on PLGA and HA (10:90) for rapid three-dimensional (3D) printing. This elastic biomaterial induced higher fusion rates than control groups in the rat PLSF model, both with and without BMP-2.[53]

As observed in Table 1, calcium-based materials constitute the target of study for SF, commonly without further combination with bioactive agents,[54,55] yet achieving optimal bone fusion in both rodent and rabbit PLSF, comparable to ABG.

Growth Factors

BMPs, discovered by Marshall Urist in 1965,[18] are nowadays well known for their potent capacity to enhance and accelerate bone formation, both *in vitro* and *in vivo*. In the field of orthopedics, BMPs were introduced in the clinic in the early 2000s; then, in 2001, the food and drug administration (FDA) approved the use of rhBMP-7 for the treatment of long bone nonunions. Specifically, for SF, rhBMP-2 was approved the next year for use in single-level anterior fusions from L4 to S1, and later for pseudarthrosis of the lumbar spine. rhBMP-7 indication was also further expanded to include PLSF.[110] The attractive outcomes of the use of these BMPs, and yet their limited approved applications, have led to extensive ''off-label'' use.[110] Consequently, numerous additional adverse effects, including life-threatening complications, have been reported and discussed elsewhere.[111,112]

Preclinical studies have analyzed the effects of BMP-2 on SF, most of those using collagen as a carrier to deliver the GF[93–95,97] with/without HA, given its high affinity for BMP-2.[65,78] Collagen coated with CaP[94] has been tested to localize delivery and to mitigate some complications associated with BMP-2 administration. The use of TCP as an additional component provides resistance to compression caused by paraspinal muscles, while offering a long-term structure for bone growth.[51,68,69,78] rhBMP-2 is currently produced by mammalian cell expression, resulting in a very expensive product. Recent studies have tested the efficacy of rhBMP produced with *Escherichia coli* to reduce costs associated with therapeutic use of this GF.[68,69] Outcomes in large animal models (ovine PLSF and caprine anterior cervical interbody fusion [ACIF]) have demonstrated bone formation and fusion equivalent to ABG.[68,69]

To overcome side effects, new delivery systems and improved engineering mechanisms are being developed to reduce the need of high dosages of BMP-2, by gradually releasing BMP for a staged and controlled bone growth.[96] Han and coworkers engineered human BMP-2 with a collagen-binding domain, to be delivered within a collagen scaffold. This allowed a sustained release of BMP-2 during collagen scaffold degradation, avoiding the burst release currently occurring when promoting bone fusion with BMP-2.[96]

Abbah *et al.* extensively studied the potential and controlled release of BMP for SF[40,42,84–86] through the development of polyelectrolyte complex (PEC) in combination with heparin and alginate beads. This GF sequestration platform provided effective bone formation in both small and large animal models—through the rodent PLSF and pig ALIF approach.[40,42,84–86]

Strategies to improve expression of BMP-2 include gene therapy, by genetically modifying MSC. Fu *et al.* transfected BM-MSC with a recombinant baculovirus encoding BMP-2 and vascular endothelial growth factor (VEGF), further delivered to a rabbit model within TCP scaffolds. After 12 weeks, the transfected group resulted in significantly improved fusion rates than nontransfected or scaffold alone.[67] Studies conducted by Sheyn *et al.* have proved increased SF with both bone marrow and adipose tissue genetically modified MSC encoding for BMPs (BM-MSC/BMP-2 or AT-MSC/BMP-6), in the rodent model.[105,106] Fibroblasts have also been the target cell source for BMP-2 expression,[109] with the aim of developing a cell-based gene therapy system for spine fusion through a single injection, avoiding surgical intervention. Other osteogenic factors such as Smad1C[101] or BMP-7[89] have been transferred to BM-MSC for SF, achieving great amounts of new bone formation after implantation in the rabbit PLSF model. Although BMP-2 *per se* exhibits potent osteogenic capacity, its combination with BMP-7 seems relevant for enhanced bone regeneration in SF. Kaito *et al.*[90] demonstrated the synergistic effect of combined BMP-2 and BMP-7 gene transfer of adipose tissue-derived MSC (AT-MSC), whereas this experimental group induced significantly higher bone formation as compared with individual BMP in a rat model, by 8 weeks.

Previous *in vitro* and *in vivo* studies have shown evidence of increased osteogenesis and bone regeneration by BMP-2/7 heterodimer as compared with the homodimers BMP-2 or -7.[113,114] Given this, an alternative approach to reduce the supraphysiological BMP clinical dosage required for effective bone repair has been proposed through the use of this heterodimer with enhanced potency. Particularly in SF, Morimoto *et al.*[97] demonstrated, by radiography and microcomputed tomography, significantly improved fusion scores in the rat model group treated with BMP-2/7 heterodimer ($p < 0.0001$) as compared with other groups, including those treated with BMP-2 or -7 homodimers.

Other proteins have shown promising features, such as NELL-1,[25,59,60] which has performed comparatively to commercial BMP-2 product.[59] NELL-1 is an osteoblast-specific GF, claimed to elude adverse effects associated to BMP-2, such as nonspecific function or ectopic bone formation.[25]

Oxysterols are osteogenic inducers while simultaneously anti-adipogenetic.[88,99] For instance, Oxy34 and Oxy49 demonstrated equal osteogenic efficacy as BMP-2 in the rat PLSF model, while presenting less adipocytes in the newly formed bone.[88] Oxy133, in particular, presents greater ease of synthesis and improved time to fusion compared with other oxysterols.[99] Other strategies have focused on the use of GFs to enhance bone formation by allografts or autografts with reduced properties, such as those obtained from older patients. As such, Park *et al.*[100] impregnated collagen sponge with angiogenic COMP-Ang1 chimeric protein, for implantation in the rat PLSF model. After 6 weeks, nearly 90% fusion rates were obtained.[100] Jing *et al.*[108] aimed at restoring bone-forming potential of aged autografts by activating their stem cell populations with WNT3A. Superior bone formation was obtained in the aged rat PLSF model, as compared with standard of care.[108]

Beyond the use of a single GF, or a certain set of GF as described earlier, platelet-rich plasma (PRP) has gained strength in the orthopedic field as an enhancer of bone regeneration.[115] Its application in SF was recently and extensively revised by Elder *et al.*,[17] where high heterogeneity of results of preclinical and clinical studies was observed. The reasons identified include lack of standardization of the PRP preparation protocol, which lead to important differences in platelet number and concentration used in the formulation.[116] Further findings include differences in GF concentrations even when similar PRP yields and concentrations are achieved. Even further, it is not clear whether the measured GF concentration of fresh PRP is maintained at the implantation site, given that GF diffusion depends on fibrinolysis of the fibrin clot formed when PRP is activated by thrombin and $CaCl_2$.[17] Nevertheless, positive outcomes were obtained in animal studies conducted with PRP: Kamoda *et al.*[66] used PRP in a rodent IF model, combined with HA, obtaining 100% fusion. No fusion was obtained with HA alone.[66] Cinotti *et al.* obtained 86% fusion in the rabbit PLSF model when combining PRP with a calcium carbonate/HA scaffold,[82] and Okamoto *et al.*[103] also obtained bone fusion comparable to ABG by implanting PRP with a gelatin β-TCP sponge in the rat PLSF model. On the other hand, Scholz *et al.*[98] observed no significant osteoinductive effect of PRP combined with mineralized collagen in the sheep cervical IF model.

Cells

Fully differentiated bone and blood vessel cells would be considered ideal for the building of new bone,[15] yet these are limited in amount and source, ultimately jeopardizing a potential cell therapy. On the other hand, stem cells, such as MSC, have demonstrated evidence of safety and efficacy for bone formation, including applications for spine fusion. MSC are multipotent stromal cells that are capable of regenerating tissues by direct differentiation or indirectly by stimulating angiogenesis.[117,118] Such cells play an additional role by limiting inflammation as well as by recruiting tissue-specific progenitor cells.[119,120] MSC can be sourced from a variety of tissues[117]; however, for SF, BM-MSC or AT-MSC are the most reported (Table 1).

Bone marrow cells

The application of BM-MSC in the distinct SF surgical techniques (posterior/anterior IF/posterolateral fusion) and animal models are acknowledged. For instance, Ye *et al.*[23] used intraoperativelly isolated BM-MSC with poly-L-lysine-enriched DBM to regenerate bone in a goat intertransverse processes fusion model, with bone fusion comparable to autologous graft. On the other hand, neither Hayashi *et al.*[56] nor Klíma *et al.*,[63] in their studies, found advantages of the use of BM-MSC on what regards posterolateral fusion and new bone formation in the rat model. In studies conducted by Abbah *et al.*,[40] in large animal models, BM-MSC seem promising, despite underperforming other groups such as those containing BMP-2, or ABG control. Biomaterial used for cell delivery greatly affects fusion outcomes, as proved by Niu *et al.*,[52] where BM-MSC induced more bone formation when delivered in the PLGA/BCP/collagen graft rather than the PLGA/HA/collagen composite. Likewise, Gu *et al.*[107] observed increased fusion by BM-MSC within mineralized silk scaffold, as compared with nonmineralized scaffold.

An allogeneic source of cells would overcome current limitations related to autologous bone marrow harvest as well as time and costs related to manufacturing of expanded cells, and further potentially increasing therapeutic efficacy by using a qualified cell source. Wheeler *et al.*[71,73] tested allogeneic BM-MSC delivered by a TCP/HA carrier for a posterolateral spine fusion in a sheep model. Although therapeutic use of these allogeneic cells was reported as safe (no adverse systemic or local tissue responses), equivalent bone fusion was obtained as with autograft after 9 months of treatment.[71,73] Studies conducted by Goldschlager *et al.*[72,75] further demonstrated more robust fusion with allogeneic BM cells than ABG in the ovine cervical IF model. These cells also outperformed the experimental group containing amnion-derived epithelial cells (AEC).[75]

An alternative approach deals with osteogenic differentiation of MSC before implantation. Yang *et al.*[92] cultured osteogenic MSC before implantation in an anterior IF model in rabbit, using a collagen sponge. Bone fusion was achieved at 8 weeks of treatment, comparable to autogenous bone graft.[92] In a large animal, Abbah *et al.*[41] achieved new bone formation as early as 3 months in the porcine ALIF model, with osteogenically induced cell sheets assembled with PCL/TCP scaffolds. Clough *et al.*[102] demonstrated low immunogenicity of these cells by administrating human osteogenically enhanced MSC to an immunocompromised rat model. As discussed in the Biomaterials and Growth Factors sections, the use of cells is not yet synonym of improved bone fusion. For instance, Cuenca-Lopez *et al.*[64] remained uncertain about the role of osteogenic MSC to SF in their sheep PLSF study. Callus interference with the scaffolds was claimed as a possible cause. As previously mentioned, biomaterial properties greatly influence fusion outcomes, even when using osteogenically induced MSC. Shamsul *et al.*,[77] also in a sheep PLSF model, observed superior fusion with TCP/HA constructs than with HA scaffold.

Synergies between rhBMP-2 and bone marrow cells have been further tested. For instance, Hu *et al.*[79] claim increased efficacy of low dosages of rhBMP-2 (2.5 μg) when mixed with BM-MSC for PLSF in a rodent model. Liu *et al.*[104] further confirmed increased effectiveness in rabbit PLSF when BM-MSC were co-delivered with BMP-2. Even a lower dose of BMP-2 (1.68 μg/mL) was found to be effective by Bae *et al.* when combined with bone marrow aspirates (BMA).[91] These findings suggest that the delivery of

low BMP-2 doses as an adjuvant of a cell source may lead to satisfying fusion rates, while reducing dose-related complications, as well therapeutic cost.

BMA can be obtained by a relatively simple and noninvasive method, providing an osteogenic material in a more expedite manner as compared with MSC. Exciting outcomes have been obtained with this cell source in the rabbit PLSF model: Tanaka *et al.*[50] combined BMA with porous HA/PLA composites, which outperformed ABG after 12 weeks; Fredericks *et al.*[83] implanted BMA with silicate-substituted HA graft, obtaining clinical and radiographic outcomes similar to ABG; and Smucker *et al.*[76] used an HA/TCP graft loaded with BMA, which resulted in biomechanical and radiographic results similar to ABG after 8 weeks.

Adipose tissue cells

AT-MSC are quite attractive for their high abundance and ease of accessibility, while providing appealing cell types to be used in bone regeneration.[121,122] It should be kept in mind, however, that cell yield and heterogeneity of cell populations obtained are reported to be likely dependent on factors including donor, tissue harvesting site, and protocols used for *in vitro* cell isolation and culture.[123] Despite evidences of improved osteogensesis by BM-MSC,[124,125] osteogenic potential of AT-MSC seems less dependent on age or osteoporosis condition,[24] as BM-MSC demonstrated to be.[126]

In the field of adipose-derived cells, three fractions of cells with distinct degrees of purification were studied for SF:

(i) Stromal Vascular Fraction (SVF)—is the immediate fraction of cells obtained after disaggregation of the adipose tissue extracellular matrix.[127,128] This is a very heterogeneous population of cells composed of nucleated blood cells, fibroblasts, smooth muscle cells, and pericytes that play important roles in vascularization, and also a 1–10% fraction of mesenchymal stromal/stem cells.[127,128] The simple and fast obtainment of these cells make them attractive for bone fusion. To that end, Helder's co-workers tested the immediate loading of SVF onto PLCL scaffolds *in vitro*[129] and later implanted them in a spine fusion goat model.[44,45] Although osteogenesis occurred *in vitro*, the presence of SVF or AT-MSC within the PLCL scaffold did not improve fusion rates.

(ii) AT-MSC—the low immunogenicity of the stromal/stem cell fraction of SVF makes it attractive for allogeneic applications.[130] In this thought, McIntosh *et al.*[131] and Lopez *et al.*[132] not only demonstrated an accelerated SF by the use of AT-MSC in a rat model but also confirmed equal efficacy of allogeneic and syngeneic cells.[131] AT-MSC were delivered in TCP/collagen scaffold. After 8 weeks, both AT-MSC groups resulted in more mature callus formation, and less inflammatory response as compared with scaffold alone.[132] In the rabbit PLSF model, Tang *et al.*[49] also obtained improved fusion when using AT-MSC combined with the nano-hydroxyapatite (nHA)/collagen (Col)/PLA scaffold, as compared with scaffold alone or scaffold combined with ABG. Regarding osteogenic differentiation of AT-MSC, as reported for BM-MSC, these have also demonstrated potential for SF in a porcine study.[58]

(iii) Subpopulations of perivascular stem cells (PSC)—these cells exhibit advantages over AT-MSC once no *in vitro* culture step is necessary: PSC are sorted directly from the SVF of the adipose tissue.[57] Chung *et al.*[57] obtained robust endochondral ossification in all dosages of PSC delivered within DBM putty in a rat model, after 4 weeks of treatment. In addition, evidence of both direct and paracrine regulation of osteogenesis by PSC was found. Later, in an elegant study by Lee and co-workers,[24] the potential of these cells was evaluated in both osteoporotic and non-osteoporotic rat models. Efficacy of human perivascular stem cells (hPSC) was tested, in combination with the NELL-1 factor mentioned earlier, and an 83.3% fusion improvement was obtained in osteoporotic rats by treatment with high doses of these bioactive agents.[24]

Animal Models

Experimental studies discussed herein were conducted in diverse animal models, as outlined in Table 2. The rat model and the PLSF approach show highest adoption. Ease of handle and housing, resilience to anesthesia, resistance to infection, and reduced costs[133] are factors that aid selection of the rat for preliminary studies. Subsequently, PLSF studies using the rabbit were the most frequent—this is a validated model, with particular advantages: It allows a true inter-

Table 2. Animal Models Used for Efficacy Evaluation of New Biomaterials and Bioactive Agents in Spinal Fusion (2010–2016)

	Posterolateral spinal fusion		*Interbody fusion*		
			Cervical/thoracic	*Lumbar*	
	Lumbar	*Lumbar paravertebral muscle*	*Anterior*	*Anterior*	*Posterior*
Rat	24,25,42,47,53,54,56,57,59,63,79,84, 86,88,90,91,95–97,99,100,102,103,106–108	105,109			66
Rabbit	49–52,55,61,62,67,74,76,80–83,89,94,101,104		92		
Sheep	64,68,71,77		43,46,48,72,93,98	60,75	73
Goat	23,70		69	44,45	
Pig/Mini-pig	65			40,41,58,85	
Monkey	78				

transverse process arthrodesis, and has a nonunion rate comparable to that in humans.[134] Large animal models further allow an IF approach, in the cervical, thoracic, or lumbar spine. The sheep was commonly selected for anterior IF of the cervical spine, whereas posterolateral fusions were most used for the lumbar spine. The vertebrae size in the sheep is comparable to humans; therefore, human surgical techniques, as well as instrumentation can be easily performed.[133] The goat and pig were majorly used for lumbar procedures, both PLSF and IF approaches, providing optimal outcomes as described in Biomaterials, Growth Factors and Cells sections.

Conclusion

Innovative and sophisticated solutions with new biomaterial and GF compositions are being proposed at a rapid pace, demonstrating strong evidence of fusion, while caring for cost and safety matters. HA and TCP remain solid players, being fundamental mineral components of an osteoconductive structure. Synthetic biodegradable polyesters, such as PCL or PLA, are expressive in SF research, acting as an inert supporting material. Their properties can be fine-tuned to achieve desired mechanical properties, degradation rates, or even biological response. The use of GF, particularly BMP-2, to accelerate bone formation is nowadays well known in SF, and their pros and cons have been thoroughly described. To overcome limitations, while taking full benefit of the consistent fusion achieved with this bioactive agent, distinct approaches are under development: (i) new delivery vehicles, with controlled release of the GF; (ii) exploration of alternative GF, such as NELL-1 or oxysterols; and (iii) gene therapy, for sustained expression of desired osteogenic factor. Approaches for SF further started to integrate cells into the equation for improved functional bone development, taking benefit of growing knowledge in the field, particularly on what regards sources, characteristics, and potential. Although bone marrow and AT-MSC has been the preferred targets of study, efficacy outcomes have not met the elevated expectations. There is much to be understood on cell behavior to fully take advantage of their potential for SF.

Acknowledgments

The authors gratefully acknowledge funding by European Regional Development Fund (FEDER), through the Competitiveness Factors Operational Programme (COMPETE), and by National funds, through the Foundation for Science and Technology (FCT), under the scope of the project POCI-01-0145-FEDER-007038; and by the project NORTE-01-0145-FEDER-000013, supported by the Northern Portugal Regional Operational Programme (NORTE 2020), under the Portugal 2020 Partnership Agreement, through the FEDER. The funders had no role in the study design, data collection and analysis, decision to publish, or preparation of this article.

Disclosure Statement

No competing financial interest exists.

References

1. Kaiser, M.G., Eck, J.C., Groff, M.W., Watters, W.C., 3rd, Dailey, A.T., Resnick, D.K., *et al.* Guideline update for the performance of fusion procedures for degenerative disease of the lumbar spine. Part 1: Introduction and methodology. J Neurosurg Spine **21,** 2, 2014.
2. Esses, S.I., and Huler, R.J. Indications for lumbar spine fusion in the adult. Clin Orthop Relat Res **279,** 87, 1992.
3. Enker, P., and Steffee, A.D. Interbody fusion and instrumentation. Clin Orthop Relat Res **300,** 90, 1994.
4. Duarte, R.M., and Vaccaro, A.R. Spinal infection: state of the art and management algorithm. Eur Spine J **22,** 2787, 2013.
5. Slone, R.M., MacMillan, M., Montgomery, W.J., and Heare, M. Spinal fixation. Part 2. Fixation techniques and hardware for the thoracic and lumbosacral spine. Radiographics **13,** 521, 1993.
6. Slone, R.M., MacMillan, M., and Montgomery, W.J. Spinal fixation. Part 1. Principles, basic hardware, and fixation techniques for the cervical spine. Radiographics **13,** 341, 1993.
7. Fischer, C.R., Cassilly, R., Cantor, W., Edusei, E., Hammouri, Q., and Errico, T. A systematic review of comparative studies on bone graft alternatives for common spine fusion procedures. Eur Spine J **22,** 1423, 2013.
8. Campana, V., Milano, G., Pagano, E., Barba, M., Cicione, C., Salonna, G., *et al.* Bone substitutes in orthopaedic surgery: from basic science to clinical practice. J Mater Sci Mater Med **25,** 2445, 2014.
9. Pape, H.C., Evans, A., and Kobbe, P. Autologous bone graft: properties and techniques. J Orthop Trauma **24 Suppl 1,** S36, 2010.
10. Dimar, J.R., 2nd, Glassman, S.D., Burkus, J.K., Pryor, P.W., Hardacker, J.W., and Carreon, L.Y. Two-year fusion and clinical outcomes in 224 patients treated with a single-level instrumented posterolateral fusion with iliac crest bone graft. Spine J **9,** 880, 2009.
11. Grabowski, G., and Cornett, C.A. Bone graft and bone graft substitutes in spine surgery: current concepts and controversies. J Am Acad Orthop Surg **21,** 51, 2013.
12. Gupta, A., Kukkar, N., Sharif, K., Main, B.J., Albers, C.E., and El-Amin Iii, S.F. Bone graft substitutes for spine fusion: a brief review. World J Orthop **6,** 449, 2015.
13. Malloy, K.M., and Hilibrand, A.S. Autograft versus allograft in degenerative cervical disease. Clin Orthop Relat Res **394,** 27, 2002.
14. Delloye, C., Cornu, O., Druez, V., and Barbier, O. Bone allografts: what they can offer and what they cannot. J Bone Joint Surg Br **89,** 574, 2007.
15. Nguyen, L.H., Duenas, V., Chen, M.Y., and Jandial, R. Progenitor cells: role and usage in bone tissue engineering approaches for spinal fusion. Adv Exp Med Biol **760,** 188, 2012.
16. Park, J.J., Hershman, S.H., and Kim, Y.H. Updates in the use of bone grafts in the lumbar spine. Bull Hosp Jt Dis **71,** 39, 2013.
17. Elder, B.D., Holmes, C., Goodwin, C.R., Lo, S.F., Puvanesarajah, V., Kosztowski, T.A., *et al.* A systematic assessment of the use of platelet-rich plasma in spinal fusion. Ann Biomed Eng **43,** 1057, 2015.
18. Urist, M.R. Bone: formation by autoinduction. Science **150,** 893, 1965.
19. Peterson, B., Whang, P.G., Iglesias, R., Wang, J.C., and Lieberman, J.R. Osteoinductivity of commercially available demineralized bone matrix. Preparations in a spine fusion model. J Bone Joint Surg Am **86-A,** 2243, 2004.
20. Tilkeridis, K., Touzopoulos, P., Ververidis, A., Christodoulou, S., Kazakos, K., and Drosos, G.I. Use of demineralized bone matrix in spinal fusion. World J Orthop **5,** 30, 2014.

21. Aghdasi, B., Montgomery, S.R., Daubs, M.D., and Wang, J.C. A review of demineralized bone matrices for spinal fusion: the evidence for efficacy. Surgeon **11,** 39, 2013.
22. Murphy, M.B., Suzuki, R.K., Sand, T.T., Chaput, C.D., and Gregory, C.A. Short term culture of human mesenchymal stem cells with commercial osteoconductive carriers provides unique insights into biocompatibility. J Clin Med **2,** 49, 2013.
23. Ye, Q., Chen, K., Huang, W., He, Y., Nong, M., Li, C., *et al.* Osteogenic ability of bone marrow stem cells intraoperatively enriched by a novel matrix. Exp Ther Med **9,** 25, 2015.
24. Lee, S., Zhang, X., Shen, J., James, A.W., Chung, C.G., Hardy, R., *et al.* Brief report: human perivascular stem cells and Nel-like protein-1 synergistically enhance spinal fusion in osteoporotic rats. Stem Cells **33,** 3158, 2015.
25. Li, W., Lee, M., Whang, J., Siu, R.K., Zhang, X., Liu, C., *et al.* Delivery of lyophilized Nell-1 in a rat spinal fusion model. Tissue Eng Part A **16,** 2861, 2010.
26. Dai, L.Y., and Jiang, L.S. Single-level instrumented posterolateral fusion of lumbar spine with beta-tricalcium phosphate versus autograft: a prospective, randomized study with 3-year follow-up. Spine (Phila Pa 1976) **33,** 1299, 2008.
27. Epstein, N.E. A preliminary study of the efficacy of beta tricalcium phosphate as a bone expander for instrumented posterolateral lumbar fusions. J Spinal Disord Tech **19,** 424, 2006.
28. Alsousou, J., Thompson, M., Hulley, P., Noble, A., and Willett, K. The biology of platelet-rich plasma and its application in trauma and orthopaedic surgery: a review of the literature. J Bone Joint Surg Br **91,** 987, 2009.
29. Stevens, M.M. Biomaterials for bone tissue engineering. Materials Today **11,** 18, 2008.
30. Yan, L.P., Silva-Correia, J., Correia, C., Caridade, S.G., Fernandes, E.M., Sousa, R.A., *et al.* Bioactive macro/micro porous silk fibroin/nano-sized calcium phosphate scaffolds with potential for bone-tissue-engineering applications. Nanomedicine (Lond) **8,** 359, 2013.
31. Correia, C., Bhumiratana, S., Sousa, R.A., Reis, R.L., and Vunjak-Novakovic, G. Sequential application of steady and pulsatile medium perfusion enhanced the formation of engineered bone. Tissue Eng Part A **19,** 1244, 2013.
32. Hannink, G., and Arts, J.J. Bioresorbability, porosity and mechanical strength of bone substitutes: what is optimal for bone regeneration? Injury **42 Suppl 2,** S22, 2011.
33. Correia, C., Grayson, W.L., Park, M., Hutton, D., Zhou, B., Guo, X.E., *et al.* In vitro model of vascularized bone: synergizing vascular development and osteogenesis. PLoS One **6,** e28352, 2011.
34. Santos, M.I., and Reis, R.L. Vascularization in bone tissue engineering: physiology, current strategies, major hurdles and future challenges. Macromol Biosci **10,** 12, 2010.
35. Thomas, K.A., Toth, J.M., Crawford, N.R., Seim, H.B., 3rd, Shi, L.L., Harris, M.B., *et al.* Bioresorbable polylactide interbody implants in an ovine anterior cervical discectomy and fusion model: three-year results. Spine (Phila Pa 1976) **33,** 734, 2008.
36. Boden, S.D. Biology of lumbar spine fusion and use of bone graft substitutes: present, future, and next generation. Tissue Eng **6,** 383, 2000.
37. Manavitehrani, I., Fathi, A., Badr, H., Daly, S., Shirazi, A.N., and Dehghani, F. Biomedical applications of biodegradable polyesters. Polymers **8,** 20, 2016.
38. Mogosanu, D., Giol, E., Vandenhaute, M., Dragusin, D., Samal, S., and Dubruel, P. Polyester biomaterials for regenerative medicine. In: Cao, S., and Zhu, H., eds. Frontiers in Biomaterials: The Design, Synthetic Strategies and Biocompatibility of Polymer Scaffolds for Biomedical Application. Sharjah, U.A.E.: Bentham Science Publishers Ltd., 2014, pp. 155–197.
39. Abbah, S.A., Lam, C.X., Hutmacher, D.W., Goh, J.C., and Wong, H.K. Biological performance of a polycaprolactone-based scaffold used as fusion cage device in a large animal model of spinal reconstructive surgery. Biomaterials **30,** 5086, 2009.
40. Abbah, S.A., Lam, C.X., Ramruttun, A.K., Goh, J.C., and Wong, H.K. Fusion performance of low-dose recombinant human bone morphogenetic protein 2 and bone marrow-derived multipotent stromal cells in biodegradable scaffolds: a comparative study in a large animal model of anterior lumbar interbody fusion. Spine (Phila Pa 1976) **36,** 1752, 2011.
41. Abbah, S.A., Lam, C.X., Ramruttun, K.A., Goh, J.C., and Wong, H.K. Autogenous bone marrow stromal cell sheets-loaded mPCL/TCP scaffolds induced osteogenesis in a porcine model of spinal interbody fusion. Tissue Eng Part A **17,** 809, 2011.
42. Abbah, S.A., Liu, J., Goh, J.C., and Wong, H.K. Enhanced control of in vivo bone formation with surface functionalized alginate microbeads incorporating heparin and human bone morphogenetic protein-2. Tissue Eng Part A **19,** 350, 2013.
43. Li, Y., Wu, Z.G., Li, X.K., Guo, Z., Wu, S.H., Zhang, Y.Q., *et al.* A polycaprolactone-tricalcium phosphate composite scaffold as an autograft-free spinal fusion cage in a sheep model. Biomaterials **35,** 5647, 2014.
44. Kroeze, R.J., Smit, T.H., Vergroesen, P.P., Bank, R.A., Stoop, R., van Rietbergen, B., *et al.* Spinal fusion using adipose stem cells seeded on a radiolucent cage filler: a feasibility study of a single surgical procedure in goats. Eur Spine J **24,** 1031, 2015.
45. Vergroesen, P.P., Kroeze, R.J., Helder, M.N., and Smit, T.H. The use of poly(L-lactide-co-caprolactone) as a scaffold for adipose stem cells in bone tissue engineering: application in a spinal fusion model. Macromol Biosci **11,** 722, 2011.
46. Yong, M.R., Saifzadeh, S., Woodruff, M., Askin, G.N., Labrom, R.D., Hutmacher, D.W., *et al.* Biological performance of a polycaprolactone-based scaffold plus recombinant human morphogenetic protein-2 (rhBMP-2) in an ovine thoracic interbody fusion model. Eur Spine J **23,** 650, 2014.
47. Chen, C., Garber, L., Smoak, M., Fargason, C., Scherr, T., Blackburn, C., *et al.* In vitro and in vivo characterization of pentaerythritol triacrylate-co-trimethylolpropane nanocomposite scaffolds as potential bone augments and grafts. Tissue Eng Part A **21,** 320, 2015.
48. Cao, L., Duan, P.G., Li, X.L., Yuan, F.L., Zhao, M.D., Che, W., *et al.* Biomechanical stability of a bioabsorbable self-retaining polylactic acid/nano-sized β-tricalcium phosphate cervical spine interbody fusion device in single-level anterior cervical discectomy and fusion sheep models. Int J Nanomedicine **7,** 5875, 2012.
49. Tang, Z.B., Cao, J.K., Wen, N., Wang, H.B., Zhang, Z.W., Liu, Z.Q., *et al.* Posterolateral spinal fusion with nano-hydroxyapatite-collagen/PLA composite and autologous adipose-derived mesenchymal stem cells in a rabbit model. J Tissue Eng Regen Med **6,** 325, 2012.
50. Tanaka, K., Takemoto, M., Fujibayashi, S., Neo, M., Shikinami, Y., and Nakamura, T. A bioactive and bioresorbable porous cubic composite scaffold loaded with bone marrow aspirate: a potential alternative to autogenous bone grafting. Spine (Phila Pa 1976) **36,** 441, 2011.

51. Matsumoto, T., Toyoda, H., Dohzono, S., Yasuda, H., Wakitani, S., Nakamura, H., *et al.* Efficacy of interspinous process lumbar fusion with recombinant human bone morphogenetic protein-2 delivered with a synthetic polymer and β-tricalcium phosphate in a rabbit model. Eur Spine J **21,** 1338, 2012.
52. Niu, C.C., Lin, S.S., Chen, W.J., Liu, S.J., Chen, L.H., Yang, C.Y., *et al.* Benefits of biphasic calcium phosphate hybrid scaffold-driven osteogenic differentiation of mesenchymal stem cells through upregulated leptin receptor expression. J Orthop Surg Res **10,** 111, 2015.
53. Jakus, A.E., Rutz, A.L., Jordan, S.W., Kannan, A., Mitchell, S.M., Yun, C., *et al.* Hyperelastic ''bone'': a highly versatile, growth factor-free, osteoregenerative, scalable, and surgically friendly biomaterial. Sci Transl Med **8,** 358ra127, 2016.
54. Hu, M.H., Lee, P.Y., Chen, W.C., and Hu, J.J. Comparison of three calcium phosphate bone graft substitutes from biomechanical, histological, and crystallographic perspectives using a rat posterolateral lumbar fusion model. Mater Sci Eng C Mater Biol Appl **45,** 82, 2014.
55. Mao, K., Cui, F., Li, J., Hao, L., Tang, P., Wang, Z., *et al.* Preparation of combined β-TCP/α-CSH artificial bone graft and its performance in a spinal fusion model. J Biomater Appl **27,** 37, 2012.
56. Hayashi, T., Lord, E.L., Suzuki, A., Takahashi, S., Scott, T.P., Phan, K., *et al.* A comparison of commercially available demineralized bone matrices with and without human mesenchymal stem cells in a rodent spinal fusion model. J Neurosurg Spine **25,** 133, 2016.
57. Chung, C.G., James, A.W., Asatrian, G., Chang, L., Nguyen, A., Le, K., *et al.* Human perivascular stem cell-based bone graft substitute induces rat spinal fusion. Stem Cells Transl Med **4,** 538, 2015.
58. Schubert, T., Lafont, S., Beaurin, G., Grisay, G., Behets, C., Gianello, P., *et al.* Critical size bone defect reconstruction by an autologous 3D osteogenic-like tissue derived from differentiated adipose MSCs. Biomaterials **34,** 4428, 2013.
59. Yuan, W., James, A.W., Asatrian, G., Shen, J., Zara, J.N., Tian, H.J., *et al.* NELL-1 based demineralized bone graft promotes rat spine fusion as compared to commercially available BMP-2 product. J Orthop Sci **18,** 646, 2013.
60. Siu, R.K., Lu, S.S., Li, W., Whang, J., McNeill, G., Zhang, X., *et al.* Nell-1 protein promotes bone formation in a sheep spinal fusion model. Tissue Eng Part A **17,** 1123, 2011.
61. Kiely, P.D., Brecevich, A.T., Taher, F., Nguyen, J.T., Cammisa, F.P., and Abjornson, C. Evaluation of a new formulation of demineralized bone matrix putty in a rabbit posterolateral spinal fusion model. Spine J **14,** 2155, 2014.
62. Smucker, J.D., and Fredericks, D.C. Assessment of Progenix(®) DBM putty bone substitute in a rabbit posterolateral fusion model. Iowa Orthop J **32,** 54, 2012.
63. Klíma, K., Vaněček, V., Kohout, A., Jiroušek, O., Foltán, R., Štulík, J., *et al.* Stem cells regenerative properties on new rat spinal fusion model. Physiol Res **64,** 119, 2015.
64. Cuenca-López, M.D., Andrades, J.A., Gómez, S., Zamora-Navas, P., Guerado, E., Rubio, N., *et al.* Evaluation of posterolateral lumbar fusion in sheep using mineral scaffolds seeded with cultured bone marrow cells. Int J Mol Sci **15,** 23359, 2014.
65. Kong, C.B., Lee, J.H., Baek, H.R., Lee, C.K., and Chang, B.S. Posterolateral lumbar fusion using *Escherichia coli*-derived rhBMP-2/hydroxyapatite in the mini pig. Spine J **14,** 2959, 2014.
66. Kamoda, H., Yamashita, M., Ishikawa, T., Miyagi, M., Arai, G., Suzuki, M., *et al.* Platelet-rich plasma combined with hydroxyapatite for lumbar interbody fusion promoted bone formation and decreased an inflammatory pain neuropeptide in rats. Spine (Phila Pa 1976) **37,** 1727, 2012.
67. Fu, T.S., Chang, Y.H., Wong, C.B., Wang, I.C., Tsai, T.T., Lai, P.L., *et al.* Mesenchymal stem cells expressing baculovirus-engineered BMP-2 and VEGF enhance posterolateral spine fusion in a rabbit model. Spine J **15,** 2036, 2015.
68. Pelletier, M.H., Oliver, R.A., Christou, C., Yu, Y., Bertollo, N., Irie, H., *et al.* Lumbar spinal fusion with β-TCP granules and variable *Escherichia coli*-derived rhBMP-2 dose. Spine J **14,** 1758, 2014.
69. Wang, H., Zhang, F., Lv, F., Jiang, J., Liu, D., and Xia, X. Osteoinductive activity of ErhBMP-2 after anterior cervical diskectomy and fusion with a β-TCP interbody cage in a goat model. Orthopedics **37,** e123, 2014.
70. Delawi, D., Kruyt, M.C., Huipin, Y., Vincken, K.L., de Bruijn, J.D., Oner, F.C., *et al.* Comparing autograft, allograft, and tricalcium phosphate ceramic in a goat instrumented posterolateral fusion model. Tissue Eng Part C Methods **19,** 821, 2013.
71. Wheeler, D.L., Lane, J.M., Seim, H.B., Puttlitz, C.M., Itescu, S., and Turner, A.S. Allogeneic mesenchymal progenitor cells for posterolateral lumbar spine fusion in sheep. Spine J **14,** 435, 2014.
72. Goldschlager, T., Rosenfeld, J.V., Ghosh, P., Itescu, S., Blecher, C., McLean, C., *et al.* Cervical interbody fusion is enhanced by allogeneic mesenchymal precursor cells in an ovine model. Spine (Phila Pa 1976) **36,** 615, 2011.
73. Wheeler, D.L., Fredericks, D.C., Dryer, R.F., and Bae, H.W. Allogeneic mesenchymal precursor cells (MPCs) combined with an osteoconductive scaffold to promote lumbar interbody spine fusion in an ovine model. Spine J **16,** 389, 2016.
74. Lee, T.H., Huang, Y.H., Chang, N.K., Lin, W.C., Chien, P.W., Su, T.M., *et al.* Characterization and spinal fusion effect of rabbit mesenchymal stem cells. BMC Res Notes **6,** 528, 2013.
75. Goldschlager, T., Ghosh, P., Zannettino, A., Williamson, M., Rosenfeld, J.V., Itescu, S., *et al.* A comparison of mesenchymal precursor cells and amnion epithelial cells for enhancing cervical interbody fusion in an ovine model. Neurosurgery **68,** 1025, discussion 34, 2011.
76. Smucker, J.D., Petersen, E.B., Nepola, J.V., and Fredericks, D.C. Assessment of Mastergraft(®) strip with bone marrow aspirate as a graft extender in a rabbit posterolateral fusion model. Iowa Orthop J **32,** 61, 2012.
77. Shamsul, B.S., Tan, K.K., Chen, H.C., Aminuddin, B.S., and Ruszymah, B.H. Posterolateral spinal fusion with ostegenesis induced BMSC seeded TCP/HA in a sheep model. Tissue Cell **46,** 152, 2014.
78. Khan, S.N., Toth, J.M., Gupta, K., Glassman, S.D., and Gupta, M.C. Early-term and mid-term histologic events during single-level posterolateral intertransverse process fusion with rhBMP-2/collagen carrier and a ceramic bulking agent in a nonhuman primate model: implications for bone graft preparation. J Spinal Disord Tech **27,** 212, 2014.
79. Hu, T., Abbah, S.A., Toh, S.Y., Wang, M., Lam, R.W., Naidu, M., *et al.* Bone marrow-derived mesenchymal stem cells assembled with low-dose BMP-2 in a three-dimensional hybrid construct enhances posterolateral spinal fusion in syngeneic rats. Spine J **15,** 2552, 2015.

80. Huang, J.W., Lin, S.S., Chen, L.H., Liu, S.J., Niu, C.C., Yuan, L.J., *et al.* The use of fluorescence-labeled mesenchymal stem cells in poly(lactide-co-glycolide)/hydroxyapatite/collagen hybrid graft as a bone substitute for posterolateral spinal fusion. J Trauma **70,** 1495, 2011.
81. Walsh, W.R., Oliver, R.A., Gage, G., Yu, Y., Bell, D., Bellemore, J., *et al.* Application of resorbable poly(lactide-co-glycolide) with entangled hyaluronic acid as an autograft extender for posterolateral intertransverse lumbar fusion in rabbits. Tissue Eng Part A **17,** 213, 2011.
82. Cinotti, G., Corsi, A., Sacchetti, B., Riminucci, M., Bianco, P., and Giannicola, G. Bone ingrowth and vascular supply in experimental spinal fusion with platelet-rich plasma. Spine (Phila Pa 1976) **38,** 385, 2013.
83. Fredericks, D.C., Petersen, E.B., Sahai, N., Corley, K.G., DeVries, N., Grosland, N.M., *et al.* Evaluation of a novel silicate substituted hydroxyapatite bone graft substitute in a rabbit posterolateral fusion model. Iowa Orthop J **33,** 25, 2013.
84. Hu, T., Abbah, S.A., Wang, M., Toh, S.Y., Lam, R.W., Naidu, M., *et al.* Novel Protamine-Based Polyelectrolyte Carrier Enhances Low-Dose rhBMP-2 in Posterolateral Spinal Fusion. Spine (Phila Pa 1976) **40,** 613, 2015.
85. Abbah, S.A., Lam, W.M., Hu, T., Goh, J., and Wong, H.K. Sequestration of rhBMP-2 into self-assembled polyelectrolyte complexes promotes anatomic localization of new bone in a porcine model of spinal reconstructive surgery. Tissue Eng Part A **20,** 1679, 2014.
86. Abbah, S.A., Liu, J., Lam, R.W., Goh, J.C., and Wong, H.K. In vivo bioactivity of rhBMP-2 delivered with novel polyelectrolyte complexation shells assembled on an alginate microbead core template. J Control Release **162,** 364, 2012.
87. Sherman, B.P., Lindley, E.M., Turner, A.S., Seim, H.B., Benedict, J., Burger, E.L., *et al.* Evaluation of ABM/P-15 versus autogenous bone in an ovine lumbar interbody fusion model. Eur Spine J **19,** 2156, 2010.
88. Johnson, J.S., Meliton, V., Kim, W.K., Lee, K.B., Wang, J.C., Nguyen, K., *et al.* Novel oxysterols have pro-osteogenic and anti-adipogenic effects in vitro and induce spinal fusion in vivo. J Cell Biochem **112,** 1673, 2011.
89. Liao, J.C. Bone marrow mesenchymal stem cells expressing baculovirus-engineered bone morphogenetic protein-7 enhance rabbit posterolateral fusion. Int J Mol Sci **17,** 1073, 2016.
90. Kaito, T., Johnson, J., Ellerman, J., Tian, H., Aydogan, M., Chatsrinopkun, M., *et al.* Synergistic effect of bone morphogenetic proteins 2 and 7 by ex vivo gene therapy in a rat spinal fusion model. J Bone Joint Surg Am **95,** 1612, 2013.
91. Bae, H.W., Zhao, L., Kanim, L.E., Wong, P., Marshall, D., and Delamarter, R.B. Bone marrow enhances the performance of rhBMP-2 in spinal fusion: a rodent model. J Bone Joint Surg Am **95,** 338, 2013.
92. Yang, W., Dong, Y., Hong, Y., Guang, Q., and Chen, X. Evaluation of anterior vertebral interbody fusion using osteogenic mesenchymal stem cells transplanted in collagen sponge. Clin Spine Surg **29,** E201, 2016.
93. Scholz, M., Schleicher, P., Sewing, A., Gelinsky, M., and Kandziora, F. Cyclic-RGD is as effective as rhBMP-2 in anterior interbody fusion of the sheep cervical spine. Spine (Phila Pa 1976) **38,** E59, 2013.
94. Majid, K., Tseng, M.D., Baker, K.C., Reyes-Trocchia, A., and Herkowitz, H.N. Biomimetic calcium phosphate coatings as bone morphogenetic protein delivery systems in spinal fusion. Spine J **11,** 560, 2011.
95. Morimoto, T., Kaito, T., Kashii, M., Matsuo, Y., Sugiura, T., Iwasaki, M., *et al.* Effect of intermittent administration of teriparatide (parathyroid hormone 1–34) on bone morphogenetic protein-induced bone formation in a rat model of spinal fusion. J Bone Joint Surg Am **96,** e107, 2014.
96. Han, X., Zhang, W., Gu, J., Zhao, H., Ni, L., Han, J., *et al.* Accelerated postero-lateral spinal fusion by collagen scaffolds modified with engineered collagen-binding human bone morphogenetic protein-2 in rats. PLoS One **9,** e98480, 2014.
97. Morimoto, T., Kaito, T., Matsuo, Y., Sugiura, T., Kashii, M., Makino, T., *et al.* The bone morphogenetic protein-2/7 heterodimer is a stronger inducer of bone regeneration than the individual homodimers in a rat spinal fusion model. Spine J **15,** 1379, 2015.
98. Scholz, M., Schleicher, P., Eindorf, T., Friedersdorff, F., Gelinsky, M., König, U., *et al.* Cages augmented with mineralized collagen and platelet-rich plasma as an osteoconductive/inductive combination for interbody fusion. Spine (Phila Pa 1976) **35,** 740, 2010.
99. Montgomery, S.R., Nargizyan, T., Meliton, V., Nachtergaele, S., Rohatgi, R., Stappenbeck, F., *et al.* A novel osteogenic oxysterol compound for therapeutic development to promote bone growth: activation of hedgehog signaling and osteogenesis through smoothened binding. J Bone Miner Res **29,** 1872, 2014.
100. Park, B.H., Song, K.J., Yoon, S.J., Park, H.S., Jang, K.Y., Zhou, L., *et al.* Acceleration of spinal fusion using COMP-angiopoietin 1 with allografting in a rat model. Bone **49,** 447, 2011.
101. Douglas, J.T., Rivera, A.A., Lyons, G.R., Lott, P.F., Wang, D., Zayzafoon, M., *et al.* Ex vivo transfer of the Hoxc-8-interacting domain of Smad1 by a tropism-modified adenoviral vector results in efficient bone formation in a rabbit model of spinal fusion. J Spinal Disord Tech **23,** 63, 2010.
102. Clough, B.H., McNeill, E.P., Palmer, D., Krause, U., Bartosh, T.J., Chaput, C.D., *et al.* An allograft generated from adult stem cells and their secreted products efficiently fuses vertebrae in immunocompromised athymic rats and inhibits local immune responses. Spine J **17,** 418, 2016.
103. Okamoto, S., Ikeda, T., Sawamura, K., Nagae, M., Hase, H., Mikami, Y., *et al.* Positive effect on bone fusion by the combination of platelet-rich plasma and a gelatin β-tricalcium phosphate sponge: a study using a posterolateral fusion model of lumbar vertebrae in rats. Tissue Eng Part A **18,** 157, 2012.
104. Liu, Z., Zhu, Y., Zhu, H., He, X., and Liu, X. Enhancement of posterolateral lumbar spine fusion using recombinant human bone morphogenetic protein-2 and mesenchymal stem cells delivered in fibrin glue. J Biomater Appl **31,** 477, 2016.
105. Sheyn, D., Rüthemann, M., Mizrahi, O., Kallai, I., Zilberman, Y., Tawackoli, W., *et al.* Genetically modified mesenchymal stem cells induce mechanically stable posterior spine fusion. Tissue Eng Part A **16,** 3679, 2010.
106. Sheyn, D., Kallai, I., Tawackoli, W., Cohn Yakubovich, D., Oh, A., Su, S., *et al.* Gene-modified adult stem cells regenerate vertebral bone defect in a rat model. Mol Pharm **8,** 1592, 2011.
107. Gu, Y., Chen, L., Niu, H.Y., Shen, X.F., and Yang, H.L. Promoting spinal fusions by biomineralized silk fibroin films seeded with bone marrow stromal cells: an in vivo animal study. J Biomater Appl **30,** 1251, 2016.

108. Jing, W., Smith, A.A., Liu, B., Li, J., Hunter, D.J., Dhamdhere, G., *et al.* Reengineering autologous bone grafts with the stem cell activator WNT3A. Biomaterials **47,** 29, 2015.
109. Olabisi, R.M., Lazard, Z., Heggeness, M.H., Moran, K.M., Hipp, J.A., Dewan, A.K., *et al.* An injectable method for noninvasive spine fusion. Spine J **11,** 545, 2011.
110. Chrastil, J., Low, J.B., Whang, P.G., and Patel, A.A. Complications associated with the use of the recombinant human bone morphogenetic proteins for posterior interbody fusions of the lumbar spine. Spine (Phila Pa 1976) **38,** E1020, 2013.
111. Carragee, E.J., Hurwitz, E.L., and Weiner, B.K. A critical review of recombinant human bone morphogenetic protein-2 trials in spinal surgery: emerging safety concerns and lessons learned. Spine J **11,** 471, 2011.
112. Schultz, D.G. FDA public health notification: life-threatening complications associated with recombinant human bone morphogenetic protein in cervical spine fusion. 2008. www.fda.gov/MedicalDevices/Safety/AlertsandNotices/PublicHealthNotifications/ucm062000.htm Accessed August 10, 2015.
113. Israel, D.I., Nove, J., Kerns, K.M., Kaufman, R.J., Rosen, V., Cox, K.A., *et al.* Heterodimeric bone morphogenetic proteins show enhanced activity in vitro and in vivo. Growth Factors **13,** 291, 1996.
114. Wang, J., Zheng, Y., Zhao, J., Liu, T., Gao, L., Gu, Z., *et al.* Low-dose rhBMP2/7 heterodimer to reconstruct peri-implant bone defects: a micro-CT evaluation. J Clin Periodontol **39,** 98, 2012.
115. Hsu, W.K., Mishra, A., Rodeo, S.R., Fu, F., Terry, M.A., Randelli, P., *et al.* Platelet-rich plasma in orthopaedic applications: evidence-based recommendations for treatment. J Am Acad Orthop Surg **21,** 739, 2013.
116. Weibrich, G., Kleis, W.K., Hitzler, W.E., and Hafner, G. Comparison of the platelet concentrate collection system with the plasma-rich-in-growth-factors kit to produce platelet-rich plasma: a technical report. Int J Oral Maxillofac Implants **20,** 118, 2005.
117. Murray, I.R., West, C.C., Hardy, W.R., James, A.W., Park, T.S., Nguyen, A., *et al.* Natural history of mesenchymal stem cells, from vessel walls to culture vessels. Cell Mol Life Sci **71,** 1353, 2014.
118. Watt, S.M., Gullo, F., van der Garde, M., Markeson, D., Camicia, R., Khoo, C.P., *et al.* The angiogenic properties of mesenchymal stem/stromal cells and their therapeutic potential. Br Med Bull **108,** 25, 2013.
119. Chen, L., Tredget, E.E., Wu, P.Y., and Wu, Y. Paracrine factors of mesenchymal stem cells recruit macrophages and endothelial lineage cells and enhance wound healing. PLoS One **3,** e1886, 2008.
120. Singer, N.G., and Caplan, A.I. Mesenchymal stem cells: mechanisms of inflammation. Annu Rev Pathol **6,** 457, 2011.
121. Gimble, J.M., Bunnell, B.A., Chiu, E.S., and Guilak, F. Concise review: adipose-derived stromal vascular fraction cells and stem cells: let's not get lost in translation. Stem Cells **29,** 749, 2011.
122. Grayson, W.L., Bunnell, B.A., Martin, E., Frazier, T., Hung, B.P., and Gimble, J.M. Stromal cells and stem cells in clinical bone regeneration. Nat Rev Endocrinol **11,** 140, 2015.
123. Baer, P.C., and Geiger, H. Adipose-derived mesenchymal stromal/stem cells: tissue localization, characterization, and heterogeneity. Stem Cells Int **2012,** 812693, 2012.
124. Im, G.I. Bone marrow-derived stem/stromal cells and adipose tissue-derived stem/stromal cells: their comparative efficacies and synergistic effects. J Biomed Mater Res A 2017. DOI: 10.1002/jbma.36089.
125. Knight, M.N., and Hankenson, K.D. Mesenchymal stem cells in bone regeneration. Adv Wound Care (New Rochelle) **2,** 306, 2013.
126. Boeloni, J.N., Ocarino, N.M., Goes, A.M., and Serakides, R. Comparative study of osteogenic differentiation potential of mesenchymal stem cells derived from bone marrow and adipose tissue of osteoporotic female rats. Connect Tissue Res **55,** 103, 2014.
127. Gimble, J.M., Grayson, W., Guilak, F., Lopez, M.J., and Vunjak-Novakovic, G. Adipose tissue as a stem cell source for musculoskeletal regeneration. Front Biosci (Schol Ed) **3,** 69, 2011.
128. Bourin, P., Bunnell, B.A., Casteilla, L., Dominici, M., Katz, A.J., March, K.L., *et al.* Stromal cells from the adipose tissue-derived stromal vascular fraction and culture expanded adipose tissue-derived stromal/stem cells: a joint statement of the International Federation for Adipose Therapeutics and Science (IFATS) and the International Society for Cellular Therapy (ISCT). Cytotherapy **15,** 641, 2013.
129. Jurgens, W.J., Kroeze, R.J., Bank, R.A., Ritt, M.J., and Helder, M.N. Rapid attachment of adipose stromal cells on resorbable polymeric scaffolds facilitates the one-step surgical procedure for cartilage and bone tissue engineering purposes. J Orthop Res **29,** 853, 2011.
130. McIntosh, K., Zvonic, S., Garrett, S., Mitchell, J.B., Floyd, Z.E., Hammill, L., *et al.* The immunogenicity of human adipose-derived cells: temporal changes in vitro. Stem Cells **24,** 1246, 2006.
131. McIntosh, K.R., Lopez, M.J., Borneman, J.N., Spencer, N.D., Anderson, P.A., and Gimble, J.M. Immunogenicity of allogeneic adipose-derived stem cells in a rat spinal fusion model. Tissue Eng Part A **15,** 2677, 2009.
132. Lopez, M.J., McIntosh, K.R., Spencer, N.D., Borneman, J.N., Horswell, R., Anderson, P., *et al.* Acceleration of spinal fusion using syngeneic and allogeneic adult adipose derived stem cells in a rat model. J Orthop Res **27,** 366, 2009.
133. Drespe, I.H., Polzhofer, G.K., Turner, A.S., and Grauer, J.N. Animal models for spinal fusion. Spine J **5,** 209S, 2005.
134. Riordan, A.M., Rangarajan, R., Balts, J.W., Hsu, W.K., and Anderson, P.A. Reliability of the rabbit postero-lateral spinal fusion model: a meta-analysis. J Orthop Res **31,** 1261, 2013.

Address correspondence to:
Rui M. Duarte, MD
School of Medicine
University of Minho
Campus de Gualtar
4710-057 Braga
Portugal

E-mail: ruimfduarte@med.uminho.pt

Received: February 10, 2017
Accepted: May 15, 2017
Online Publication Date: June 28, 2017

CHAPTER II

Aims

Aims

Management of instability, deformities and degenerative spine pathologies frequently lead to spinal fusion, where bone growth is promoted to stabilize the related spine segment [1]. Currently, lumbar interbody fusion (IF) procedures require primary stabilization through vertebral fixation systems (cages, screws and rods) [2,3]. Such hardware cause increased damage to surrounding anatomical structures, material may fail or migrate, and neurological damage can occur if material is misplaced [4]. Non-union is also associated to limited bone formation by bone graft or substitutes applied [5].

This project brings the hypothesis of a paradigm-shifting surgical approach for spinal arthrodesis, through the development of a new biomaterial for instrumentation-free interbody fusion (BIOLIF).

The main objectives of this project are:

i. Development and *in vitro* evaluation of a new PCL-based foam with physicochemical, biological and mechanical properties capable to stabilize the spine without instrumentation, while simultaneously providing an osteogenic environment for mature bone development and successful interbody fusion.

ii. Design, production and *ex vivo* testing of a novel surgical tool for delivery of the foam into the intervertebral space, following minimally invasive spine surgery techniques.

iii. *in vivo* assessment of the surgical feasibility and biological performance of the proposed approach (biomaterial and surgical device) for spinal fusion in a large animal model (pig).

References

[1] M.G. Kaiser, J.C. Eck, M.W. Groff, W.C. Watters, A.T. Dailey, D.K. Resnick, T.F. Choudhri, A. Sharan, J.C. Wang, P. V. Mummaneni, S.S. Dhall, Z. Ghogawala, Guideline update for the performance of fusion procedures for degenerative disease of the lumbar spine. Part 1: Introduction and methodology, J. Neurosurg. Spine. 21 (2014) 2–6. https://doi.org/10.3171/2014.4.SPINE14257.

[2] R. Roy-Camille, G. Saillant, C. Mazel, Internal fixation of the lumbar spine with pedicle screw plating, Clin. Orthop. Relat. Res. (1986). https://doi.org/10.1097/00003086-198602000-00003.

[3] S.D. Kuslich, C.L. Ulstrom, S.L. Griffith, J.W. Ahern, J.D. Dowdle, G. Tipton, The Bagby and Kuslich method of lumbar interbody fusion: History, techniques, and 2-year follow-up results of a United States prospective, multicenter trial, Spine (Phila. Pa. 1976). (1998). https://doi.org/10.1097/00007632-199806010-00019.

[4] P.G. Campbell, S. Yadla, J. Malone, M.G. Maltenfort, J.S. Harrop, A.D. Sharan, J.K. Ratliff, Complications related to instrumentation in spine surgery: A prospective analysis, Neurosurg. Focus. (2011). https://doi.org/10.3171/2011.7.FOCUS1134.

[5] C.R. Fischer, R. Cassilly, W. Cantor, E. Edusei, Q. Hammouri, T. Errico, A systematic review of comparative studies on bone graft alternatives for common spine fusion procedures, Eur. Spine J. 22 (2013) 1423–35. https://doi.org/10.1007/s00586-013-2718-4.

SECTION 2.

CHAPTER III

Subcritical carbon dioxide foaming of polycaprolactone for bone tissue regeneration

This chapter is based on the following publication: **Duarte RM**, Correia-Pinto J, Reis. RL and Duarte ARC, *Subcritical carbon dioxide foaming of polycaprolactone for bone tissue regeneration*; The Journal of Supercritical Fluids 140 (2018) 1–10. DOI: 10.1016/j.supflu.2018.05.019

The Journal of Supercritical Fluids 140 (2018) 1–10

Contents lists available at ScienceDirect

The Journal of Supercritical Fluids

journal homepage: www.elsevier.com/locate/supflu

Subcritical carbon dioxide foaming of polycaprolactone for bone tissue regeneration

Rui M. Duarte[a,b,d,e], Jorge Correia-Pinto[a,b,d,f], Rui L. Reis[c,d], Ana Rita C. Duarte[c,d,*,1]

[a] School of Medicine, University of Minho, Campus de Gualtar, 4710-057, Braga, Portugal
[b] Life and Health Sciences Research Institute (ICVS), School of Medicine, University of Minho, Campus de Gualtar, 4710-057, Braga, Portugal
[c] 3B´s Research Group – Biomaterials, Biodegradables and Biomimetics, University of Minho, Headquarters of the European Institute of Excellence on Tissue Engineering and Regenerative Medicine, Avepark – Parque de Ciência e Tecnologia, 4805-017, Barco GMR, Portugal
[d] ICVS/3B's-PT Government Associate Laboratory, Braga, Guimarães, Portugal
[e] Orthopedic Surgery Department, Hospital de Braga, Sete Fontes-São Victor, 4710-243, Braga, Portugal
[f] Pediatric Surgery Department, Hospital de Braga, Sete Fontes-São Victor, 4710-243, Braga, Portugal

GRAPHICAL ABSTRACT

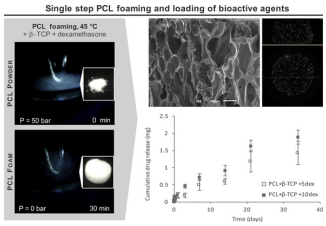

ARTICLE INFO

Keywords:
Polycaprolactone
Carbon dioxide
Subcritical
Bone regeneration
Scaffolds
Bioactive agents

ABSTRACT

The preparation of three-dimensional polycaprolactone scaffolds using dense CO_2 as foaming agent, without supercritical conditions, was evaluated in this study towards future applications in bone repair. Herein, 3D foams were obtained at 5.0 MPa and 45 °C. To induce bioactivity, β-tricalcium phosphate (β-TCP, 10 wt%) and dexamethasone (5 and 10 wt%) were dispersed in the scaffolds. Foams revealed a pore size range of 164–882 μm, 73–99% porosity and 79–99% interconnectivity, assessed by micro-computed tomography, and a Young modulus of 1.76–2.92 MPa. Dexamethasone did not impair morphology of the matrices in comparison with PCL + β-TCP, which presented a water uptake of nearly 100% after 14 days. A sustained release of dexamethasone was achieved over 35 days in physiologic solution. This study reports the feasibility of using dense CO_2 to produce in one-step a porous matrix loaded with active agents opening new possibilities towards injectable systems for *in situ* foaming.

1. Introduction

The development of 3D architectures for tissue engineering has challenged many researchers involved in different fields of knowledge. The ability to create a three-dimensional scaffold, which meets the morphological, mechanical, chemical and biological requirements for good cellular performance and tissue integration, is not straightforward. In this sense, the pursue for different processing techniques

* Corresponding author at: 3B´s Research Group – Biomaterials, Biodegradables and Biomimetics, University of Minho, Headquarters of the European Institute of Excellence on Tissue Engineering and Regenerative Medicine, Avepark – Parque de Ciência e Tecnologia, 4805-017, Barco GMR, Portugal.
E-mail addresses: aduarte@dep.uminho.pt, aduarte@fct.unl.pt (A.R.C. Duarte).
[1] Present address: Departamento de Química, Faculdade de Ciências e Tecnologia, Universidade Nova de Lisboa, 2829-516 Caparica, Portugal.

https://doi.org/10.1016/j.supflu.2018.05.019
Received 7 December 2017; Received in revised form 21 May 2018; Accepted 21 May 2018
Available online 22 May 2018

which can offer the most appropriate construct for the application of such purpose has been the goal of many different works reported in the literature. One of the techniques that has been extensively studied for polymer processing is the use of gas and/or supercritical foaming. This technique was firstly proposed by Mooney and co-workers back in 1996 [1] to produce a highly porous and interconnected structure for tissue engineering and regenerative medicine. In the work reported, foaming of poly(-lactic-co-glycolic acid) without the use of organic solvents was described. The thermodynamic principle underlying the gas foaming is the plasticization effect of the gas on the polymeric matrix, decreasing its glass transition and/or melting temperature. Upon decompression cells start to nucleate and the pores are formed [2–6]. Carbon dioxide is the supercritical fluid used per excellence, particularly due to its low critical properties (P_c = 7.4 MPa and T_c = 31 °C), but also due to its innocuity. The main constraint of the gas/supercritical foaming technique is, however, the limited ability of carbon dioxide to decrease the glass transition temperature of crystalline polymers, hence this processing can only be applied to amorphous or semi-crystalline polymers and the extent of foaming will be directly related to the affinity of carbon dioxide to the polymer.

Since the pioneering work of Mooney, different polymers were tested. Particularly interesting for biomedical applications are different derivatives of polyesters such as poly(L-lactic acid) [7,8], poly(DL-lactic acid) [9,10], poly(lactic-co-glycolic acid) with different ratios of lactic and glycolic [9,11] and polycaprolactone (PCL). In this work we selected polycaprolactone, a FDA-approved polymer used for several biomedical applications, which has attracted attention in bone tissue engineering for its biocompatibility, bioabsorbability and mechanical properties [12]. Particularly in spinal fusion, PCL has demonstrated to yield successful bone fusion and maturation of newly formed bone, in large animal models such as pig [13,14] and sheep [15,16], outperforming bone graft [17,18].

Several techniques are used to process PCL and PCL composites towards achieving optimal performing physicochemical properties for bone applications, such techniques including particulate leaching [19], compressive moulding [20], melt spinning [21], wet spinning [22], electrospinning [23], or fused deposition modeling (FDM) [13] / 3D-printing [24], which yield a pre-fabricated scaffold suitable for implantation. The use of gas and/or supercritical foaming technique and experimental conditions proposed herein, brings the possibility of foam injection, for in situ formation of the 3D porous scaffold. The settled material shall achieve the specific format and dimensions of the osseous defect. Multiple manuscripts have reported different experimental conditions for gas and/or supercritical foaming of PCL, including polymers of several molecular weights and the presence of additives, as detailed in Table 1.

Most of the work refers to supercritical fluid foaming, i.e. conditions in which carbon dioxide was used above its critical parameters of pressure and temperature. There are however two exceptions. Cotugno et al [26] report the foaming of polycaprolactone, in a two-step approach. The polymer is initially molten at temperatures higher than its melting temperature and pressurized with CO_2. Afterwards the system is cooled and, upon depressurization of the system to ambient pressure, the foaming takes place. In this work [26] it is however difficult to assess which experiments are carried out at sub or supercritical conditions as the final pressure, before depressurization is not mentioned. Another work reported in the literature, by Di Maio and co-workers [40] presents several experiments were carried out to foam polycaprolactone in a temperature range from 28 to 45 °C and a pressure range from 2.8 to 5.5 MPa. Although the manuscript presented does not provide extensive morphological characterization of the foams generated, it is possible to conclude that the foams prepared have small pore size diameter in the range of 20–80 μm and a density between 0.05 and 0.25 g/cm^3. The different approaches followed by Di Maio et al [40] aims the understanding of the effect of the operating conditions on the morphology of the scaffolds, but also the thermodynamics underlying

Table 1
Summary of the supercritical fluid studies on foaming of polycaprolactone reported in the literature.

Additives	Operating parameters			Morphological properties		Mechanical properties	
	Pressure range (MPa)	Temperature range (°C)	Molecular weight (Da)	Porosity (%)	Pore size (μm)	Compressive modulus (MPa)	Reference
Talc	6.2	70	–	Data not shown	Data not shown	Data not shown	[25]
	6.9[a]	24–30[b]	80,000	Data not shown	100 Pin > Pc CO_2 450 - 700 P in. < Pc CO_2	Data not shown	[26]
	8.0–16.0	40	85,000	Data not shown	40–160	Data not shown	[27]
Ethanol	12.3–20.5	35–45	80,000	Data not shown	40–80	Data not shown	[28]
	21.0–45.0	20–50	14,000	Data not shown	Data not shown	Data not shown	[29]
Ethyl lactacte	20.0	40–45	80,000	65-80%	50–200	Data not shown	[30–32]
5-fluorouracil, nicotinamide and triflusal	20.0	40	80,000	61-74%	87–337	Data not shown	[33]
NaCl	8.0	50	30–50,000	Data not shown	427	Data not shown	[34]
HA	20.0	37	65,000	~90%	50–70 and 100–300	Data not shown	[35]
	20.0–30.0	40-60	80,000	Data not shown	80–200	Data not shown	[36]
Elastin + NaCl	6.5	70	80,000	70-90 %	200–500	Data not shown	[37]
	7.8–20.0	25-50	69–120, 000	65-90 %	170–350	Data not shown	[38]
	10.0–20.0	30-45	74,000	Data not shown	110–360	Data not shown	[39]
	2.8–5.9	29-45[b]	80,000	Data not shown	80–300	Data not shown	[40]
Mesoporous silica particles Dexamethasone +	14.0–25.0	35	40,000	20–50%	no macroporosity evaluated	20–250	[41]
	8.2	60	70,000	Data not shown	Data not shown	Data not shown	[42]

[a] Psat bewteen 6.9 and 32 MPa.
[b] T sat = 70 °C.

the process. A more applied research has been reported by Annabi [37] and De Matos [41] which relates specifically to the preparation PCL based 3D architectures for tissue engineering and regenerative medicine.

In 2003 David Tomasko and co-workers [43] have highlighted the main constrains of using carbon dioxide as foaming agent claiming that "The challenges of CO_2 as a foaming agent are associated with the higher pressure operation, dimensional instability during the foam-shaping process (…)" [43]. 15 years later, the industry is still reluctant when it comes to high-pressure and supercritical technology. Despite the significant advances at the scale-up and translation from lab to bench scale the perception that working under high pressures and the requirement of sophisticated and expensive equipment, continues to hinder the use of supercritical fluid technologies at a larger scale.

In this work, we evaluated the possibility to prepare 3D scaffolds from polycaprolactone under subcritical carbon dioxide atmosphere. The possibility to use milder processing conditions may open new strategies in bone regeneration, particularly through the development of a portable surgical tool for *in situ* foaming and foam delivery.

2. Materials and methods

2.1. Materials

Poly-ε-caprolactone (PCL) (Mn 45,000 Da and 80,000 Da) in granular form was obtained from Sigma Aldrich and milled to powder using an ultra-centrifugal mill (Retsch ZM200) under liquid nitrogen. β-tricalcium phosphate (β-TCP) (CAS 7758-87-4) and dexamethasone (dex) (CAS50-02-2) were also obtained from Sigma Aldrich. Carbon dioxide (99.998 mol %) was supplied by Air liquid. All reagents were used as received without further purification.

2.2. Subcritical carbon dioxide foaming

The scaffolds were prepared by subcritical carbon dioxide foaming at 5.0 MPa and 45 °C. In each experiment c.a. 500 mg of PCL was loaded in a stainless steel cylindrical mold with 2 cm inner diameter and 1 cm height, which was placed inside the high-pressure vessel (2.5 cm inner diameter, 40 cm height) (Fig. 1). The vessel was heated by means of an electric thin band heater (OGDEN) connected to a temperature controller, which maintained the temperature within ± 1 °C. The system was pressurized with carbon dioxide until the operational pressure was attained inside the vessel, measured with a pressure transducer. The system was closed for two hours to allow the plasticization of the polymer. Afterwards the system was slowly depressurized (depressurization rate ~0.15 MPa/min).

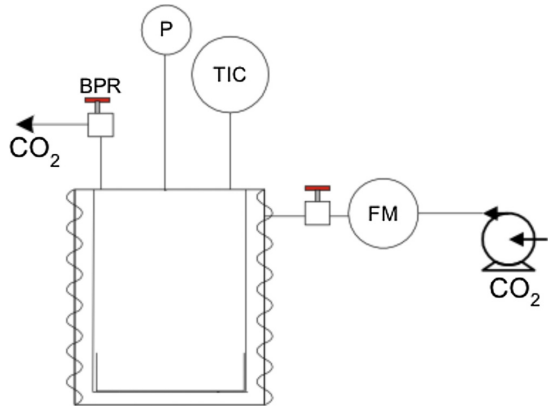

Fig. 1. Schematic representation of the supercritical foaming equipment. BPR: Back Pressure Regulator, P: Pressure Transducer, TIC: Temperature Controller, FM: Flow Meter, CO_2: Carbon Dioxide.

Table 2
Summary of the different formulations prepared in this work (PCL (Mn 45,000 Da) mass was kept constant in all formulations, 500 mg were used).

#	Designation	β-TCP (wt %)	Dexamethasone (wt %)
1	PCL	–	–
2	PCL + β-TCP	10	–
3	PCL + β-TCP + dex5	10	5
4	PCL + β-TCP + dex10	10	10

When β-TCP and dexamethasone were loaded in the 3D construct, they were previously physically mixed with the PCL polymer and afterwards loaded in the mold. The foaming procedure was the same as described above.

A summary of the samples prepared is listed in Table 2:

2.3. Characterization of the 3D structures

2.3.1. Scanning electron microscopy (SEM)

Porous matrices obtained from the different formulations were observed by a Leica Cambridge S360 Scanning Electron Microscope (SEM). Cross sections of the specimens were examined after fracturing in liquid nitrogen. The matrices were fixed by mutual conductive adhesive tape on aluminum stubs and covered with gold palladium using a sputter coater.

2.3.2. Micro-computed tomography (micro-CT)

The morphological structure and the calculation of the morphometric parameters that characterize the samples were evaluated by micro-computed tomography (micro-CT) using a Skyscan 1272 equipment (Bruker, Germany) with penetrative X-rays of 50 KeV and 200 μA, in high-resolution mode with a pixel size of 21.6 μm A CT analyzer (v1.15.4.0, 2012–2015, Bruker Micro-CT) was used to calculate the parameters from the 2D images of the matrices.

2.3.3. Compressive mechanical analysis

Compressive mechanical analysis of the materials produced were measured using an INSTRON 5540 (Instron Int. Ltd, High Wycombe, UK) universal testing machine with a load cell of 1 kN. The scaffolds were cut in cylindrical shape with 5 mm diameter and 4 mm height. Compression testing was carried out at a crosshead speed of 2 mm.min^{-1}, until a maximum reduction in sample weight of 60%. The compressive modulus is defined as the initial linear modulus on the stress/strain curves. The data presented is the result of the average of at least five measurements.

2.4. Water uptake and degradation studies

The water uptake ability of the matrices prepared was assessed for a period up to 14 days. Scaffolds of PCL and PCL + β-TCP prepared by dense gas foaming were weighed and immersed in 5 mL of an isotonic solution (Phosphate Buffered Saline, PBS) at pH = 7.4. The samples were placed in a water bath at 37 °C. After predetermined periods of time (1, 3, 7 and 14 days) the samples were weighed in order to determine the water uptake of the scaffolds.

Water uptake was determined using the following Eq. (1):

$$\%\, water\ uptake\ = \frac{w_w - w_i}{w_i} \times 100 \quad (1)$$

where w_w is the weight of the wet sample and w_i is the weight of the initial sample.

The pH of each solution was also measured in order to determine the effect of polymer degradation on the acidity of the medium.

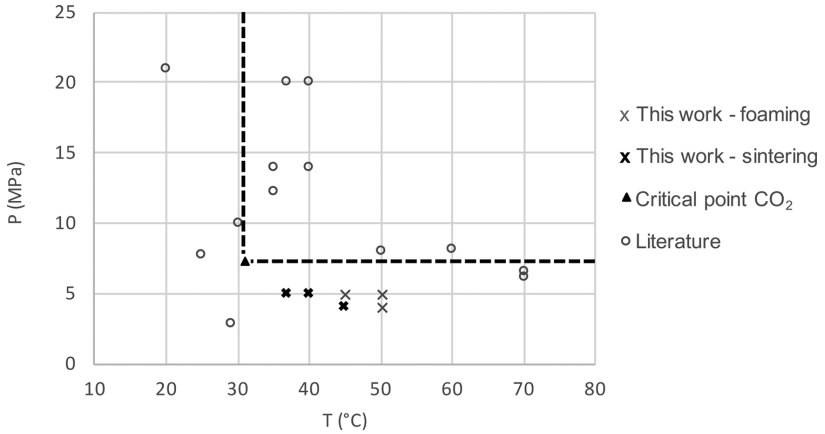

Fig. 2. Schematic representation of processing conditions (pressure and temperature) used in the work reported in the literature (circle symbol) as well as the conditions proposed herein (cross symbol).

After immersion for 28 days the samples were dried at room temperature and weighed to determine the weight loss, which was calculated according to Eq. (2):

$$\%\, weight\ loss = \left| \frac{w_f - w_i}{w_i} \right| \times 100 \quad (2)$$

where w_f is the final weight of the dry sample after immersion and w_i is the initial weight of the sample.

2.5. Drug release studies

In vitro release studies of dexamethasone from PCL foams were performed by incubating the drug-loaded matrices in 20 mL of PBS, at pH 7.4 under horizontal shaking at 37 °C [23,44]. The release was performed in sink conditions. At appropriate time intervals (5 min, 30 min, 1 h, 1.5 h, 2 h, 3 h, 4 h, 6 h, 24 h, 72 h, 7 days, 14 days, 21 days, 34 days), aliquots of 300 µL were withdrawn, and fresh volume of PBS was added to the suspension to replace the sample. The samples were quantified by UV-spectroscopy on a multi-well microplate reader (Synergy HT, Bio-Tek Instruments), using a quartz 96 well-plate. The optical density of dexamethasone was read at 245 nm. The results were presented as an average of three measurements.

2.6. Cytotoxicity studies

An immortalized mouse lung fibroblasts cell line (L929), from European Collection of Cell Cultures, UK, was maintained in basal culture medium DMEM (Dulbecco's modified Eagle's medium; Sigma–Aldrich, Germany), supplemented with 10% FBS (heat-inactivated fetal bovine serum, Biochrom AG, Germany) and 1% A/B (antibiotic–antimycotic solution, Gibco, UK). Confluent L929 cells were harvested, seeded in a 96 well plate at 1×10^3 cells/well using supplemented DMEM medium, and cultured for 24 h. The indirect contact was performed by replacing the culture medium with leachables of the materials. The leachables were obtained after 24 h of extraction using a ratio 100 mg of material in 1 mL supplemented DMEM. The samples were cultured for 48 h under a 5% CO_2 atmosphere at 37 °C, after which cell metabolic activity was determined by the MTS assay (Cell Titer 96 Aqueous One Solution Cell Proliferation Assay (Promega, USA). Absorbance was measured at 490 nm using a microplate reader (Synergie HT, Bio-Tek, USA). Optical density was determined for sample and compared to polystyrene tissue culture plate, used as a negative control and latex extract used as a positive control. All cytotoxicity screening tests were performed using three replicates.

3. Results and discussion

In this work, we have evaluated the possibility to foam polycaprolactone under subcritical carbon dioxide atmosphere. Literature review (Table 1) suggests that successful foaming of this polymer requires conditions above the critical parameters of carbon dioxide and little has been reported in what concerns the use of carbon dioxide at lower P, T conditions. The first variable optimized was the molecular weight of polycaprolactone as gas foaming is highly dependent on the molecular weight of the polymers. In this work, we tested different polycaprolactone polymers, with molecular weights of 45 000 and 80 000 Da. The experiments carried out have shown that under the processing conditions aimed in this study, i.e., below 5.0 MPa and 50 °C, polycaprolactone with a molecular weight of 80 000 Da did not foam. According to literature (Table 1), much higher conditions are required to achieve foaming of PCL 80 000 Da, i.e: pressure up to 20.0 MPa and/or temperatures above the melting temperature of the polymer. On the other hand, PCL 45 000 Da processed under 5.0 MPa and 50 °C could be foamed and was, for this reason, selected to proceed the optimization process. Two different pressures (4.0 and 5.0 MPa) and different temperatures (between 37 to 50 °C) were tested, in order to further optimize the gas foaming process and determine the best operating conditions to prepare a 3D architecture able to meet the requirements set for bone tissue engineering. These experiments were performed with an exposure time of 2 h. Fig. 2 highlights the different set of operating conditions reported in the literature for the foaming of PCL and the ones tested in this work.

At 4.0 MPa and 45 °C, sintering of the particles takes place. Sintering under dense carbon dioxide atmosphere has been reported in the literature and relies on a minor plasticization effect of carbon dioxide [45]. In the experiments performed the polymer particles are fused, but a very fragile structure is obtained. The structure cannot be handled without compromising its integrity. On the other hand, increasing pressure to 5.0 MPa and 37 °C, a homogeneous and robust architecture is obtained, however we can consider that under these conditions still sintering and not foaming occurred. It is only when temperature is increased to 45 °C, with a carbon dioxide pressure of 5.0 MPa that foaming takes place. From the same amount of starting material, the sample prepared at 5.0 MPa and 45 °C has expanded much more than the sample prepared at 37 °C, presenting a larger volume and hence, lower density. From these results, we concluded that the best operating conditions were 45 °C and 5.0 MPa and these were therefore used for further processing of the constructs.

The optimization of the required contact time for plasticization is

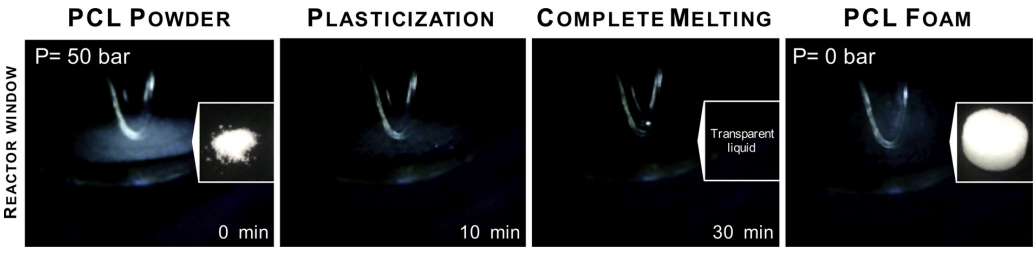

Fig. 3. Effect of time on the plasticization and foaming of polycaprolactone under dense carbon dioxide atmosphere at 45 °C.

another parameter which is crucial for the success of the polymer foaming. The plasticization of polycaprolactone was assessed using a high-pressure visual cell with a sapphire window. Imaging of the process was performed through sequential images which were captured in time lapse mode by computer software controlled program equipped with a Logitech (HD1080 P) camera. Fig. 3 shows selected images of the foaming process as a function of time.

The images demonstrate that upon pressurization of the high-pressure cell, the polymer starts to plasticize after 10 min and after 30 min it is completely in the molten state. In the decompression cycle, it is observed that the foaming occurs in the late stage of decompression of the vessel, when pressure is below 1.0 MPa. These observations are particularly relevant to optimize processing time. Fanovich and co-workers reported visual observations of the gas foaming for the system with polycaprolactone [39] and evaluated the temperature effect at 35 and 40 °C and pressure of 15.0 up to 20.0 MPa. Under these conditions the PCL scaffolds are molten after 30 min in contact with the supercritical fluid. No major differences are observed in terms of the time requested for polymer plasticization/melting either in sub or supercritical conditions. This is particularly true when large differences in CO_2 density are compared. For instance, in our work, the CO_2 density of the gas phase is ~0.104 g/cm^3 (determined using a web computation tool provided by Penn State – Earth and Mineral Sciences Energy Institute), while in the work by Fanovich, CO_2 density used was 0.839 g/cm^3 in the experiments carried out in supercritical conditions (35 °C and 15.0 MPa).

The morphological analysis of the 3D constructs produced was evaluated by scanning electron microscopy and by micro computed tomography. Fig. 4 presents the images from the cross sections observed.

Table 3
Morphological characterization of the scaffolds by microCT.

	PCL	PCL + β- TCP	PCL + β-TCP + 5 dex	PCL + β-TCP + 10 dex	Trabecular bone [47]
Porosity (%)	73	90	98	84	52–96
Pore Interconnectivity (%)	79	97	99	95	–
Mean pore size (μm)	164	383	882	664	450–1310
Density (mm^{-1})	28	54	66	31	7-34
Degree of anisotropy	1.42	1.48	1.38	1.48	1.1–2.38

The scaffolds present a very homogenous architecture with uniform pore distribution in all formulations, as observed by SEM. Differences in pore size and interconnectivity among formulations is evident by SEM images and further confirmed by micro-CT characterization (Table 3). The values of the different morphological parameters were determined by image analysis after micro-computed tomography. The interconnectivity of the scaffold is calculated according to the formula: $I = |(V_{totalpore} - V_{disconnectedpore})/V_{totalpore}| \times 100$, where the volume of the disconnected pore stands for the disconnected pore volume which was defined to be higher than 50 μm. The degree of isotropy is a measure of the 3D symmetry or the presence or absence of preferential alignment of structures along a particular directional axis. Bone is known to be an anisotropic structure and this morphological characteristic of trabecular bone also plays an important role in the mechanical strength of

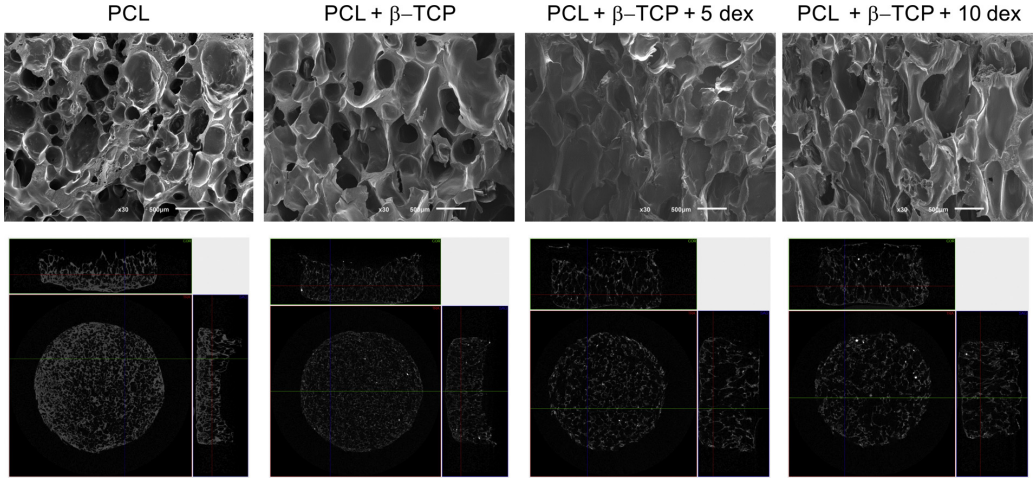

Fig. 4. Scanning electron microscopy (top row, scale bar: 500 μm) and micro-computed tomography images (bottom row) of the different formulations processed at 45 °C and 5.0 MPa.

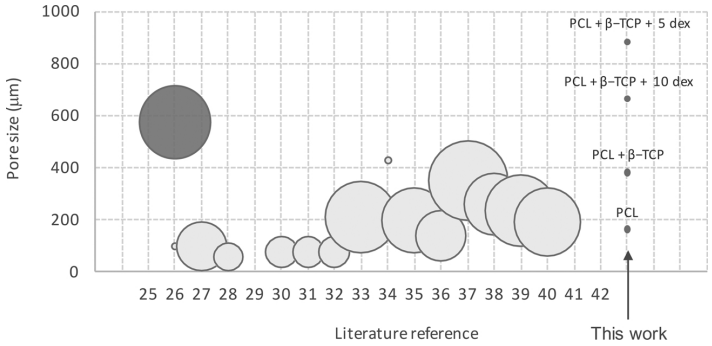

Fig. 5. Comparison of pore size of the PCL foams prepared in the literature (Table 1) and those described in this work (light grey – supercritical foaming conditions; dark grey – subcritical foaming conditions). Circle diameter represent the range of pore size reported in each work.

the architecture produced [46].

In terms of porosity, the values obtained in this work are in accordance with what is reported in the literature (Table 1), which is between 60 and 90%. In some cases, the porosity of the matrices produced is even slightly higher than what has been previously reported. There is one exception, presented by de Matos, that reports porosity values between 20 and 50%. However, the porosity reported was determined by mercury intrusion porosimetry and this may explain the low porosity reported by the authors [41]. Pore size is the parameter which can be compared from a larger set of data. Fig. 5 presents a schematic representation of the pore size distribution of the matrices reported in the literature in comparison to the ones obtained in this work. The size of the bubbles represents the range of pore size obtained at the different conditions employed in each cited work. As it can be observed the pore size is much higher when subcritical P, T conditions are used in the foaming process (dark grey data set), possibly due to a distinct expansion profile of the foam.

Most important however, is the establishment of a comparison with the data from trabecular bone reported in the literature [47]. The morphological analysis of the scaffolds is in very good agreement with this data (Table 3) suggesting that the scaffolds prepared under subcritical carbon dioxide atmosphere can be interesting for bone regeneration applications.

The 3D reconstruction of the structures prepared can also be obtained by micro-computed tomography. Fig. 6 presents the reconstructed 3D architectures of the scaffolds PCL and PCL + β-TCP. This technique also allows the visualization of the distribution of β-TCP within the construct due to the inherently different densities of the polymer and the inorganic/ ceramic part. As it can be observed the foaming with β-TCP particles dispersed renders a uniform dispersion of the ceramic part within the structure.

The mechanical properties of the 3D constructs produced were evaluated in compression mode. For an open cellular material, usually stress-strain curves are characterized by three regions, a linear elastic regime, a plateau and a densification region [48]. Fig. 7 displays a representative image of the deformation that occurs upon loading and a scheme of the typical stress-strain deformation of a porous polymeric structure (“Example”). The elastic regime is characterized as a reversible region where the deformation applied can be reversed, the cell walls bend, but have the ability to fully recover the shape when the load or stress applied is removed. The plateau characteristic of the initial plastic region is a region characterized by the fracture of some cells and the disruption of the structure. If the force continues to be applied a densification region is observed, cell walls collapse and the deformation is irreversible [49].

A closer look at the initial mechanical properties of the two structures (Fig. 7) highlights the fact that both PCL and PCL + β-TCP structures prepared under these operating conditions have a limited elastic and plateau region, and the samples present a plastic behavior typical of elastomeric materials. The elastic regime of both PCL and PCL + β-TCP is limited to up to 1 and 5% strain, respectively. It is hence, in this region that the elastic modulus is determined. The Young modulus calculated from the initial slope of the curve (up to 1% strain) corresponds to 2.97 ± 0.7 MPa and 1.76 ± 0.7 MPa for PCL and PCL + β-TCP, respectively.

De Matos and co-workers report the compressive modulus of composite PCL + mesoporous silica particles scaffolds prepared by supercritical fluid foaming at 35 °C and 14.0 to 25.0 MPa. In their work the reported scaffolds present a compressive modulus of 20–150 MPa [45]. It would perhaps be expected that β-TCP could enhance the mechanical properties of the scaffold, however, the mechanical properties are also strictly connected to the morphological features of the three-dimensional architectures. In our work, the mechanical properties of the scaffolds produced are much lower than those reported by De Matos, but the morphological features are also different, the porosity of the PCL + β-TCP structures herein prepared have a much higher porosity value (90 vs 20–50%) and the content of ceramic filler much lower (10 vs 30 wt%). Hence, the higher porosity, pore size and interconnectivity observed for the PCL + β-TCP may explain this decrease in the Young modulus. Other authors have reported the decrease in mechanical

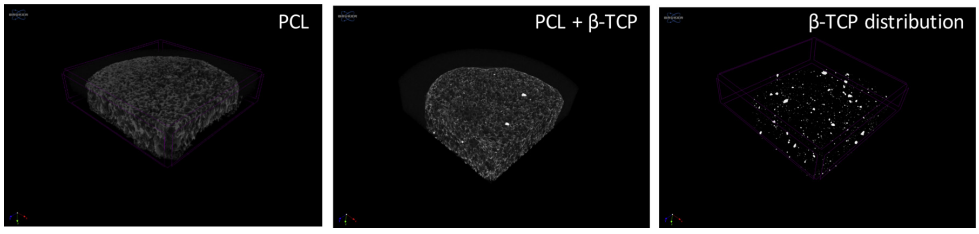

Fig. 6. Micro-computed tomography 3D reconstruction images of the scaffolds produced at 45 °C, 5.0 MPa.

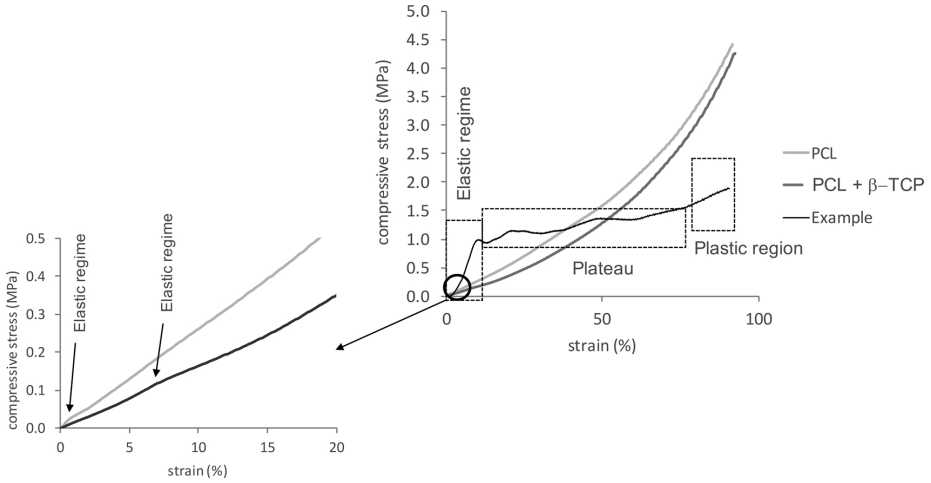

Fig. 7. Strain-stress curves obtained in compression mode for the 3D constructs PCL and PCL + β-TCP, compared with a typical stress-strain curve as Example. Bottom left: A close-up of the elastic regime area.

properties after the addition of hydroxyapatite or bioglass in PCL scaffolds [50–52]. The production of hybrid scaffolds loaded with inorganic fillers has not only the purpose to reinforce the structure but also, and most importantly to create a bioactive structure. The desired scaffold shall result from a fine balance between mechanical properties and bioactivity. Mechanical properties of bone, and particularly those in spine surgery, far exceeds the values herein obtained. Bone has very high mechanical properties which depend greatly on its hierarchical structure. While cortical bone is a compact structure, cancellous bone is composed of irregular, sinuous convolutions of lamellae, and these differences are highly noticeable in the elastic modulus of 0.1 to 0.5 GPa for cancellous bone and 12 to 18 GPa for cortical bone; and a compressive strength situated between 130 and 180 MPa for cortical bone [53]. Chen and co-workers [52] report the development of porous foams as bone augments and grafts, and even though the mechanical properties of the polycaprolactone scaffolds produced are relatively low when compared to cancellous one, the *in vivo* study performed demonstrated a good performance of the scaffolds [52]. It should be highlighted that it is in fact, not only one property but a combination of different features that may offer distinct advantages over other materials, particularly in which concerns the enhancement of bone regeneration. Polymeric scaffolds designed for tissue engineering and regenerative medicine applications have to meet a particular set of requirements, highly tailored towards compatibility and integration with surrounding tissue at implantation site. On what regards morphological properties, scaffolds for bone repair should present open and interconnected pores and adequate pore size, allowing for cell growth and vascularization. Scaffolds should ensure sufficient mechanical strength to withstand the tissue-specific biological forces and maintain cell physical integrity. Adequate surface properties, both chemically and topographically, should promote cell adhesion and proliferation. When working with biodegradable structures, its degradation rate should match the growth rate of the neotissue. Sterilization of the final product should be thought early in scaffold design, so that it will not compromise the structure properties [54–56]. It is, hence, extremely difficult to produce an implant that meets all the ideal criteria. Furthermore, as the characteristics and features of the matrices are related, sometimes the enhancement of one property may compromise another. For all the above, the aim is to develop scaffolds which, despite being far from the optimal conditions, show evidences that may lead to motivating outputs when implanted *in vivo*.

Another important feature, related with the surface properties of the scaffolds prepared is the water uptake ability. The measurement of the water uptake ability provides an indication of the bulk hydrophilicity and thus the susceptibility of the scaffolds to suffer hydrolysis. Furthermore, this feature is also related with the diffusion of nutrients and oxygen to the cells together with the elimination of cell wastes, which occurs in an aqueous environment. Fig. 8(A) presents the water uptake of the PCL and PCL + β-TCP formulations tested. Both formulations present different water uptake abilities, where PCL + β-TCP attains nearly 70% at the first 24 h, reaching 100% by the end of the 2-week time-frame, while PCL foams achieve nearly half water uptake at

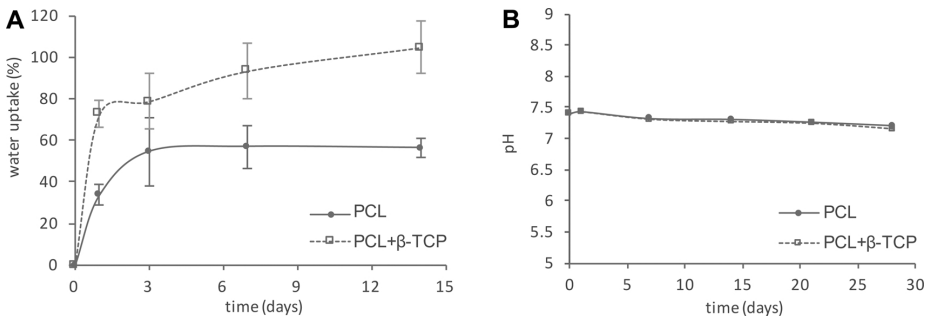

Fig. 8. Water uptake of the scaffolds (A) and pH of the solution (B) as a function of time for the scaffolds PCL (closed symbols) and PCL + β-TCP (open symbols).

same time-points. After 14 days of immersion, the water uptake has reached the plateau region for PCL (at approx. 50%), yet not for PCL + β-TCP, which shall be able to uptake more water at longer time-points. These observations can be justified by the differences observed in the morphological properties of the scaffolds. Larger pores and higher porosity and interconnectivity facilitate water diffusion into the bulk of the sample contributing to an enhancement of the water uptake ability of the scaffold. Additionally, the presence of β-TCP, has been reported to promote higher hydrophilicity of polycaprolactone scaffolds, as described by Zhou and co-workers [57]. One of the concerns when using synthetic polyesters is the possibility of degradation by hydrolysis and production of acidic residues due to the cleavage of the carboxylic groups [21]. For this reason, it is important to follow the pH of the solution in which the scaffolds are immersed. In this work, we have evaluated the changes in pH of a physiological solution throughout 28 days. As it can be seen in Fig. 8(B), the pH of the solution did not change significantly upon the duration of this study. Furthermore, we have quantified the degree of degradation by weight loss and after 28 days, the materials present an average degradation of 1 wt. %, for all samples tested. These results demonstrate the high stability of polycaprolactone scaffolds in physiological solution. It has been recognized that polycaprolactone presents a long degradation time, which in vivo may vary between two and four years, given that its degradation occurs mostly by hydrolytic processes [7,48].

It has long been recognized that scaffolds for tissue engineering should move from a merely inert structure towards a bioactive support, which is able to promote the necessary cues for an improved regeneration process. In addition to a ceramic material, we have evaluated the possibility to homogeneously disperse a second bioactive agent, namely dexamethasone. Dexamethasone was chosen due to the potential of this drug to direct stem cell differentiation towards the osteogenic lineage [58,59]. Two different drug concentrations were evaluated, and as demonstrated by the morphological analysis (Table 2), the presence of both β-TCP and dexamethasone did not compromise the porosity and interconnectivity of PCL scaffolds produced under dense carbon dioxide atmosphere. In fact, a more porous and interconnected structure with larger pores seems to be obtained with this supplementation, which could be the result of distinct expansion profile of the foam. This cause-effect shall be further analyzed in future studies. The morphological differences of each formulation are expected to have an impact on mechanical performance upon application, whereas a fine balance between supplementation of bioactive agents and such mechanical properties shall be achieved. It was found that, for instance addition of β-TCP did not result in augmented young modulus upon compression as compared to non-supplemented PCL, possibly due to the higher porosity and pore size. Nevertheless, its morphology and bioactivity shall offer a more osteoinductive and osteoconductive environment aimed towards improved osteointegration. Pore size and porosity are intimately related with surface area, whereas structures with higher surface area, are more exposed to water molecules which shall lead to faster hydrolytic degradation of the PCL component. These can be fine-tuned in order to reach the best performing structure on what regards matching new bone formation and scaffold degradation rates, as well as controlled release of bioactive agents such as the dexamethasone. The *in vitro* drug release profile was followed up to 35 days in an isotonic physiological solution and the results are presented in Fig. 9.

Dexamethasone was sustainably released from the scaffolds within one month. Up to 24 h there are no relevant differences between the two systems, loaded with 5 or 10 wt% of dexamethasone. The release profile presented a lag time of 2 h before dexamethasone could be detected in the release media. Between 2 and 6 h there is an eventual burst release as the drug concentration in solution increased. From this point onwards, there is a controlled release of the drug from the scaffold. The release profile of both structures presents a parallel trend, suggesting that the mechanisms underlying the release are the same and the differences encountered are only due to the differences in the loaded concentrations. At the end of this study, and as it would be expected, the cumulative amount of dexamethasone in solution is higher for the samples prepared with 10 wt% dex, however, these samples have a slower release rate than the scaffolds impregnated with 5 wt% dex. After 35 days, the scaffolds loaded with 5 wt% have released 100% of the drug impregnated while the scaffolds loaded with 10 wt% have released approximately 75% of the drug.

One of the most important requirements in a scaffold for tissue engineering and regenerative medicine is the biocompatibility of the material. Hence, the cytotoxicity of the materials prepared was evaluated by an indirect contact in which the cells are cultured in the presence of the materials leachables extracted for 24 h. Cell viability determined by MTS assay was determined as a function of the cell viability of the cells cultured with DMEM culture media. The results for the different formulations are presented in Fig. 10.

The results demonstrate that the leachables of the different structures prepared do not compromise the viability and metabolic activity of the cells and hence could be used as scaffolds for tissue engineering applications.

4. Conclusions

In this work, we evaluated the possibility to prepare 3D scaffolds from polycaprolactone under dense subcritical carbon dioxide atmosphere. Processing technologies, carried out to pressures up to 5.0 MPa can encourage the development of new materials, the use of cheaper equipment, eliminating the need for cooling systems, liquid pumps, compressors and all the negative connotation of the “high-pressure” concept without the need to go up to supercritical conditions. Unlike the studies reported in the literature, it was possible to create porous structures without the need to use supercritical condition, i.e pressures below 74 MPa. The structures prepared present interesting morphological and mechanical properties to be used as scaffolds in bone tissue engineering and regenerative medicine and open new perspectives for the treatment of bone defects by *in situ* foaming, through the development of a portable surgical tool. Furthermore, osteoconductive and osteoinductive active agents were incorporated into PCL in a single operating step: β-tricalcium phosphate and dexamethasone were homogeneously dispersed within the PCL matrix. Dexamethasone was released sustainably from the constructs, with a higher delivery rate during the first week of the study, enhancing the functionality of the PCL scaffold. The cytotoxicity of the materials produced was also studied and the different formulations tested did not show any compromise of the cell viability after 48 h of contact. Overall, the results obtained prove that this novel hybrid structure might be a promising approach as a multifunctional template for regenerative medicine applications.

Declarations of interest

None.

Acknowledgments

The research leading to these results has received funding from the European Union Seventh Framework Programme (FP7/2007-2013) under grant agreement number REGPOT-CT2012-316331-POLARIS. It was also funded by the project “Novel smart and biomimetic materials for innovative regenerative medicine approaches” (RL1-ABMR-NORTE-01-0124-FEDER-000016) co-financed by North Portugal Regional Operational Programme (ON.2 – O Novo Norte), under the National Strategic Reference Framework (NSRF), through the European Regional Development Fund (ERDF) and the project NORTE-01-0145-FEDER-000013, supported by the Northern Portugal Regional Operational Programme (NORTE 2020), under the Portugal

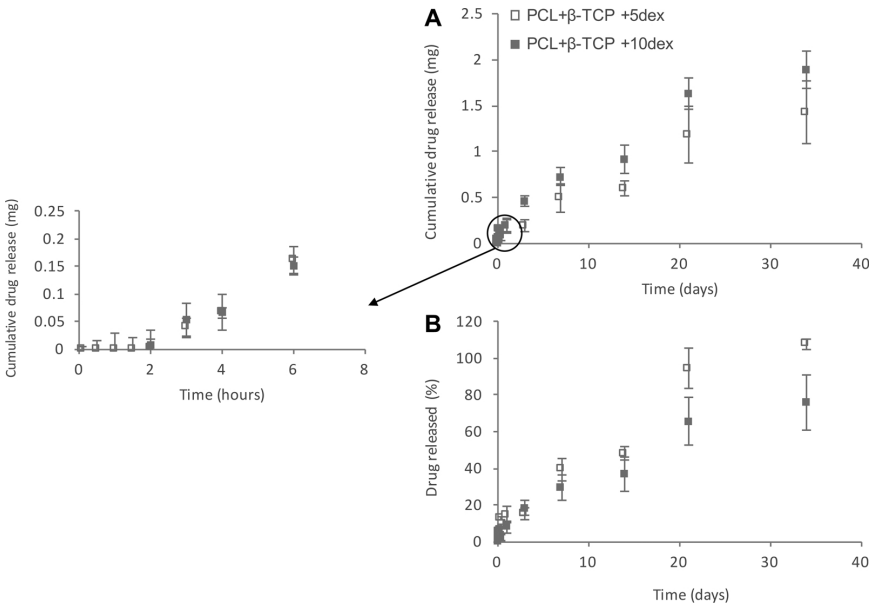

Fig. 9. In vitro release profile of the samples loaded with 5 wt% dex (open symbols) and 10 wt% dex (closed symbols), represented as Cumulative drug released (mg) (A) or Percentage of drug released (%). Bottom left: A close-up of the early time-points.

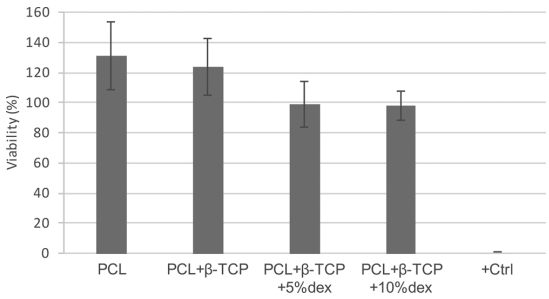

Fig. 10. Cytotoxicity assay: cell viability (%) determined by indirect contact.

2020 Partnership Agreement. The authors would like to acknowledge the funding of the project Associate Laboratory ICVS/3B's, under grant agreement number POCI-01-0145-FEDER-007038 supported by FEDER, through the Competitiveness Factors Operational Programme (COMPETE), and by National funds, through the Foundation for Science and Technology (FCT).

References

[1] D.J. Mooney, D.F. Baldwin, N.P. Suh, J.P. Vacanti, R. Langer, Novel approach to fabricate porous sponges of poly(D,L-lactic-co-glycolic acid) without the use of organic solvents, Biomaterials 17 (1996) 1417–1422, http://dx.doi.org/10.1016/0142-9612(96)87284-X.

[2] A.R.C. Duarte, J.F. Mano, R.L. Reis, Perspectives on: supercritical fluid technology for 3D tissue engineering scaffold applications, J. Bioact. Compat. Polym. 24 (2009) 385–400, http://dx.doi.org/10.1177/0883911509105796.

[3] L.J.M. Jacobs, M.F. Kemmere, J.T.F. Keurentjes, Sustainable polymer foaming using high pressure carbon dioxide: a review on fundamentals, processes and applications, Green Chem. 10 (2008) 731, http://dx.doi.org/10.1039/b801895b.

[4] S.P. Nalawade, F. Picchioni, L.P.B.M. Janssen, Supercritical carbon dioxide as a green solvent for processing polymer melts: processing aspects and applications, Prog. Polym. Sci. 31 (2006) 19–43, http://dx.doi.org/10.1016/j.progpolymsci.2005.08.002.

[5] S.K. Goel, E.J. Beckman, Generation of microcellular polymeric foams using supercritical carbon dioxide. Effect of pressure and temperature on nucleation, Polym. Eng. Sci. 34 (1994) 1137–1147, http://dx.doi.org/10.1002/pen.760341407.

[6] A.I. Cooper, Polymer synthesis and processing using supercritical carbon dioxide, J. Mater. Chem. 10 (2000) 207–234, http://dx.doi.org/10.1039/a906486i.

[7] L.M. Mathieu, M.O. Montjovent, P.E. Bourban, D.P. Pioletti, J.A.E. Månson, Bioresorbable composites prepared by supercritical fluid foaming, J. Biomed. Mater. Res. Part A 75 (2005) 89–97, http://dx.doi.org/10.1002/jbm.a.30385.

[8] G. Georgiou, L. Mathieu, D.P. Pioletti, P.E. Bourban, J.A.E. Månson, J.C. Knowles, S.N. Nazhat, Polylactic acid-phosphate glass composite foams as scaffolds for bone tissue engineering, J. Biomed. Mater. Res. Part B Appl. Biomater. 80 (2007) 322–331, http://dx.doi.org/10.1002/jbm.b.30600.

[9] H. Tai, M.L. Mather, D. Howard, W. Wang, L.J. White, J.A. Crowe, S.P. Morgan, A. Chandra, D.J. Williams, S.M. Howdle, K.M. Shakesheff, Control of pore size and structure of tissue engineering scaffolds produced by supercritical fluid processing, Eur. Cells Mater. 14 (2007) 64–76, http://dx.doi.org/10.22203/eCM.v014a07.

[10] V.E. Santo, A.R.C. Duarte, E.G. Popa, M.E. Gomes, J.F. Mano, R.L. Reis, Enhancement of osteogenic differentiation of human adipose derived stem cells by the controlled release of platelet lysates from hybrid scaffolds produced by supercritical fluid foaming, J. Control. Release 162 (2012) 19–27, http://dx.doi.org/10.1016/j.jconrel.2012.06.001.

[11] K.C. Baker, R. Bellair, M. Manitiu, H.N. Herkowitz, R.M. Kannan, Structure and mechanical properties of supercritical carbon dioxide processed porous resorbable polymer constructs, J. Mech. Behav. Biomed. Mater. 2 (2009) 620–626, http://dx.doi.org/10.1016/j.jmbbm.2008.11.006.

[12] D. Mondal, M. Griffith, S.S. Venkatraman, Polycaprolactone-based biomaterials for tissue engineering and drug delivery: current scenario and challenges, Int. J. Polym. Mater. Polym. Biomater. 65 (2016) 255–265, http://dx.doi.org/10.1080/00914037.2015.1103241.

[13] S.A. Abbah, C.X.L. Lam, D.W. Hutmacher, J.C.H. Goh, H.K. Wong, Biological performance of a polycaprolactone-based scaffold used as fusion cage device in a large animal model of spinal reconstructive surgery, Biomaterials 30 (2009) 5086–5093, http://dx.doi.org/10.1016/j.biomaterials.2009.05.067.

[14] S.A. Abbah, C.X.F. Lam, K.A. Ramruttun, J.C.H. Goh, H.-K. Wong, Autogenous bone marrow stromal cell sheets-loaded mPCL/TCP scaffolds induced osteogenesis in a porcine model of spinal interbody fusion, Tissue Eng. Part A 17 (2011) 809–817, http://dx.doi.org/10.1089/ten.tea.2010.0255.

[15] Y. Li, Z. gang Wu, X. kang Li, Z. Guo, S. hua Wu, Y. quan Zhang, L. Shi, S. hin Teoh, Y. chun Liu, Z. yong Zhang, A polycaprolactone-tricalcium phosphate composite scaffold as an autograft-free spinal fusion cage in a sheep model, Biomaterials 35 (2014) 5647–5659, http://dx.doi.org/10.1016/j.biomaterials.2014.03.075.

[16] M.R.N.O. Yong, S. Saifzadeh, G.N. Askin, R.D. Labrom, D.W. Hutmacher, C.J. Adam, Biological performance of a polycaprolactone-based scaffold plus recombinant human morphogenetic protein-2 (rhBMP-2) in an ovine thoracic interbody fusion model, Eur. Spine J. 23 (2014) 650–657, http://dx.doi.org/10.1007/s00586-013-3085-x.

[17] R.J. Kroeze, T.H. Smit, P.P. Vergroesen, R.A. Bank, R. Stoop, B. van Rietbergen, B.J. van Royen, M.N. Helder, Spinal fusion using adipose stem cells seeded on a radiolucent cage filler: a feasibility study of a single surgical procedure in goats, Eur. Spine J. 24 (2015) 1031–1042, http://dx.doi.org/10.1007/s00586-014-

3696-x.
[18] P.-P.A. Vergroesen, R.-J. Kroeze, M.N. Helder, T.H. Smit, The use of poly(L-lactide-co-caprolactone) as a scaffold for adipose stem cells in bone tissue engineering: application in a spinal fusion model, Macromol. Biosci. 11 (2011) 722–730, http://dx.doi.org/10.1002/mabi.201000433.
[19] R.C. Thomson, M.J. Yaszemski, J.M. Powers, A.G. Mikos, Fabrication of biodegradable polymer scaffolds to engineer trabecular bone, J. Biomater. Sci. Polym. Ed. 7 (1995) 23–38, http://dx.doi.org/10.1163/156856295X00805.
[20] V.M. Correlo, L.F. Boesel, E. Pinho, A.R. Costa-Pinto, M.L. Alves Da Silva, M. Bhattacharya, J.F. Mano, N.M. Neves, R.L. Reis, Melt-based compression-molded scaffolds from chitosan-polyester blends and composites: morphology and mechanical properties, J. Biomed. Mater. Res. Part A 91 (2009) 489–504, http://dx.doi.org/10.1002/jbm.a.32221.
[21] M.E. Gomes, H.S. Azevedo, A.R. Moreira, V. Ellä, M. Kellomäki, R.L. Reis, Starch-poly(epsilon-caprolactone) and starch-poly(lactic acid) fibre-mesh scaffolds for bone tissue engineering applications: structure, mechanical properties and degradation behaviour, J. Tissue Eng. Regen. Med. 2 (2008) 243–252, http://dx.doi.org/10.1002/term.89.
[22] I.B. Leonor, M.T. Rodrigues, M.E. Gomes, R.L. Reis, In situ functionalization of wet-spun fibre meshes for bone tissue engineering, J. Tissue Eng. Regen. Med. 5 (2011) 104–111, http://dx.doi.org/10.1002/term.294.
[23] A. Martins, A.R.C. Duarte, S. Faria, A.P. Marques, R.L. Reis, N.M. Neves, Osteogenic induction of hBMSCs by electrospun scaffolds with dexamethasone release functionality, Biomaterials 31 (2010) 5875–5885, http://dx.doi.org/10.1016/j.biomaterials.2010.04.010.
[24] I.F. Cengiz, M. Pitikakis, L. Cesario, P. Parascandolo, L. Vosilla, G. Viano, J.M. Oliveira, R.L. Reis, Building the basis for patient-specific meniscal scaffolds: from human knee MRI to fabrication of 3D printed scaffolds, Bioprinting 1–2 (2016) 1–10, http://dx.doi.org/10.1016/j.bprint.2016.05.001.
[25] J. Reignier, J. Tatibouët, R. Gendron, Batch foaming of poly(ε{lunate}-caprolactone) using carbon dioxide: impact of crystallization on cell nucleation as probed by ultrasonic measurements, Polym. (Guildf.) 47 (2006) 5012–5024, http://dx.doi.org/10.1016/j.polymer.2006.05.040.
[26] S. Cotugno, E. Di Maio, G. Mensitieri, S. Iannace, G.W. Roberts, R.G. Carbonell, H.B. Hopfenberg, Characterization of microcellular biodegradable polymeric foams produced from supercritical carbon dioxide solutions, Ind. Eng. Chem. Res. 44 (2005) 1795–1803, http://dx.doi.org/10.1021/ie049445c.
[27] Q. Xu, X. Ren, Y. Chang, J. Wang, L. Yu, K. Dean, Generation of microcellular biodegradable polycaprolactone foams in supercritical carbon dioxide, J. Appl. Polym. Sci. 94 (2004) 593–597, http://dx.doi.org/10.1002/app.20726.
[28] I. Tsivintzelis, E. Pavlidou, C. Panayiotou, Biodegradable polymer foams prepared with supercritical CO2-ethanol mixtures as blowing agents, J. Supercrit. Fluids 42 (2007) 265–272, http://dx.doi.org/10.1016/j.supflu.2007.02.009.
[29] E. Kiran, K. Liu, K. Ramsdell, Morphological changes in poly(ε-caprolactone) in dense carbon dioxide, Polym. (Guildf.) 49 (2008) 1853–1859, http://dx.doi.org/10.1016/j.polymer.2008.02.017.
[30] A. Salerno, M.A. Fanovich, C.D. Pascual, The effect of ethyl-lactate and ethyl-acetate plasticizers on PCL and PCL-HA composites foamed with supercritical CO2, J. Supercrit. Fluids 95 (2014) 394–406, http://dx.doi.org/10.1016/j.supflu.2014.10.007.
[31] A. Salerno, E. Di Maio, S. Iannace, P.A. Netti, Solid-state supercritical CO2 foaming of PCL and PCL-HA nano-composite: effect of composition, thermal history and foaming process on foam pore structure, J. Supercrit. Fluids 58 (2011) 158–167, http://dx.doi.org/10.1016/j.supflu.2011.05.009.
[32] A. Salerno, U. Clerici, C. Domingo, Solid-state foaming of biodegradable polyesters by means of supercritical CO2/ethyl lactate mixtures: towards designing advanced materials by means of sustainable processes, Eur. Polym. J. 51 (2014) 1–11, http://dx.doi.org/10.1016/j.eurpolymj.2013.11.015.
[33] A. Salerno, J. Saurina, C. Domingo, Supercritical CO2 foamed polycaprolactone scaffolds for controlled delivery of 5-fluorouracil, nicotinamide and triflusal, Int. J. Pharm. 496 (2015) 654–663, http://dx.doi.org/10.1016/j.ijpharm.2015.11.012.
[34] T.-Y. Bak, M.-S. Kook, S.-C. Jung, B.-H. Kim, Biological effect of gas plasma treatment on CO 2 gas Foaming/Salt leaching fabricated porous polycaprolactone scaffolds in bone tissue engineering, J. Nanomater. 2014 (2014) 1–6, http://dx.doi.org/10.1155/2014/657542.
[35] A. Salerno, S. Zeppetelli, E. Di Maio, S. Iannace, P.A. Netti, Design of bimodal PCL and PCL-HA nanocomposite scaffolds by two step depressurization during solid-state supercritical CO2 foaming, Macromol. Rapid Commun. 32 (2011) 1150–1156, http://dx.doi.org/10.1002/marc.201100119.
[36] E. Markočič, M. Škerget, Ž. Knez, Effect of temperature and pressure on the behavior of poly(ε-caprolactone) in the presence of supercritical carbon dioxide, Ind. Eng. Chem. Res. 52 (2013) 15594–15601, http://dx.doi.org/10.1021/ie402256a.
[37] N. Annabi, A. Fathi, S.M. Mithieux, A.S. Weiss, F. Dehghani, Fabrication of porous PCL/elastin composite scaffolds for tissue engineering applications, J. Supercrit. Fluids 59 (2011) 157–167, http://dx.doi.org/10.1016/j.supflu.2011.06.010.
[38] M. Karimi, M. Heuchel, T. Weigel, M. Schossig, D. Hofmann, A. Lendlein, Formation and size distribution of pores in poly(ε-caprolactone) foams prepared by pressure quenching using supercritical CO2, J. Supercrit. Fluids 61 (2012) 175–190, http://dx.doi.org/10.1016/j.supflu.2011.09.022.
[39] M.A. Fanovich, P. Jaeger, Sorption and diffusion of compressed carbon dioxide in polycaprolactone for the development of porous scaffolds, Mater. Sci. Eng. C 32 (2012) 961–968, http://dx.doi.org/10.1016/j.msec.2012.02.021.
[40] E. Di Maio, G. Mensitieri, S. Iannace, L. Nicolais, W. Li, R.W. Flumerfelt, Structure optimization of polycaprolactone foams by using mixtures of CO2 and N2 as blowing agents, Polym. Eng. Sci. 45 (2005) 432–441, http://dx.doi.org/10.1002/pen.20289.
[41] M.B.C. De Matos, A.P. Piedade, C. Alvarez-Lorenzo, A. Concheiro, M.E.M. Braga, H.C. De Sousa, Dexamethasone-loaded poly(É-caprolactone)/silica nanoparticles composites prepared by supercritical CO2 foaming/mixing and deposition, Int. J. Pharm. 456 (2013) 269–281, http://dx.doi.org/10.1016/j.ijpharm.2013.08.042.
[42] C. Marrazzo, E. Di Maio, S. Iannace, Conventional and nanometric nucleating agents in poly(e-caprolactone) foaming: crystals vs. Bubbles nucleation, Polym. Eng. Sci. 48 (2008) 336–344, http://dx.doi.org/10.1002/pen.20937.
[43] D.L. Tomasko, H. Li, D. Liu, X. Han, M.J. Wingert, L.J. Lee, K.W. Koelling, A review of CO 2 applications in the processing of polymers, Ind. Eng. Chem. Res. 42 (2003) 6431–6456, http://dx.doi.org/10.1021/ie030199z.
[44] A.R.C. Duarte, J.F. Mano, R.L. Reis, Dexamethasone-loaded scaffolds prepared by supercritical-assisted phase inversion, Acta Biomater. 5 (2009) 2054–2062, http://dx.doi.org/10.1016/j.actbio.2009.01.047.
[45] A.R.C. Duarte, V.E. Santo, A. Alves, S.S. Silva, J. Moreira-Silva, T.H. Silva, A.P. Marques, R.A. Sousa, M.E. Gomes, J.F. Mano, R.L. Reis, Unleashing the potential of supercritical fluids for polymer processing in tissue engineering and regenerative medicine, J. Supercrit. Fluids 79 (2013) 177–185, http://dx.doi.org/10.1016/j.supflu.2013.01.004.
[46] A. Odgaard, Three-dimensional methods for quantification of cancellous bone architecture, Bone 20 (1997) 315–328, http://dx.doi.org/10.1016/S8756-3282(97)00007-0.
[47] L.M. Mathieu, T.L. Mueller, P. Bourban, D.P. Pioletti, R. Müller, J.-A.E. Månson, Architecture and properties of anisotropic polymer composite scaffolds for bone tissue engineering, Biomaterials 27 (2006) 905–916, http://dx.doi.org/10.1016/j.biomaterials.2005.07.015.
[48] L.J. Gibson, Biomechanics of cellular solids, J. Biomech. 38 (2005) 377–399, http://dx.doi.org/10.1016/j.jbiomech.2004.09.027.
[49] L.J. Gibson, M.F. Ashby, Cellular Solids: Structure and Properties, (1990), http://dx.doi.org/10.2277/0521499119.
[50] J. Ródenas-Rochina, J.L.G. Ribelles, M. Lebourg, Comparative study of PCL-HAp and PCL-bioglass composite scaffolds for bone tissue engineering, J. Mater. Sci. Mater. Med. 24 (2013) 1293–1308, http://dx.doi.org/10.1007/s10856-013-4878-5.
[51] P.S.P. Poh, D.W. Hutmacher, B.M. Holzapfel, A.K. Solanki, M.M. Stevens, M.A. Woodruff, *In vitro* and *in vivo* bone formation potential of surface calcium phosphate-coated polycaprolactone and polycaprolactone/bioactive glass composite scaffolds, Acta Biomater. 30 (2016) 319–333, http://dx.doi.org/10.1016/j.actbio.2015.11.012.
[52] C. Chen, L. Garber, M. Smoak, C. Fargason, T. Scherr, C. Blackburn, S. Bacchus, M.J. Lopez, J.A. Pojman, F. Del Piero, D.J. Hayes, In vitro and in vivo characterization of pentaerythritol triacrylate-co-trimethylolpropane nanocomposite scaffolds as potential bone augments and grafts, Tissue Eng. Part A 21 (2015) 320–331, http://dx.doi.org/10.1089/ten.tea.2014.0018.
[53] K. Rezwan, Q.Z. Chen, J.J. Blaker, A.R. Boccaccini, Biodegradable and bioactive porous polymer/inorganic composite scaffolds for bone tissue engineering, Biomaterials 27 (2006) 3413–3431, http://dx.doi.org/10.1016/j.biomaterials.2006.01.039.
[54] A.R. Boccaccini, J.A. Roelher, L.L. Hench, V. Maquet, R. Jrme, A composites approach to tissue engineering, Ceram. Eng. Sci. Proc. (2008) 805–816, http://dx.doi.org/10.1002/9780470294758.ch90.
[55] M. Navarro, A. Michiardi, O. Castan, J.A. Planell, Review. biomaterials in orthopaedics, J. R. Soc. Interface 5 (2008) 1137–1158, http://dx.doi.org/10.1098/rsif.2008.0151.
[56] V. Karageorgiou, D. Kaplan, Porosity of 3D biomaterial scaffolds and osteogenesis, Biomaterials 26 (2005) 5474–5491, http://dx.doi.org/10.1016/j.biomaterials.2005.02.002.
[57] Y. Zhou, D.W. Hutmacher, S.L. Varawan, T.M. Lim, In vitro bone engineering based on polycaprolactone and polycaprolactone-tricalcium phosphate composites, Polym. Int. 56 (2007) 333–342, http://dx.doi.org/10.1002/pi.2138.
[58] N. Jaiswal, S.E. Haynesworth, A.I. Caplan, S.P. Bruder, Osteogenic differentiation of purified, culture-expanded human mesenchymal stem cells in vitro, J. Cell. Biochem. 64 (1997) 295–312, http://dx.doi.org/10.1002/(sici)1097-4644(19970264:2<295::aid-jcb12>3.0.co;2-i.
[59] C. Correia, W. Grayson, R. Eton, J.M. Gimble, R.A. Sousa, R.L. Reis, G. Vunjak-Novakovic, Human adipose-derived cells can serve as a single-cell source for the in vitro cultivation of vascularized bone grafts, J. Tissue Eng. Regen. Med. 8 (2014) 629–639, http://dx.doi.org/10.1002/term.1564.

CHAPTER IV

Advancing spinal fusion: interbody stabilization by in situ foaming of a chemically modified polycaprolactone

This chapter is based on the following publication: **Duarte RM**, Correia-Pinto J, Reis RL and Duarte ARC, *Advancing spinal fusion: interbody stabilization by in situ foaming of a chemically modified polycaprolactone;* Journal of Tissue Engineering and Regenerative Medicine (2020) 1–11. DOI: 10.1002/term.3111

Received: 3 December 2019 | Revised: 21 July 2020 | Accepted: 22 July 2020

DOI: 10.1002/term.3111

RESEARCH ARTICLE

WILEY

Advancing spinal fusion: Interbody stabilization by in situ foaming of a chemically modified polycaprolactone

Rui M. Duarte[1,2,3,4] | **Jorge Correia-Pinto**[1,2,3,5] | **Rui L. Reis**[3,6,7] | **Ana Rita C. Duarte**[3,6]

[1]School of Medicine, University of Minho, Campus de Gualtar, Braga, Portugal

[2]Life and Health Sciences Research Institute (ICVS), School of Medicine, University of Minho, Campus de Gualtar, Braga, Portugal

[3]ICVS/3B's—PT Government Associate Laboratory, Braga/Guimarães, Portugal

[4]Orthopedic Surgery Department, Hospital de Braga, Sete Fontes-São Victor, Braga, Portugal

[5]Pediatric Surgery Department, Hospital de Braga, Braga, Portugal

[6]3B's Research Group, I3B's—Research Institute on Biomaterials, Biodegradables and Biomimetics, University of Minho, Headquarters of the European Institute of Excellence in Tissue Engineering and Regenerative Medicine, Guimarães, Portugal

[7]The Discoveries Centre for Regenerative and Precision Medicine, Headquarters at University of Minho, Guimarães, Portugal

Correspondence
Ana Rita C. Duarte, 3B's Research Group, I3B's—Research Institute on Biomaterials, Biodegradables and Biomimetics, University of Minho, Headquarters of the European Institute of Excellence in Tissue Engineering and Regenerative Medicine, Avepark—Parque de Ciência e Tecnologia, Zona Industrial da Gandra, 4805-017 Barco, Guimarães, Portugal.
Email: aduarte@fct.unl.pt

Present Address
Ana Rita C. Duarte, LAQV-REQUIMTE, Chemistry Department, Faculdade de Ciências e Tecnologia, Universidade Nova de Lisboa, 2829-516 Caparica, Portugal.

Funding information
European Regional Development Fund, Grant/Award Numbers: NORTE-01-0145-FEDER-000013, POCI-01-0145-FEDER-007038, RL1-ABMR-NORTE-01-0124-FEDER-000016; European Union Seventh Framework Programme, Grant/Award Number: REGPOT-CT2012-316331-POLARIS

Abstract

Spinal fusion (SF) surgery relies on medical hardware such as screws, cages and rods, complemented by bone graft or substitute, to stabilize the interventioned spine and achieve adequate bone ingrowth. SF is technically demanding, lengthy and expensive. Advances in material science and processing technologies, proposed herein, allowed the development of an adhesive polymeric foam with the potential to dismiss the need for invasive hardware in SF. Herein, 3D foams of polycaprolactone doped with polydopamine and polymethacrylic acid (PCL pDA pMAA) were created. For immediate bone stabilization, in situ hardening of the foam is required; therefore, a portable high-pressure device was developed to allow CO_2 foaming within bone defects. Foams were characterized by scanning electron microscopy, Fourier transform infrared spectroscopy and X-ray photoelectron spectroscopy. Adhesive properties of PCL pDA pMAA outperformed PCL when tested using glass surfaces ($p < 0.001$) or spinal plugs ($p < 0.05$). No cytotoxicity was observed, and bioactivity was confirmed by the CaP layer formed upon 7 days immersion in simulated body fluid. As proof of concept, PCL pDA pMAA was extruded in-between ex vivo porcine vertebrae, and micro-computed tomography revealed similar properties to those of trabecular bone. This novel system presents great promise for instrumentation-free interbody fusion.

KEYWORDS
carbon dioxide foaming, dopamine, polycaprolactone, polymethacrylic acid, spinal fusion, tissue engineering

1 | INTRODUCTION

The design of bone adhesives is one of the most challenging fields in the intersection of polymer and biomedical engineering. Management of some orthopaedic ailments, particularly those related with bone degeneration and trauma, frequently lead to the need for bone defect filling and stabilization towards achievement of bone fusion (R. M. Duarte, Varanda, Reis, Duarte, & Correia-Pinto, 2017; Slevin et al., 2016). In the majority of spinal surgeries, achievement of a solid bone fusion between vertebras is paramount. Bone filling is typically achieved by bone graft or bone graft substitute, whereas stabilization occurs through the use of fixation systems such as screws, cages and rods. Such hardware cause increased damage to surrounding anatomical structures, and material may mechanically fail or migrate (Shillingford et al., 2019; Yilar, 2019). Non-union is also associated to limited bone formation by bone graft or substitutes applied. No technological breakthrough has yet been proposed to substitute such approach.

In orthopaedic clinical practice, one can find synthetic materials used to achieve fixation between interfaces, where bone cements of poly(methyl methacrylate) (PMMA) are chief, yet no adhesive traits can be claimed to these given that fixation occurs essentially through mechanical interlock of the material with the porous bone (Farrar, 2012; Heiss et al., 2006), and biocompatibility issues are a common concern (Farrar, 2012; Heiss et al., 2006). Biologically derived adhesives, such as fibrin glues, show superior adhesiveness, biocompatibility and biodegradation as compared with synthetic solutions, yet their low mechanical properties are more suited for soft tissues (Farrar, 2012; Heiss et al., 2006). Multiple routes are under investigation towards achieving appropriate tissues adhesives, whereas great attention has been given to the 3,4-dihydroxy-L-phenylalanine (DOPA) amino acid found in mussels, for their extraordinary bonding capacity in wet environments and at ambient temperature (Neto et al., 2014). Its analogue dopamine has the ability to self-polymerize, which provides a versatile and easy way to functionalize and coat a large variety of materials, from metals to ceramics and polymers (Lee, Dellatore, Miller, & Messersmith, 2007; Liu, Ai, & Lu, 2014). Not only polydopamine (pDA) enhances the adhesive properties of the material but also may induce bioactivity of the structures, particularly by inducing mineralization of the structure and the formation of a bone-like hydroxyapatite (HA) layer, promoting bone–bone bonding (Mabrouk et al., 2015; Xie, Zhong, Ma, Shuler, & Lim, 2013; Zhang et al., 2014). For instance, the poor bioadhesiveness and biomineralization of polycaprolactone (PCL) can both be reverted by coating with pDA (Choi, Lee, Kim, & Jang, 2016; M. Kim, Kim, Lee, & Jang, 2016). PCL is a biocompatible, bioresorbable polymer (up to 3–4 years (Woodruff & Hutmacher, 2010), FDA approved for several applications in the human body, and widely studied for the preparation of bone implants (Dash & Konkimalla, 2012; Martina & Hutmacher, 2007; Woodruff & Hutmacher, 2010). PCL is an inert material, with such interesting template for rational design of specific chemical modifications towards conferring desired bioactive properties, and therefore explored in this study.

Herein, the authors propose the development of an adhesive polymeric foam by (i) improving the PCL pDA adhesive properties through additional modification with polymethacrylic acid (pMAA) and (ii) achieving in situ foaming through use of carbon dioxide technology. pMAA belongs to the acrylate family of synthetic adhesives. Despite their excellent adhesive properties, the use of these materials has been hindered particularly due to their toxicity. Nonetheless, the possibility to control its concentration in a polymeric blend may overcome biocompatibility issues, while still enhancing the adhesiveness of the matrices, as demonstrated by J. H. Kim, Lim, and Park (2013).

In previous work (R. M. Duarte, Correia-Pinto, Reis, & Duarte, 2018), the authors reported successful carbon dioxide foaming of PCL in subcritical, physiologically friendly conditions (5.0 MPa and 45°C), while incorporating bioactive agents such as dexamethasone and β-tricalcium phosphate (TCP), to aid osteogenesis. The use of CO_2 as a porogen agent has significant advantages over others, namely, the fact that this is a physical foaming agent. No chemical reaction takes place upon foaming, reducing the risk of production of any by-products that may be toxic. On the other hand, CO_2 foaming can be carried out under milder operating conditions due to the ability of CO_2 to act as a plasticizing agent and reduce the glass transition temperature and melting temperature of the polymer. Additionally, the polymer viscosity is also reduced improving the ease of manipulation and allowing an appropriate working time (A. R. C. Duarte, Mano, & Reis, 2009; A. R. C. Duarte et al., 2013; Nalawade, Picchioni, & Janssen, 2006). In this work, it is evaluated not only the possibility to design a new bone adhesive but also the ability to create a porous foam structure which can be directly delivered into the lesion site.

2 | MATERIALS AND METHODS

2.1 | PCL doping with dopamine and pMAA

pDA was grafted on the surface of PCL particles following the reported procedure by M. Kim et al. (2016) and Choi et al. (2016). Briefly, PCL beads (PCL average Mn 45.000, Sigma) were milled to powder using a Ultra Centrifugal Mill (Retsch ZM200) under liquid nitrogen. A solution of 10×10^{-3} M Tris–HCl (CAS 1185-53-1, Sigma) was prepared and the pH adjusted to 8.5, using a sodium hydroxide (CAS 1310-73-2, Fisher Chemical, UK) solution (1 M). Dopamine-hydrochloride (CAS 62-31-7, Sigma) was added to the solution (2 mg/ml) as well as the PCL powder, and the solution was stirred overnight. The change in colour to dark brown indicates that the polymerization took place. The powder was recovered by filtration and dialysed for 3 days in order to eliminate any residual monomer that did not react (Choi et al., 2016; M. Kim et al., 2016). The final samples of PCL pDA were recovered and dried by freeze-drying. Grafting pMAA to PCL pDA powder was carried out in a subsequent step. In the formulation described in this work 20% wt/wt pMAA in respect to PCL pDA was tested. Based on the procedure reported by J. H. Kim et al. (2013), 10 wt% of *N*-(3-dimethylaminopropyl)-*N*′-

ethylcarbodiimide polymer-bound (EDC; EC-No 217-579-2, Sigma) and *N*-hydroxysuccinimide (NHS; CAS 6066-82-6, Sigma) were dissolved in poly(methacrylic acid, sodium salt) (pMAA) solution (CAS 54193-36-1, Sigma). The correspondent amount of PCL pDA was then added, together with 1-ml phosphate-buffered solution (PBS tablets, Sigma). The reaction was allowed to take place for 4 h, after which the samples were precipitated with absolute ethanol (CAS 64-17-5, Panreac) for 12 h. Finally, the monomers that did not react were washed with absolute ethanol, and the sample was left to air dry at room temperature.

2.2 | Scanning electron microscopy

Morphological properties of PCL, PCL pDA and PCL pDA pMAA samples in particulate form were analysed by scanning electron microscopy (SEM; JSM-6010 LV, JEOL, Japan). The samples were fixed by mutual conductive adhesive tape on aluminium stubs and were sputter-coated with gold before analysis.

2.3 | FTIR analysis

Fourier transformed infrared (FTIR) analysis was used to evaluate the chemical modifications of PCL doped with pDA and pMAA and compared with unmodified PCL and its intermediate PCL pDA. The samples were powdered and mixed with potassium bromide, and the mixture was moulded into a transparent pellet using a press (Pike). Spectra were recorded at 32 scans with a resolution of 2 cm^{-1} (Shimadzu-IR Prestige 21).

2.4 | X-ray photoelectron spectroscopy

X-ray photoelectron spectroscopy (XPS) was used to evaluate the surface chemistry of the samples prepared to confirm the doping of PCL with dopamine. The C 1s, O 1s, N 1s, Na 1s and survey spectra were recorded using a Kratos Axis-Supra instrument. Monochromatic X-ray source Al Kα (1486.6 eV) was used for all samples and experiments. The residual vacuum in the analysis chamber was maintained at around 8.5×10^{-9} torr. The samples were fixed to the sample holder with double-sided carbon tape. Charge referencing was done by setting the binding energy of C 1s photo peak at 285.0 eV C 1s hydrocarbon peak. An electron flood gun was employed to minimize surface charging, that is, charge compensation.

2.5 | Mechanical characterization—Adhesion to glass surface

Adhesion tests of the PCL, PCL pDA and PCL pDA pMAA materials were performed in a first approach using a glass substrate, as reported by Neto et al. 2014). A contact area of 20 × 25 mm was employed. The powder was dispersed in a glass plate so that the area of contact was covered upon melting, which took place at 60°C in a heating plate. The two glass substrates were superimposed and maintained until solidification of the material. The bonded glass slides were placed on a universal testing machine with a load cell of 1 kN (INSTRON 5540, Instron Int. Lda, High Wycombe, UK) in tensile mode and a crosshead speed of 2 mm/min was applied. The load was applied until detachment, which was confirmed by the graphic. The lap shear bonding strength was determined from the maximum of the force–deformation curve obtained. The results are presented as the average of at least three samples.

2.6 | Cytotoxicity studies

The cytotoxicity evaluation was performed in accordance with ISO 10993-5:2009 guidelines (International Organization for Standardization, 2009). The L929 cell line (ECACC, UK) was maintained in basal culture medium (DMEM; Sigma-Aldrich, Germany), supplemented with 10% heat-inactivated fetal bovine serum (FBS; Biochrom AG, Germany) and 1% A/B (antibiotic–antimycotic solution, Gibco, UK). Confluent L929 cells were harvested and seeded in a 96-well plate (BD Biosciences, USA). Briefly, 100 μl of cell suspension with a concentration of 1×10^4 cells per millilitre were added to the well. The materials' leachables were obtained after 24 h of extraction (5% CO_2, 37°C) using a ratio 100 mg of material in 1-ml supplemented DMEM, according to ISO 10993-12:2004 (International Organization for Standardization, 2004). A latex extract was used as positive control for cell death, and for negative control, cell culture medium was used. The samples were cultured for 24 h, and cell metabolic activity was evaluated by the MTS assay (CellTiter 96® AQueous One Solution, Promega, USA). The formazan product was quantified reading the absorbance at 490 nm (Synergy HT, Bio-Tek Instruments, USA). The results are presented as a function of the negative control and correspond to the average of at least three measurements (±standard deviation).

2.7 | Development of a portable high-pressure extrusion device

A dedicated portable high-pressure device was designed for in situ polymer foaming. Herein, a stainless-steel (316SS) reactor was built in order to withstand up to 120 bar pressure, 100°C temperature and up to 4-ml volume, ensuring a sterile extruded foam while safe and user-friendly in a surgery room. The high-pressure device includes a mechanical piston for complete extrusion of material upon depressurization of the high-pressure chamber, through a thin tip for controlled application of the porous foam.

2.8 | In situ foaming of PCL pDA pMAA into ex vivo IVD space

In situ foaming of the polymer through the high-pressure device was tested by using ex vivo porcine vertebrae. The intervertebral disc (IVD) was removed and vertebrae surfaces debrided by the aid of a surgical curette. Briefly, 1 g of PCL pDA pMAA powder was loaded into the high-pressure chamber, which was then sealed and pressurized with carbon dioxide at 50 bar (Air Liquide, 99.998 mol %). As control, same amount of PCL pDA pMAA powder was loaded into a standard 5-ml plastic syringe and maintained at ambient pressure. Both devices were heated up to 60°C in a water bath to promote the plasticization of the polymer, and after 15 min of settling time under these conditions, the polymers were extruded into the defect sites. Once the system is ready for delivery, the tip of the device is placed at lesion site so that, once the chamber is open, depressurization drives the piston inwards the chamber, which per se allows extrusion of the foam into the lesion. Upon depressurization carbon dioxide suffers a sudden drop in temperature, characteristic of the Joule–Thomson effect. In this sense, after depressurization, the temperature of the polymer also decreases significantly, promoting the hardening of the polymer within less than a minute. On the other hand, the polymer extruded through the syringe does not suffer such drastic temperature drop and is still in the molten state in the lesion site, solidifying after few minutes.

2.9 | Mechanical characterization—Adhesion in-between spinal plugs

Ex vivo porcine spinal plugs (6 × 6 × 15 mm) were prepared from adjacent vertebrae. The IVD was removed and vertebrae surfaces debrided by the aid of a bone curette. Extruded PCL formulations were applied in-between spinal plugs. The shear bond strength test was performed with a crosshead speed of 2 mm/min until complete fracture or detachment of the specimens (Neto et al., 2014). The maximum force (N) was recorded on a computer and divided by the bonded area (in mm^2) in order to calculate the bond strength (N/cm^2). The fractures were observed under a stereomicroscope (STEMI 1000, ZEISS). The results are presented as the average of at least three samples.

2.10 | Micro-computed tomography

The morphological structure and the calculation of the morphometric parameters that characterize the 3D extruded foams were evaluated by micro-computed tomography (micro-CT) using a Skyscan 1272 equipment (Bruker, Germany) with penetrative X-rays of 50 keV and 200 μA, in high-resolution mode with a pixel size of 21.6 μm. A CT analyser (v1.15.4.0, 2012-2015, Bruker Micro-CT) was used to calculate the parameters from the 2D images of the matrices.

2.11 | Bioactivity studies

To evaluate the bioactivity of PCL pDA pMAA, samples extruded through the high-pressure device (approximately 15 mg) were soaked in 10 ml of simulated body fluid (SBF) solution during 1, 3, 7 and 14 days at 37°C. The SBF was prepared by dissolving NaCl, $NaHCO_3$, KCl, $K_2HPO_4.3H_2O$, $MgCl_2.6H_2O$ and Na_2SO_4 in distilled water and buffered with tris(hydroxymethyl)aminomethane buffer and HCl to reach a pH value of 7.4, following the protocol described by Kokubo and Takadama (2006). All chemicals were purchased from Sigma-Aldrich, and the tests were carried out in sterile conditions. Upon removal from SBF, the samples were rinsed with sterile distilled water and air-dried before further analysis. PCL samples were used as control.

2.12 | SEM coupled with EDS

The morphology and composition of the CaPs deposited on the surface of the matrices was investigated with a JSM-6010 LV, JEOL microscope with an integrated energy-dispersive X-ray spectroscope (EDS; INCAx-Act, PentaFET Precision, Oxford Instruments). To perform SEM, a conductive gold coating was applied to the samples. For EDS, the analyses were conducted at low vacuum and without any coating.

2.13 | X-ray diffraction analysis

X-ray diffraction analysis (XRD) was used to evaluate the crystalline planes of the CaPs precipitated on the surface of the samples. The XRD diffraction patterns were collected on a Bruker D8 Discover, at a voltage of 40 kV and a current of 40 mA in a $2q$ range from 10° to 60° with a step size of 0.02°.

2.14 | Statistical analysis

Statistical analysis was performed using GraphPad Prism 7.03 for Windows. Normality was evaluated after Shapiro–Wilk test. When data follows a normal distribution, one-way ANOVA followed by Tukey test was used.

3 | RESULTS

In this work, a two-step approach was followed for the functionalization of PCL with pDA and pMAA. SEM images (Figure 1) show the morphological appearance of the pure PCL powder, the intermediate PCL powder modified with pDA and the final formulation composed of PCL pDA pMAA. At a higher magnification image, difference in roughness was most visible with the pDA and pMAA modification. Chemical analysis of the polymers was carried out by

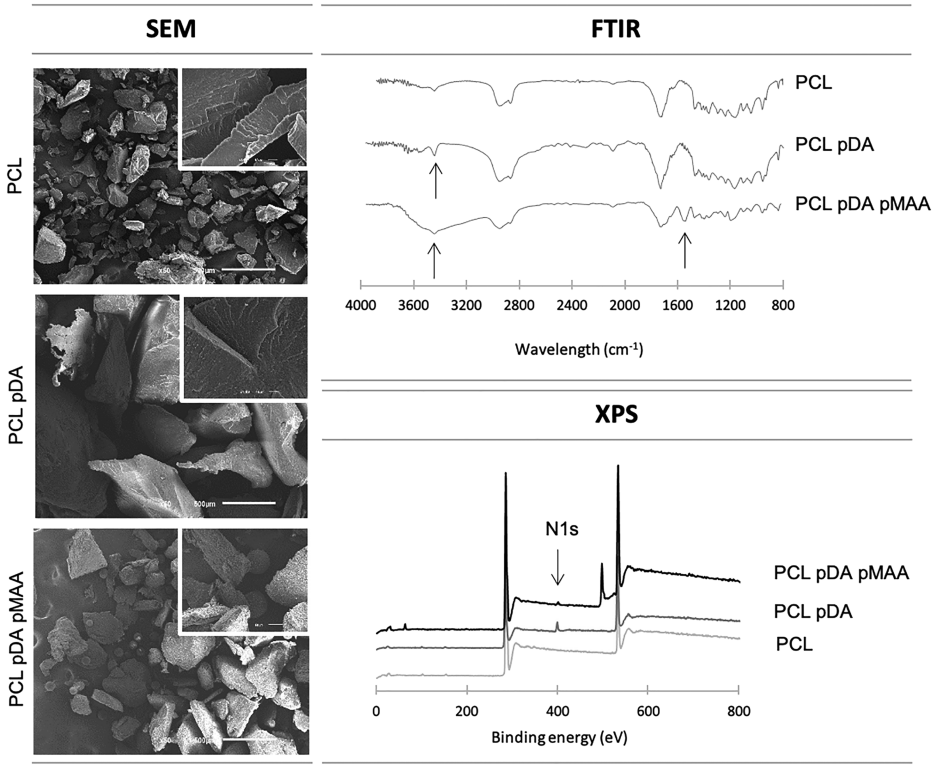

FIGURE 1 Morphological appearance of PCL, PCL pDA and PCL pDA pMAA analysed by scanning electron microscopy (SEM; scale bars 500 μm [main image] and 10 μm [insert image]) and confirmation of chemical modification of the samples by Fourier transformed infrared (FTIR) and X-ray photoelectron spectroscopy (XPS)

FTIR and XPS (Figure 1). By FTIR, it is possible to observe, as indicated by the arrows in the figure, the characteristic peak of the amine N–H stretching group in pDA at 3,440 cm^{-1} (Li et al., 2015). The presence of a single band indicates that the secondary amine has reacted with PCL and a primary amine is present in the PCL pDA formulation. This is consistent with the information reported in the literature, namely, on the description of the chemical reaction involved between dopamine and different substrates at pH 8.5 and Tris solution (B. H. Kim et al., 2011; Liu et al., 2014). When pMAA is grafted, the amine group of dopamine may react with the carboxylic group of methacrylic acid and an amide is possibly formed. These observations are supported by the appearance of the characteristic bands of N–H bending of the amide II band at 1,550–1,510 cm^{-1} and the N–H stretch at 3,500–3,400 cm^{-1}. The successful doping of PCL with pDA was further confirmed by XPS. Surface analysis has shown that there was indeed a modification of the surface chemistry proven by the presence of the peak at 400.2 eV of the N 1s peak, which is absent in the case of pure PCL (M. Kim et al., 2016).

The adhesive properties of the novel materials were characterized by mechanical testing. In a first approach, the adhesive properties were tested in a glass surface (Figure 2). Two glass plates were glued with the different materials and were subjected to a tensile force to evaluate the maximum load at detachment. Figure 2a represents the load applied versus the extension and as can be observed, both PCL pDA and PCL pDA pMAA present similar behaviour and higher adhesive properties than PCL itself. Both pDA modified samples present maximum load before detachment between 200 and 300 N, whereas highest values were observed for the PCL pDA (265 N load).

The adhesion strength can be determined from the maximum load taking into consideration the surface area (Figure 2b). PCL presents an adhesive strength of 0.074 (±0.02) N/cm^2, PCL pDA of 16.2 (±2.4) N/cm^2 and PCL pDA pMAA of 13.7 (±0.6) N/cm^2. These results provide evidences that modifying PCL with pDA and pDA plus methacrylic acid significantly enhances the mechanical properties of the polymer, particularly the adhesive properties of PCL ($p < 0.001$). The differences in adhesion strength between PCL pDA and PCL pDA pMAA are, however, not significantly different. Adhesion properties were further evaluated using bone tissue (ex vivo spinal plugs) and extruded polymer foam.

To achieve such in situ foaming, a safe and user-friendly portable high-pressure device was developed based on the principles of gas foaming and extrusion (Figure 3a). Such device was built, optimized to guarantee optimal performance in the surgical procedure, namely, outlet length and diameter, as well as spatiotemporal control of foam exit. Extruded foams and nonextruded materials were tested for cytotoxicity. Biocompatibility was assessed by the MTS assay, according to the

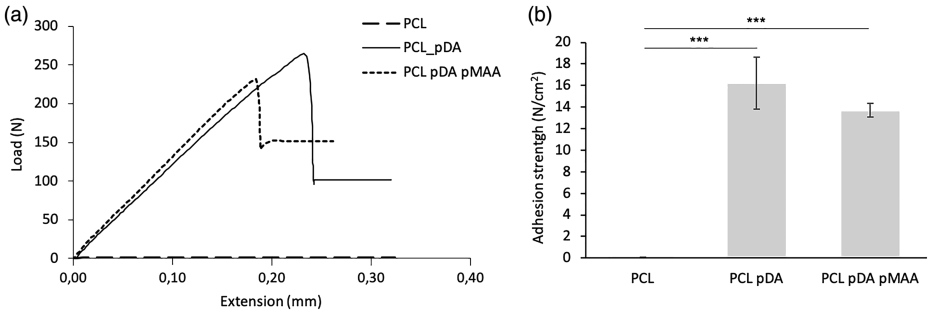

FIGURE 2 Adhesion testing on glass surface. (a) Force versus displacement curve for the different samples studied and (b) adhesion strength for the different samples studied, $^{***}p < 0.001$

protocol described in the ISO 10993-5:2009 (International Organization for Standardization, 2009). Extracts of the different formulations were tested, and the viability was determined as a function of the negative control (Figure 3b). None of the formulations are cytotoxic, once viability is above 70% in all groups. PCL pDA pMAA before and after extrusion presents distinct effect on cell viability (72.36% and 85.28%, respectively), whereas the final form of the biomaterial after extrusion presents a more favourable cellular response ($p = 0.0003$), possibly due to a purification effect by CO_2, where nonreacted monomers were eventually removed by the CO_2.

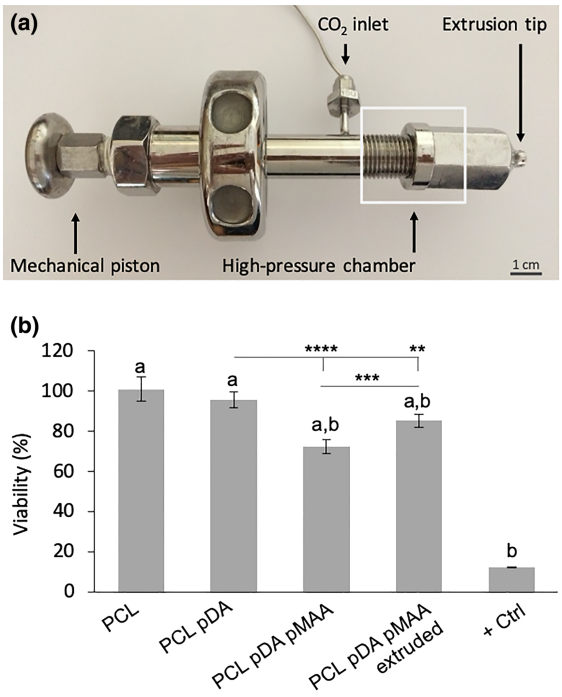

FIGURE 3 (a) Picture of portable high-pressure device built for in situ foaming. (b) Viability data obtained from culture of L929 cell line with the materials' extracts: *a*, $p < 0.0001$ versus Positive Ctrl; *b*, $p < 0.0001$ versus PCL, $^{****}p < 0.0001$, $^{***}p = 0.0003$, $^{**}p = 0.0037$ [Colour figure can be viewed at wileyonlinelibrary.com]

Using this device, the adhesive strength of extruded PCL, PCL pDA and PCL pDA pMAA was then evaluated in spinal plugs, cut with a regular geometry (Figure 4). As observed in Figure 4a,b, PCL pDA pMAA presents higher adhesive properties than nonmodified PCL ($p < 0.05$). After tensile testing, PCL and PCL pDA materials detached from one of the bone interfaces (Figure 4c,d), whereas the PCL pDA pMAA maintained fully adhered (Figure 4e). PCL pDA pMAA material–bone interface remained intact at both ends after testing, whereas breaking site occurred at bone vertebra (yellow arrow; Figure 4e).

In order to mimic the anterolateral surgical approach for lumbar interbody fusion, PCL pDA pMAA was extruded through the high-pressure portable device into a defect created in the IVD space of an ex vivo porcine spine (Figure 5). Extrusion of the polymer within the lesion boundaries happened in a controlled manner, and hardening of the foam occurred within few seconds allowing immediate stabilization of the vertebrae. A similar behaviour was observed for PCL pDA pMAA extruded via standard syringe (control group); however, the solidification is not immediate. The solidified structures were taken from the defect site, and the morphological parameters were analysed by micro-CT. Figure 5 presents the three axial cross-sections of both samples. The sample injected through the syringe (Figure 5a) is highly compact and presents residual porosity and no interconnectivity. On the other hand, the sample extruded through the high-pressure device (Figure 5b) presents an interesting morphological profile, which is comparable to trabecular bone (Mathieu et al., 2006; Table 1). To the best of our knowledge, it is herein described a successful approach for the in situ foaming of polymers for bone defect filling.

The bioactive properties of PCL pDA pMAA were evaluated in a SBF, and PCL samples were used as a control. The samples were extruded through the device in the conditions described above (60°C and 50 bar). Figure 6 presents the SEM images of the materials after immersion as well as the chemical characterization of the CaPs precipitated on the surface, carried out by EDS and XRD.

SEM images demonstrate the presence of precipitated CaPs on the surface of the materials as early as Day 1 and a layer-like structure at Days 7 and 14. PCL samples, used as control, did not show presence of any crystals as reported in the literature (Poh et al., 2016). This confirms the hypothesis that pDA not only provides adhesive

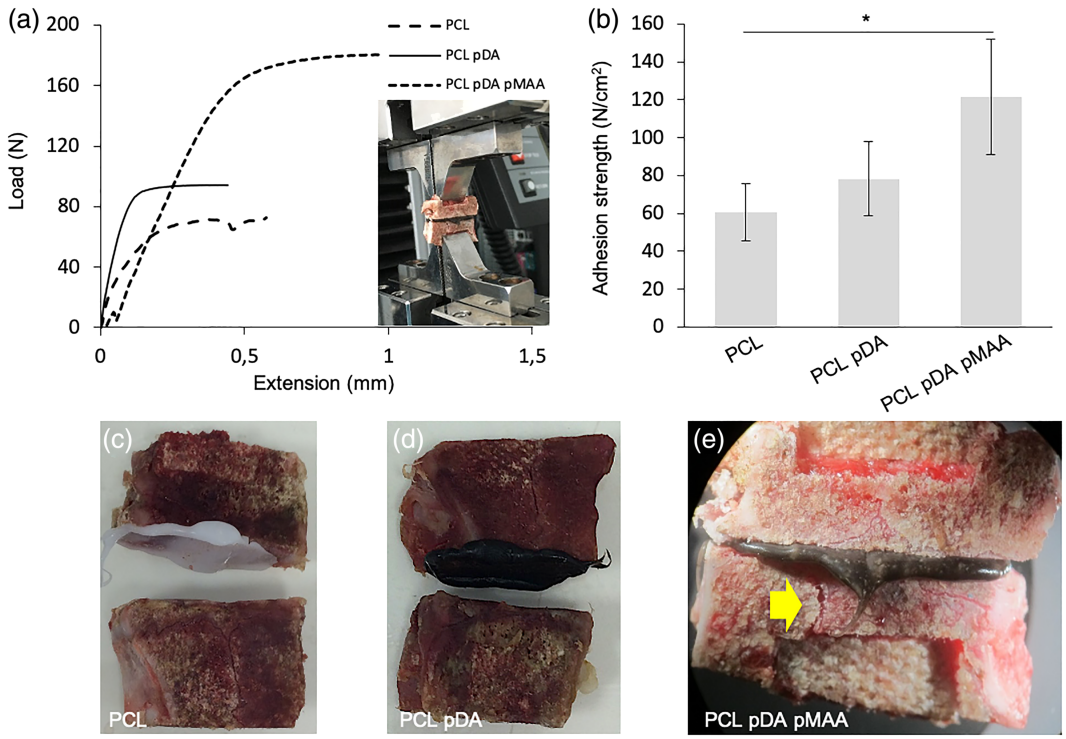

FIGURE 4 Adhesion testing of the three formulations on ex vivo spinal plugs. (a) Force versus displacement curve and photograph of sample under testing, (b) adhesion strength ($^{*}p < 0.05$) and (c–e) macroscopic pictures of spinal plugs with different formulations after tensile testing. Yellow arrow points to site of fracture [Colour figure can be viewed at wileyonlinelibrary.com]

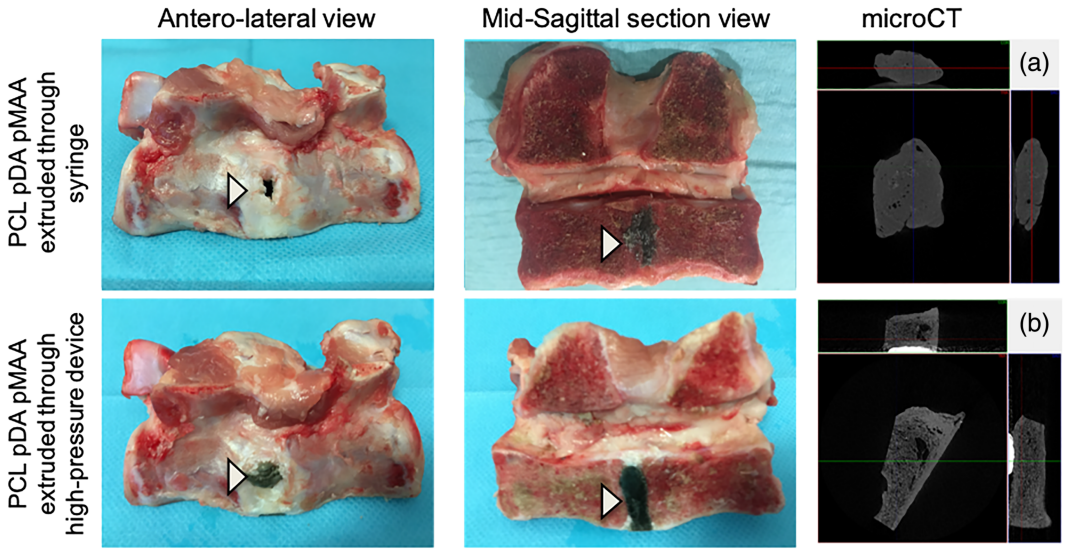

FIGURE 5 Ex vivo testing of anterolateral surgical technique in a porcine spine and micro-computerized tomography cross-section images (a and b) of the samples. Top row: PCL pDA pMAA extruded through a syringe; bottom row: PCL pDA pMAA extruded through the portable high-pressure device into the intervertebral disc space. Material indicated by arrow-head [Colour figure can be viewed at wileyonlinelibrary.com]

TABLE 1 Morphological parameters of the samples extruded into the intervertebral disc space, determined by micro-computed tomography (micro-CT)

	PCL pDA pMAA extruded by syringe	PCL pDA pMAA extruded by high-pressure device	Reference values for trabecular bone (Mathieu et al., 2006)
Porosity (%)	3	45	52–96
Interconnectivity (%)	-	28	-
Mean pore size (μm)	-	169	450–1,310
Density (mm^{-1})	2	17	7–34
Degree of anisotropy	2	2.06	1.1–2.38

analysis confirmed the formation of a partially crystalline HA layer. The figure also highlights the main diffraction peak characteristic of HA at 2θ = 32° (contribution of the (211), (112) and (300) planes of apatite), and in addition, it is visible that another characteristic peak of the CaP layer formed at 2θ = 22.9°, which corresponds to the (111) diffraction peak.

4 | DISCUSSION

PCL pDA pMAA bone adhesive was developed in this study achieving strong bone–bone attachment when challenged in-between ex vivo porcine spinal plugs (Figure 4). The modification of the PCL-based material has been successfully proven by the chemical analysis performed, which is consistent with the work reported by other authors

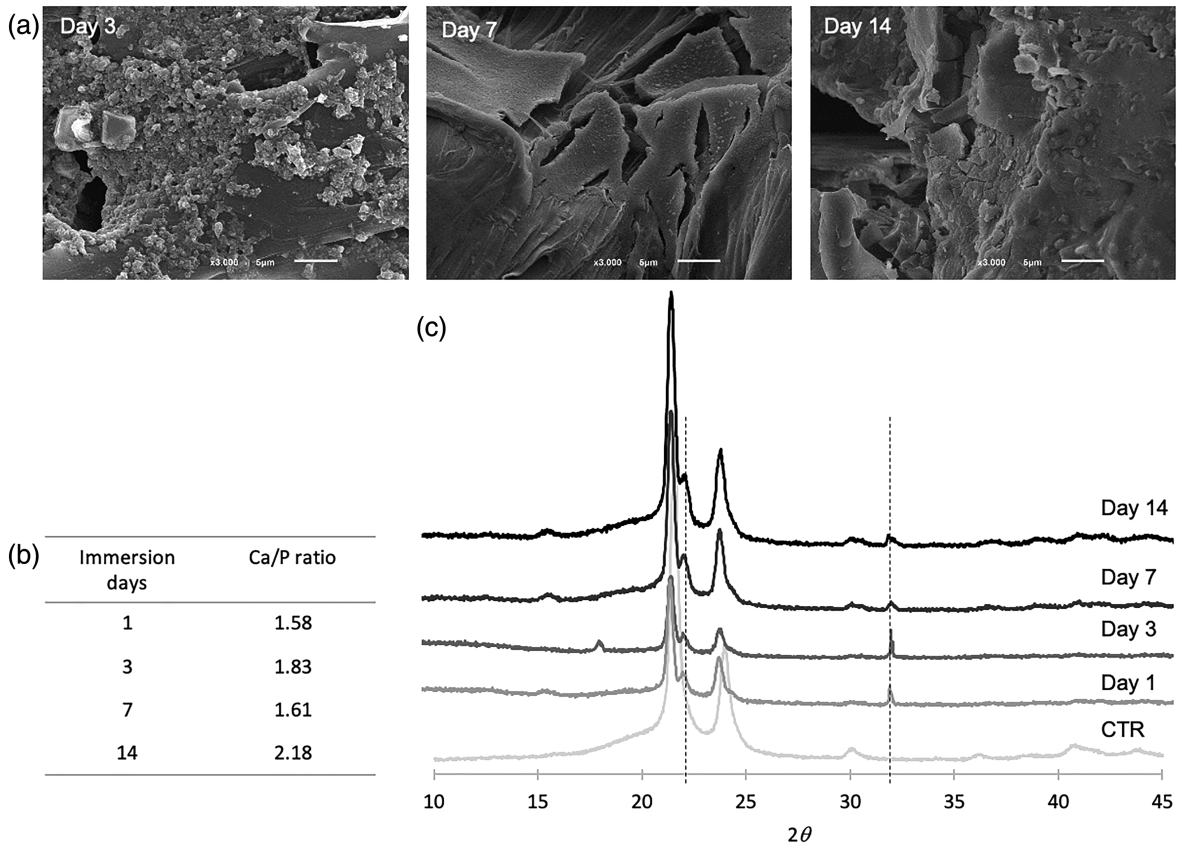

FIGURE 6 (a) Scanning electron microscopy (SEM) images of PCL pDA pMAA immersed in simulated body fluid (SBF) solution at different time points (scale bar: 5 μm), (b) Ca/P atomic ratio calculated from the energy-dispersive X-ray spectroscope (EDS) data and (c) X-ray diffraction analysis (XRD) spectra of PCL pDA pMAA immersed at different time points, compared with PCL as control (CTR)

properties to PCL but also seems to induce some degree of mineralization of the structures. The results of the EDS analysis demonstrate that there may be different CaPs present on the layer and XRD

who followed similar strategy to confer adhesive properties to PCL microspheres (M. Kim et al., 2016). As compared with other bone adhesives (Farrar, 2012; Shah & Meislin, 2013), the proposed PCL

pDA pMAA formulation revealed to have adequate adhesive properties (Figure 4), to be noncytotoxic (Figure 3b) and bioactive (Figure 6). The adhesion strength obtained for the new PCL pDA pMAA to the compact bone surfaces (121.53 ± 30.0 N/cm^2) is threefold to fourfold superior than values reported for the PMMA bone cement currently used in orthopaedics practice for implant fixation (35 N/cm^2 on compact bone; Farrar, 2012) Other approaches have reached similar levels of adhesion by pretreating bone and/or using intermediate bonding material (Farrar, 2012). In addition to enhanced adhesion, the system proposed herein offers a biocompatible, bioabsorbable and mechanically relevant backbone to sustain bone ingrowth (Manavitehrani et al., 2016; Mogosanu et al., 2014). The development of porous and interconnected structures from PCL has been explored through various different techniques (Dash & Konkimalla, 2012). In this work, a portable high-pressure device was developed for in situ polymer foaming based on the principles of gas foaming and extrusion. Carbon dioxide (CO_2) foaming can be carried out under milder operating conditions due to the ability of CO_2 to act as a plasticizing agent and reduce the glass transition temperature and melting temperature of the polymer. Additionally, the polymer viscosity is also reduced improving the ease of manipulation and allowing an appropriate working time (A. R. C. Duarte et al., 2009, 2013; Nalawade et al., 2006). Following the same principle, extrusion using CO_2 has become particularly interesting for the development of porous structures in a continuous mode; however, its potential has not been fully explored as large quantities of raw materials are usually required in an extruder (Matuana & Diaz, 2010; Sauceau, Fages, Common, Nikitine, & Rodier, 2011). Curia, De Focatiis, and Howdle (2015) have demonstrated the effect of CO_2 on melting temperature depression and the viscosity reduction of PCL under different operating conditions. Their work shows that PCL (Mw 10,000) pressurized with 50 bar suffers a decrease in melting temperature of nearly 10°C and a reduction in viscosity of nearly 50% comparing with its value at the same temperature at ambient pressure. As opposed to the implantation of a premanufactured 3D scaffold, in situ foaming of the proposed PCL pDA pMAA allows foam impregnation and adherence to bone before hardening, resulting in immediate stabilization of osseous structures. Such approach circumvents the use of any additional instrumentation for bone stabilization. In addition, while the foam is injected in-between osseous structures, it adapts to defect geometry and volume, resulting in optimal filling of the defect. Herein, a dedicated surgical tool was developed to deliver the adhesive foam into bone defects (Figure 3a). This tool functions as a portable reactor, where specific pressure, temperature and volume (previously validated in the static reactor) are created to generate the foam. Such porous foam was successfully achieved (Figure 5) while maintaining adhesion properties (Figure 4).

Typical functionalization of PCL for bone applications include reinforcement with a mineral component such as β-TCP (Abbah, Lam, Hutmacher, Goh, & Wong, 2009; Abbah, Lam, Ramruttun, Goh, & Wong, 2011b), or CaP with or without further addition with BMP-2 (Abbah, Lam, Ramruttun, Goh, & Wong, 2011a; Yong et al., 2014), yet herein, the combination of pDA and pMAA provided the adhesive properties to PCL, while simultaneously inducing mineralization of the structure (Figure 6). In a previous work, the authors have successfully incorporated dexamethasone and TCP via carbon dioxide foaming of PCL, which could be added to the formulation to further improve osteogenesis (R. M. Duarte et al., 2018). This ability to induce the formation of a bone-like HA layer has been reported to be a factor that strongly enhances the integration of the scaffold with the bone tissue and therefore pivotal for a successful healing and tissue regeneration (El-Ghannam & Ducheyne, 2011; Hill, 2011). SBF, which contains ion concentration similar to those of human blood plasma, is a standard in vitro tool used to test formation of such apatite layer on the surface of materials and therefore assess their bone-bonding bioactivity (Kokubo & Takadama, 2006). Xie et al. (2013) have previously reported the biomineralization of PCL fibres prepared by electrospinning and coated with pDA. In their work, a 10× concentrated solution of SBF was used resulting in deposition of crystals on the surface of the fibres immediately after 1 h. However, such a concentrated solution does not mimic the in vivo physiological environment. Mabrouk et al. (2015) prepared PCL-based microspheres coated with pDA and observed that in a normal SBF solution, the rate of CaP deposition is much slower than in the work of Xie et al. (2013), whereas only after 21 days of immersion, a CaP layer was visible. In the case of the samples prepared in the present work, after 1 day of immersion, some crystals are visible, whereas a layer-like structure starts to be formed at Days 7 and 14. Such layer is composed of different CaPs that can tend to a more stable HA layer at longer immersion time points.

5 | CONCLUSION

To the best of our knowledge, the new PCL pDA pMAA biopolymer, foamed through the dedicated portable high-pressure device directly into a bone defect, is pioneer in achieving immediate stabilization of osseous components, while resulting in a 3D structure with morphological properties similar to those found in trabecular bone. This PCL-based biopolymer was synthesized to achieve improved bioactive and adhesive properties aiming application as bone adhesive for diverse trauma and pathology-driven needs in bone surgery. The system composed of the adhesive polymer and the in situ foaming device opens a promising route towards instrumentation-free spinal fusion.

ACKNOWLEDGEMENTS

The research leading to these results has received funding from the European Union Seventh Framework Programme (FP7/2007-2013) under the grant REGPOT-CT2012-316331-POLARIS; the project 'Novel smart and biomimetic materials for innovative regenerative medicine approaches' (RL1-ABMR-NORTE-01-0124-FEDER-000016) cofinanced by North Portugal Regional Operational Programme (ON.2—O Novo Norte), under the National Strategic Reference Framework (NSRF), through the European Regional Development Fund (ERDF); and the project NORTE-01-0145-FEDER-000013,

supported by the Northern Portugal Regional Operational Programme (NORTE 2020), under the Portugal 2020 Partnership Agreement. The authors would like to acknowledge the funding of the project Associate Laboratory, under grant agreement number POCI-01-0145-FEDER-007038.

CONFLICT OF INTEREST

The authors confirm that there are no known conflicts of interest associated with this publication and there has been no significant financial support for this work that could have influenced its outcome.

ORCID

Rui M. Duarte https://orcid.org/0000-0002-7714-3865
Jorge Correia-Pinto https://orcid.org/0000-0002-9265-6896
Rui L. Reis https://orcid.org/0000-0002-4295-6129
Ana Rita C. Duarte https://orcid.org/0000-0003-0800-0112

REFERENCES

Abbah, S. A., Lam, C. X. F., Ramruttun, A. K., Goh, J. C. H., & Wong, H. K. (2011a). Fusion performance of low-dose recombinant human bone morphogenetic protein 2 and bone marrow-derived multipotent stromal cells in biodegradable scaffolds: A comparative study in a large animal model of anterior lumbar interbody fusion. *Spine*, *36*(21), 1752–1759. https://doi.org/10.1097/BRS.0b013e31822576a4

Abbah, S. A., Lam, C. X. F., Ramruttun, K. A., Goh, J. C. H., & Wong, H.-K. (2011b). Autogenous bone marrow stromal cell sheets-loaded mPCL/-TCP scaffolds induced osteogenesis in a porcine model of spinal interbody fusion. *Tissue Engineering Part A*, *17*(5–6), 809–817. https://doi.org/10.1089/ten.tea.2010.0255

Abbah, S. A., Lam, C. X. L., Hutmacher, D. W., Goh, J. C. H., & Wong, H. K. (2009). Biological performance of a polycaprolactone-based scaffold used as fusion cage device in a large animal model of spinal reconstructive surgery. *Biomaterials*, *30*(28), 5086–5093. https://doi.org/10.1016/j.biomaterials.2009.05.067

Choi, W., Lee, S., Kim, S. H., & Jang, J. H. (2016). Polydopamine inter-fiber networks: New strategy for producing rigid, sticky, 3D fluffy electrospun fibrous polycaprolactone sponges. *Macromolecular Bioscience*, *16*, 824–835. https://doi.org/10.1002/mabi.201500375

Curia, S., De Focatiis, D. S. A., & Howdle, S. M. (2015). High-pressure rheological analysis of CO_2-induced melting point depression and viscosity reduction of poly(ε-caprolactone). *Polymer (United Kingdom)*, *69*, 17–24. https://doi.org/10.1016/j.polymer.2015.05.026

Dash, T. K., & Konkimalla, V. B. (2012). Poly-e-caprolactone based formulations for drug delivery and tissue engineering: A review. *Journal of Controlled Release*, *158*(1), 15–33. https://doi.org/10.1016/j.jconrel.2011.09.064

Duarte, A. R. C., Mano, J. F., & Reis, R. L. (2009). Perspectives on: Supercritical fluid technology for 3D tissue engineering scaffold applications. *Journal of Bioactive and Compatible Polymers*, *24*(4), 385–400. https://doi.org/10.1177/0883911509105796

Duarte, A. R. C., Santo, V. E., Alves, A., Silva, S. S., Moreira-Silva, J., Silva, T. H., … Reis, R. L. (2013). Unleashing the potential of supercritical fluids for polymer processing in tissue engineering and regenerative medicine. *The Journal of Supercritical Fluids*, *79*, 177–185. https://doi.org/10.1016/j.supflu.2013.01.004

Duarte, R. M., Correia-Pinto, J., Reis, R. L., & Duarte, A. R. C. (2018). Subcritical carbon dioxide foaming of polycaprolactone for bone tissue regeneration. *The Journal of Supercritical Fluids*, *140*, 1–10. https://doi.org/10.1016/j.supflu.2018.05.019

Duarte, R. M., Varanda, P., Reis, R. L., Duarte, A. R. C., & Correia-Pinto, J. (2017). Biomaterials and bioactive agents in spinal fusion. *Tissue Engineering Part B: Reviews*, *23*(6), 540–551. https://doi.org/10.1089/ten.teb.2017.0072

El-Ghannam, A., & Ducheyne, P. (2011). 1.109—Bioactive ceramics. In *Comprehensive biomaterials* (pp. 157–179). Netherlands: Elsevier Ltd. https://doi.org/10.1016/B978-0-08-055294-1.00021-0

Farrar, D. F. (2012). Bone adhesives for trauma surgery: A review of challenges and developments. *International Journal of Adhesion and Adhesives*, *33*, 89–97. https://doi.org/10.1016/j.ijadhadh.2011.11.009

Heiss, C., Kraus, R., Schluckebier, D., Stiller, A. C., Wenisch, S., & Schnettler, R. (2006). Bone adhesives in trauma and orthopedic surgery. *European Journal of Trauma.*, *32*, 141–148. https://doi.org/10.1007/s00068-006-6040-2

Hill, R. G. (2011). 1.110—Bioactive glass-ceramics. In *Comprehensive biomaterials* (pp. 181–186). Netherlands: Elsevier Ltd. https://doi.org/10.1016/B978-0-08-055294-1.00022-2

International Organization for Standardization. (2004). Biological evaluation of medical devices—Part 12: Sample preparation and reference materials. ISO 10993-12.

International Organization for Standardization. (2009). Biological evaluation of medical devices—Part 5: Tests for in vitro cytotoxicity. ISO 10993-5.

Kim, B. H., Lee, D. H., Kim, J. Y., Shin, D. O., Jeong, H. Y., Hong, S., … Kim, S. O. (2011). Mussel-inspired block copolymer lithography for low surface energy materials of Teflon, graphene, and gold. *Advanced Materials*, *23*(47), 5618–5622. https://doi.org/10.1002/adma.201103650

Kim, J. H., Lim, J. I., & Park, H. K. (2013). Porous chitosan-based adhesive patch filled with poly(L-3,4-dihydroxyphenylalanine) as a transdermal drug-delivery system. *Journal of Porous Materials*, *20*(1), 177–182. https://doi.org/10.1007/s10934-012-9587-9

Kim, M., Kim, J. S., Lee, H., & Jang, J. H. (2016). Polydopamine-decorated sticky, water-friendly, biodegradable polycaprolactone cell carriers. *Macromolecular Bioscience*, *16*(5), 738–747. https://doi.org/10.1002/mabi.201500432

Kokubo, T., & Takadama, H. (2006). How useful is SBF in predicting in vivo bone bioactivity? *Biomaterials*, *27*(15), 2907–2915. https://doi.org/10.1016/j.biomaterials.2006.01.017

Lee, H., Dellatore, S. M., Miller, W. M., & Messersmith, P. B. (2007). Mussel-inspired surface chemistry for multifunctional coatings. *Science*, *318*(5849), 426–430. https://doi.org/10.1126/science.1147241

Li, C., Zhan, Y., He, L., Chen, Z., Ji, W., Su, W., & Wu, B. (2015). Antibacterial activity materials via electrospun poly(ε-caprolactone) nanofibers containing very few silver nanoparticles on the surface. *Journal of Computational and Theoretical Nanoscience*, *12*(9), 2639–2642. https://doi.org/10.1166/jctn.2015.4155

Liu, Y., Ai, K., & Lu, L. (2014). Polydopamine and its derivative materials: Synthesis and promising applications in energy, environmental, and biomedical fields. *Chemical Reviews*, *114*(9), 5057–5115. https://doi.org/10.1021/cr400407a

Mabrouk, M., Bijukumar, D., Mulla, J. A. S., Chejara, D. R., Badhe, R. V., Choonara, Y. E., … Pillay, V. (2015). Enhancement of the biomineralization and cellular adhesivity of polycaprolactone-based hollow porous microspheres via dopamine bio-activation for tissue engineering applications. *Materials Letters*, *161*, 503–507. https://doi.org/10.1016/j.matlet.2015.08.146

Manavitehrani, I., Fathi, A., Badr, H., Daly, S., Shirazi, A. N., & Dehghani, F. (2016). Biomedical applications of biodegradable polyesters. *Polymers*, *8*, 20. https://doi.org/10.3390/polym8010020

Martina, M., & Hutmacher, D. W. (2007). Biodegradable polymers applied in tissue engineering research: A review. *Polymer International*, *56*(2), 145–157. https://doi.org/10.1002/pi.2108

Mathieu, L. M., Mueller, T. L., Bourban, P., Pioletti, D. P., Müller, R., & Månson, J.-A. E. (2006). Architecture and properties of anisotropic polymer composite scaffolds for bone tissue engineering. *Biomaterials*, *27*(6), 905–916. https://doi.org/10.1016/j.biomaterials.2005.07.015

Matuana, L. M., & Diaz, C. A. (2010). Study of cell nucleation in microcellular poly(lactic acid) foamed with supercritical CO_2 through a continuous-extrusion process. *Industrial and Engineering Chemistry Research*, *49*(5), 2186–2193. https://doi.org/10.1021/ie9011694

Mogosanu, D., Giol, E., Vandenhaute, M., Dragusin, D., Samal, S., & Dubruel, P. (2014). Polyester biomaterials for regenerative medicine. In S. Cao, & H. Zhu (Eds.), *Frontiers in biomaterials: The design, synthetic strategies and biocompatibility of polymer scaffolds for biomedical application* (p. 155). eBook: Bentham Science Publishers Ltd.

Nalawade, S. P., Picchioni, F., & Janssen, L. P. B. M. (2006). Supercritical carbon dioxide as a green solvent for processing polymer melts: Processing aspects and applications. *Progress in Polymer Science (Oxford)*, *31*(1), 19–43. https://doi.org/10.1016/j.progpolymsci.2005.08.002

Neto, A. I., Cibrão, A. C., Correia, C. R., Carvalho, R. R., Luz, G. M., Ferrer, G. G., … Mano, J. F. (2014). Nanostructured polymeric coatings based on chitosan and dopamine-modified hyaluronic acid for biomedical applications. *Small*, *10*, 2459–2469. https://doi.org/10.1002/smll.201303568

Poh, P. S. P., Hutmacher, D. W., Holzapfel, B. M., Solanki, A. K., Stevens, M. M., & Woodruff, M. A. (2016). In vitro and in vivo bone formation potential of surface calcium phosphate-coated polycaprolactone and polycaprolactone/bioactive glass composite scaffolds. *Acta Biomaterialia*, *30*, 319–333. https://doi.org/10.1016/j.actbio.2015.11.012

Sauceau, M., Fages, J., Common, A., Nikitine, C., & Rodier, E. (2011). New challenges in polymer foaming: A review of extrusion processes assisted by supercritical carbon dioxide. *Progress in Polymer Science (Oxford)*, *36*(6), 749–766. https://doi.org/10.1016/j.progpolymsci.2010.12.004

Shah, N. V., & Meislin, R. (2013). Current state and use of biological adhesives in orthopedic surgery. *Orthopedics*, *36*(12), 945–956. https://doi.org/10.3928/01477447-20131120-09

Shillingford, J. N., Laratta, J. L., Sarpong, N. O., Alrabaa, R. G., Cerpa, M. K., Lehman, R. A., … Fischer, C. R. (2019). Instrumentation complication rates following spine surgery: A report from the Scoliosis Research Society (SRS) morbidity and mortality database. *Journal of Spine Surgery.*, *5*, 110–115. https://doi.org/10.21037/jss.2018.12.09

Slevin, O., Ayeni, O. R., Hinterwimmer, S., Tischer, T., Feucht, M. J., & Hirschmann, M. T. (2016). The role of bone void fillers in medial opening wedge high tibial osteotomy: A systematic review. *Knee Surgery, Sports Traumatology, Arthroscopy*, *24*(11), 3584–3598. https://doi.org/10.1007/s00167-016-4297-5

Woodruff, M. A., & Hutmacher, D. W. (2010). The return of a forgotten polymer—Polycaprolactone in the 21st century. *Progress in Polymer Science (Oxford)*, *35*(10), 1217–1256. https://doi.org/10.1016/j.progpolymsci.2010.04.002

Xie, J., Zhong, S., Ma, B., Shuler, F. D., & Lim, C. T. (2013). Controlled biomineralization of electrospun poly(ε-caprolactone) fibers to enhance their mechanical properties. *Acta Biomaterialia*, *9*(3), 5698–5707. https://doi.org/10.1016/j.actbio.2012.10.042

Yilar, S. (2019). Comparison of the accuracy of cannulated pedicle screw versus conventional pedicle screw in the treatment of adolescent idiopathic scoliosis: A randomized retrospective study. *Medicine*, *98*, e14811. https://doi.org/10.1097/MD.0000000000014811

Yong, M. R. N. O., Saifzadeh, S., Askin, G. N., Labrom, R. D., Hutmacher, D. W., & Adam, C. J. (2014). Biological performance of a polycaprolactone-based scaffold plus recombinant human morphogenetic protein-2 (rhBMP-2) in an ovine thoracic interbody fusion model. *European Spine Journal*, *23*(3), 650–657. https://doi.org/10.1007/s00586-013-3085-x

Zhang, D., George, O. J., Petersen, K. M., Jimenez-Vergara, A. C., Hahn, M. S., & Grunlan, M. A. (2014). A bioactive "self-fitting" shape memory polymer scaffold with potential to treat cranio-maxillo facial bone defects. *Acta Biomaterialia*, *10*(11), 4597–4605. https://doi.org/10.1016/j.actbio.2014.07.020

How to cite this article: Duarte RM, Correia-Pinto J, Reis RL, Duarte ARC. Advancing spinal fusion: Interbody stabilization by in situ foaming of a chemically modified polycaprolactone. *J Tissue Eng Regen Med*. 2020;1–11. https://doi.org/10.1002/term.3111

CHAPTER V

Biologic Lumbar Interbody Fusion (BIOLIF): instrumentation-free spinal fusion in a porcine model

This chapter is based on the following manuscript: **Duarte RM**, Miranda A, Carneiro V, da Silva Morais A, Oliveira T, Reis RL, Duarte ARC, Correia-Pinto J, *Biologic Lumbar Interbody Fusion (BIOLIF): instrumentation-free spinal fusion in a porcine model; submitted.*

Abstract

Medical hardware is required to ensure adequate spine stability and intervertebral spacing in Spinal Fusion (SF) surgery. Such instrumentation inevitably impacts healthy surrounding anatomical structures; material may fail or migrate; and neurological damage can occur if material is misplaced. An adhesive, structural, osteoconductive and biodegradable foam, applied by a minimally invasive approach, is proposed in this study as an alternative to spinal hardware.

Assess *in vivo* performance of a biologic approach for lumbar interbody fusion (BIOLIF) by *in situ* foaming and hardening of a new polycaprolactone grafted with polydopamine and polymethacrylic acid (PCL pDA pMAA). This foam shall maintain disc height and provide an adequate osteoconductive environment for bone ingrowth and interbody fusion.

Adult domestic pigs underwent single level anterolateral lumbar interbody fusion using the non-instrumented BIOLIF approach (n=5) or PEEK cage with bone autograft and instrumentation (n=3) as positive control. Animals were sacrificed 6 months after surgical intervention. Animal mobility was assessed during immediate post-op period. Lumbar spine radiologic imaging was performed during follow-up (0, 6 months). Spinal fusion and spinal alignment were scored through radiological imaging. Range of motion (ROM) and stiffness was quantified by non-destructive biomechanical testing and bone ingrowth was assessed by micro-computed tomography and histological analysis.

Minimally invasive *in situ* foaming of PCL pDA pMAA (BIOLIF) was technically feasible, leading to reduced surgical time ($p<0.05$). Animals in BIOLIF approach demonstrated no surgical complications and a higher mobility ($p<0.05$) at immediate post-op. Increased spinal stiffness and reduced ROM was equivalent in both groups, and a significantly higher bone volume was observed in BIOLIF approach ($p<0.05$) at termination.

The BIOLIF approach may drive a possible paradigm-shift for certain lumbar spinal fusion surgeries by avoiding use of surgical hardware.

1. INTRODUCTION

Spinal fusion surgery has evolved remarkably over the last century, with three main technical and technological breakthroughs: initially in 1911 [1], autologous graft was implemented as a fundamental agent in promoting spinal fusion; later in the 1960s the work developed by Roy-Camille [2] demonstrated fusion rate improvement through the use of fixation devices (pedicle screws), by which spinal stability was achievable. Pedicle screw fixation represents a landmark in the field of spinal surgery. Most recently, in the 1980s with the introduction of interbody spacers by Bagby and Kuslich (titanium cages) [3] a new disruptive step was taken in the field of spinal fusion. Since then, over the last 30 years, technological developments have been centered at improving accuracy of hardware placement, as well as functionality and integration of such hardware, through design, fixation capacity and specific coating properties [4–6].

However, two main problems subsist: fusion rate and hardware related complications. Application of fixation systems cause increased damage to surrounding tissues (vertebrae, muscle, ligaments), material may fail or migrate, and neurological damage can occur if material is misplaced [7,8]. Spinal fusion failure is also associated to limited bone formation by bone graft or substitutes applied [8]. No technological breakthrough has yet been proposed to overcome these limitations. Herein, a biological interbody fusion material (BIOLIF) is proposed as an injectable, structural, adhesive, and biodegradable foam, for immediate interbody fixation and spatial filling, while providing a chemical and physical setting supportive of bone ingrowth. BIOLIF consists of polycaprolactone doped with polydopamine and polymethacrylic acid (PCL pDA pMAA), foamed *in situ* by extrusion, using a dedicated portable surgical device, where carbon dioxide functions as the porogen agent and plasticizer. It has demonstrated its technological traits in previous *in vitro* and *ex vivo* studies [9]**:** i) *in situ* foaming and hardening of the polymer led to immediate stabilization of the vertebra, avoiding instrumentation; ii) a Ca-P layer was formed *in vitro* upon immersion of the foam in simulated body fluid, whereas such attribute may stimulate bone formation *in vivo* by native cells or *ex vivo* processed cells; iii) the extruded foam proved non-cytotoxic according to established ISO 10993-5 evaluation.

These preclinical results on both safety and performance of the BIOLIF approach supported further investigations in a large animal model. Polycaprolactone (PCL), FDA-approved for several biomedical applications, has attracted attention in tissue engineering for its biocompatibility, bioabsorbability and mechanical properties [10]. Specifically in spinal fusion, PCL-based systems have resulted in consistent interbody fusion in several experimental conditions, when tested in large animal models such as the pig [11–13] and sheep [14,15]. In these studies, instrumentation of the spine with standard screws and

rods were used for immediate stabilization. The porcine spine, as per its anatomical similarity to the human spine [16], biomechanical characteristics [17] and reported performance in previous spinal fusion experiments [11–13], was deemed suitable for the purposes of the present study. Herein, a anterolateral lumbar interbody fusion procedure was conducted in the adult domestic pig, with high fidelity to the standard approach in humans, in order to evaluate: 1) surgical feasibility; 2) interbody bone fusion upon 6 months of implantation; 3) no adverse biological effects or reactions to the full BIOLIF intervention.

2. Materials and Methods

2.1. BIOLIF foam synthesis and delivery device

The PCL pDA pMAA BIOLIF foam composition was prepared by grafting polycaprolactone (PCL) with dopamine (pDA) and polymethacrylic acid (pMAA) as described in our previous work [9]. Briefly, the grafting was carried out in a two-step approach, first reacting dopamine hydrochloride (CAS 62-31-7, Sigma) with polycaprolactone (average Mn 45.000, Sigma) and in a second step, poly(methacrylic acid, sodium salt) (CAS 54193-36-1, Sigma) was grafted using EDC-NHS (N-(3-dimethylaminopropyl)-N′-ethylcarbodiimide polymer-bound (EDC) (EC-No 217-579-2, Sigma) and N-hydroxysuccinimide (NHS) (CAS 6066-82-6, Sigma) as crosslinker and initiating agents, respectively. A customized portable reactor, previously described in Duarte et al [9], was built for *in situ* extrusion of the composition as an injectable foam. The device was designed to withstand the required pressure and temperature to generate the foam, while user-friendly: size and format equivalent to a 20 cc syringe, manageable within the very narrow surgical site and comprising a tip suitable for delivering the foam directly into the intervertebral space. Before the surgical intervention, the portable device was pre-loaded with 1.0 g of the PCL pDA pMAA powder, heated up to 60° and pressurized with 50 bar carbon dioxide (Air Liquide, 99.998 mol%) to induce foaming [9].

2.2. The porcine animal model and surgical approach

The porcine model, well established in the literature for spinal fusion studies [12,13,18], was selected to conduct the anterolateral lumbar approach. The similarity of the spinal anatomy with humans [16], in shape and size, was considered key for an adequate feasibility evaluation of the BIOLIF approach. This study was approved by the ethical review board of our University. We selected 8 adult domestic pigs (*Sus scrofa domesticus*) weighting 35-45 Kg. All surgeries were performed under general anesthesia with endotracheal intubation. The animals were fasted for 8 hours prior to surgery and premedicated with an

association of ketamine (20 mg/kg, intramuscular [IM]), xilazine (2 mg/kg, IM) and atropine (0.05 mg/kg, IM). Anesthetic induction was performed with propofol (6 mg/kg, intravenously [IV]) and maintained with continuous infusion of propofol (20 mg/kg/h, IV). Multimodal analgesia was provided by buprenorphine (0.05 mg/kg, IM) and carprofen (4 mg/kg, subcutaneous [SC]). The pig was placed in the lateral decubitus position and the surgical field was prepared. An anterolateral retroperitoneal approach was used to expose the lumbar spine and the intervertebral disc space, through a corridor between the peritoneum and psoas muscle. The disc space was identified, followed by annulotomy and discectomy conducted with the aid of a pituitary rongeur. The surfaces of the exposed vertebral endplates were decorticated with a bone curette. Such preparatory steps were conducted for all experimental animals independently of study group. Two treatments were then randomly allocated to animals: non-instrumented BIOLIF foam (n=5), or PEEK cage with autograft and instrumentation as positive control (n=3) (Figure 1).

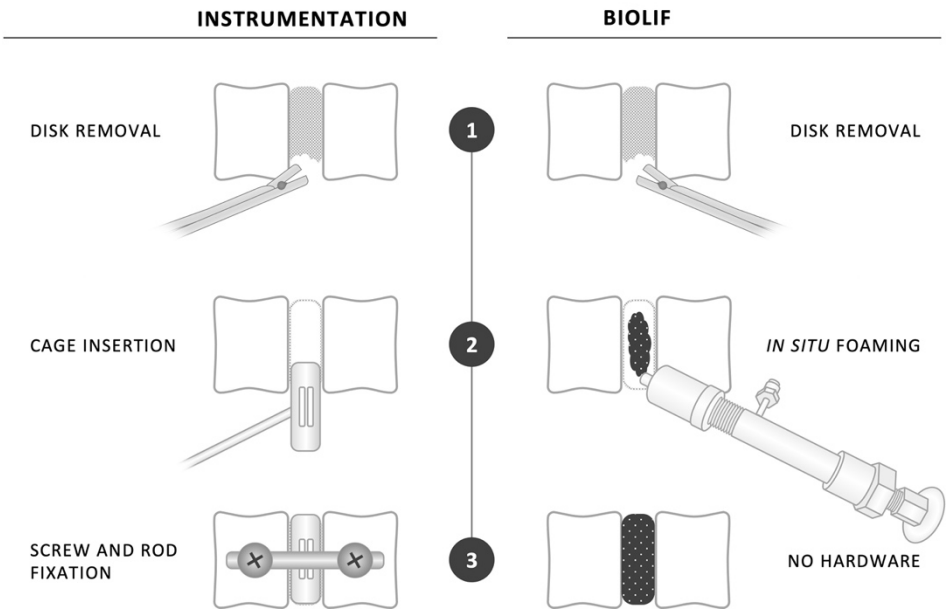

Figure 1. Graphical representation of main surgical steps required for spinal fusion in Instrumentation and BIOLIF approach.

2.3. SURGICAL TREATMENT: BIOLIF VS INSTRUMENTATION

Once the surgical site was prepared, the pre-loaded BIOLIF delivery device was positioned with its tip in the intervertebral space, towards release of the injectable foam. Hardening of the foam was allowed for a few seconds and no instrumentation was used for vertebral fixation.

For the Instrumentation group, pedicle screws (5.5 x 35mm, polyaxial, EXPEDIUM® Spine System, DePuy-Synthes) were placed in the middle lateral side, one in each adjacent vertebra. An additional step was performed to collect autologous iliac crest bone graft (ICBG). A CFRP cage (15x12x5 mm, height × width × length, respectively carbon fiber reinforced polymer IF cage ®, DePuy-Synthes) was then filled with the ICBG and placed in the interbody space. The pedicle screws were connected by a precut 5.5 x 40 mm titanium rod. Routine closure was performed, and surgery time for both groups was recorded.

At the end of the surgical procedure, animals were treated with the antibiotic ceftiofur hydrochloride (3 mg/kg, IM), which was maintained for 3 days at 24-hour intervals. Post-operative analgesia was provided by buprenorphine (0.05 mg/kg, IM) at 12-hour intervals and carprofen (4 mg/kg, SC) every 24 h. All animals were allowed *ad libitum* feeding and movement upon recovery from surgery and daily monitoring was conducted for any signs of adverse events or complications, incisional site infection, lameness, neurologic and ambulatory status for 6 months, at which animals were euthanized with pentobarbital (200 mg/mL, IV).

2.4. IN-LIFE ASSESSMENTS

Animal mobility during the first 48h was measured through the use of a commercial pedometer [19] and radiographic imaging was conducted at post-op and at termination (6-months).

2.5. POST-MORTEM TESTING

Immediately upon euthanasia, the treated segment was exposed and excised 2 levels above and below for further set of assessments. Specimens were examined for any sign of infection, necrosis or dislodgment of material and gross appearance was recorded by photography. Interbody stability was assessed by manual palpation and radiographic imaging at sagittal and coronal views, evaluated by two reviewers. For manual palpation, torsional and bending forces at fusion segment and adjacent interbody spaces was performed. The treated segment was considered fused if there was no motion and a stiffness similar to the osseous structure. The fusion was graded by a 3 point-scale [20]: 0 - motion comparable to unfused levels; 1 – reduced motion without stiffness; 2 – no motion and rigid. For radiographic

evaluation, a four-point grading score was used [20]: 0 – no fusion; 1 – bone connectivity gap >2mm; 2 - bone connectivity gap < 2mm; 3 - complete fusion. To evaluate if a normal spine alignment was maintained during the interbody fusion process, sagittal and coronal lumbar alignment was determined by measuring the Cobb angle, using Surgimap software (v2.3.2.1; Nemaris Inc., New York, USA).

2.5.1. MICROCT SCANNING AND ANALYSIS

microCT analysis was conducted to evaluate the microstructural morphology and bone ingrowth at the intervertebral segment. Specimens were scanned at an isotropic resolution of 78 μm using the vivaCT 80, SCANCO Medical AG, Switzerland, and quantitative measurements of bone volume / tissue volume (BV/TV) expressed as a percentage, were performed using its proprietary software. For analysis, the region of interest (ROI) was set as a circular disc (8-mm diameter x 10-mm height), at the center of the intervertebral segment [11,13,21]. For qualitative scoring of bone fusion, the images were classified by four independent raters according with modified Bridwell interbody fusion grading criteria [22] (Grade I – Fused with bony bridging and trabeculae remodeling; Grade II – Not fully bony bridged and remodeled, but with no lucencies above and below the cage; Grade III – A definite lucency at the top or bottom of the cage and screw; Grade IV – Definitely not fused with false motion.)

2.5.2. NON-DESTRUCTIVE MECHANICAL TESTING

Non-destructive mechanical testing was conducted to evaluate stiffness of the intervertebral segment in the three principle kinematic directions: flexion-extension (FE), right-left lateral bending (LB) and right-left axial rotation (AR), using a hydraulic material testing machine (Instron, model 8874, United States). Optical markers were placed in the vertebral bodies and tracked by high-resolution cameras. Loads were applied until reaching a moment of 4 Nm, at a constant angular velocity of 0.5 deg/s and each movement direction was tested for 5 consecutive cycles [21,23]. For flexion-extension (FE) and lateral bending (LB) testing, the specimens were placed horizontally in a custom-made three-point bending device where equal moments is ensured at the multiple levels of the lumbar spine. The axial rotation (AR) was tested in a vertical position. When a moment of +4 Nm was measured, the Instron reversed its loading direction until -4 Nm was reached. The range of motion (ROM) was obtained by using a video analysis and modelling software (Tracker v6.0.0, Open Source Physics). For each individual test (FE, LB, and AR), the stiffness (Nm/degree) of the stabilized spinal construct was calculated as the slope of the moment-ROM curve [21,23].

2.5.3. HISTOLOGICAL EVALUATION

Samples were trimmed to remove excessive vertebras until reaching the treated level and stored in 10% neutral buffered formalin. Specimens were decalcified and cut in half in the coronal plane, to conduct both hard and soft tissue histology. For the first, samples were embedded in methyl methacrylate, sectioned in 10 μm, while for the later, samples followed standard paraffin embedding and sectioning at 5 μm. Samples were stained for Haematoxylin & Eosin and Masson's Trichrome and imaged (Olympus BX61).

2.5.4. STATISTICAL ANALYSIS

Statistical analysis was performed with SPSS, version 26 and JASP, version 0.15. The Independent Samples *t* Test was used to compare treatment groups for spinal alignment, and BV/TV ratio. Normality was assessed with Shapiro-Wilk test. The two-way ANOVA was used to compare stiffness and ROM considering treatment groups and replicas. Tukeys multiple comparison tests were used to compare treatment groups. Effect size was measured with partial eta2 ($\eta 2$). Levene's test was used to assess homoscedasticity, confirmed for $p<0.05$ in all measures. Histograms and normal QQ plots were used to assess residuals normality. This assumption was confirmed for all measures.

3. RESULTS

Surgical interventions of both experimental groups occurred without complications. Minimally invasive *in situ* foaming of PCL pDA pMAA (BIOLIF) was technically feasible: the foam was delivered into the intervertebral space, through the custom-built surgical device and hardening of the foam occurred within seconds. Immediate fixation of the adjacent vertebral structures was achieved. For Instrumentation (control) group, surgical application of PEEK cage filled with ICBG and short segment instrumentation occurred routinely. Total surgery time for BIOLIF group was on average 28.0 min ± 4.6 min, 47.2% less time than required for the Instrumentation group (53.0 min ± 9.5 min) ($p<0.05$) (Figure 2a). Intra-operative visualization confirmed appropriate placement of material in both experimental groups (Figure 2b). Immediate post-op X-ray demonstrated maintenance of intervertebral disc space, normal disc alignment and structural integrity in both experimental groups (Figure 2c). Animals treated by BIOLIF demonstrated 50.5 % higher mobility at 48h post-op (mean steps 43907 vs 22184), as compared to animals treated by Instrumentation ($p<0.05$) (Figure 2d). No complications were observed during the 6-month follow-up period.

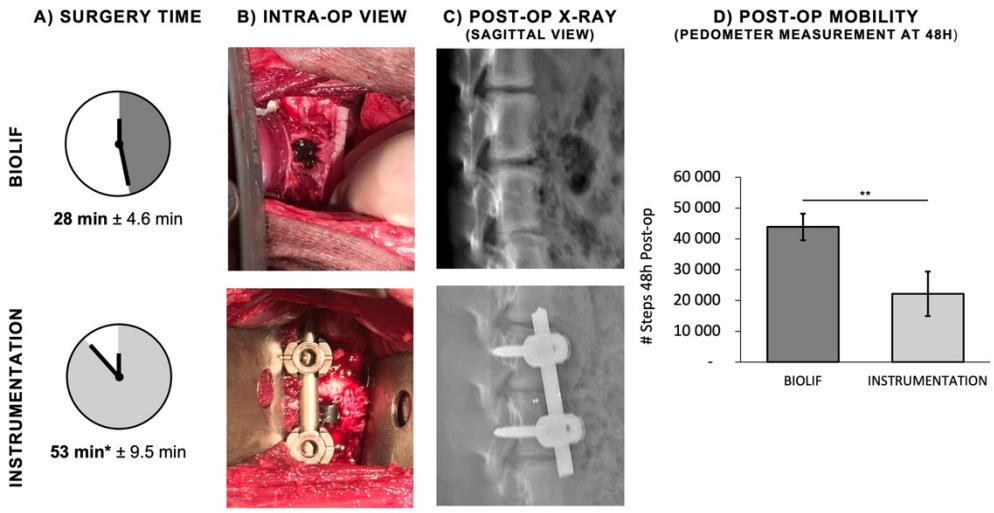

Figure 2. Surgical annotations and in-life assessments: a) Surgery time (*p<0.05), b) Photograph of intra-operative view, c) Post-op X-ray (sagittal view), d) Post-op mobility (pedometer measurement at 48h) (**p<0.05).

At termination, no signs of necrosis, infection or hardware failure were observed by gross macroscopic evaluation (Figure 3a). Manual palpation was conducted to obtain a first impression of interbody mobility, whereas, as observed in Figure 3c, most samples (BIOLIF and Instrumentation) were rated grade 2, indicative of limited interbody mobility and increased stiffness. Radiological imaging of the BIOLIF group revealed solid bone fusion in-between the two adjacent vertebrae (indicated by *, Figure 3b). Here, 70% of BIOLIF evaluations and 50% of Instrumentation assessments were classified in grades 2 and 3 (2: bone connectivity gap < 2mm; 3: complete fusion) (Figure 3d).

The porcine spine, in contrast to what occurs in humans, is characterized by presenting lumbar kyphosis around 5 degrees [24], as observed for the non-treated blank (Figure 4). In our study, sagittal Cobb angles measured were similar between both experimental groups (p>0.05), and equivalent to blank (p>0.05). Regarding coronal Cobb angles, there were no statistical significance between treatment groups, yet differences were measured when instrumentation compared to the blank (p<0.05).

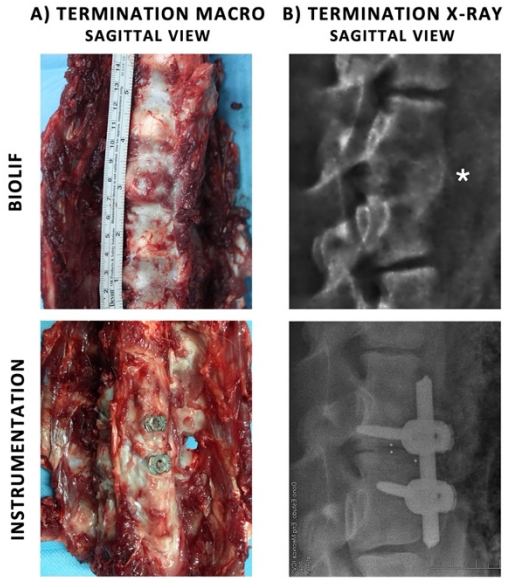

C)

Treatment	n	MANUAL PALPATION SCORE 0	1	2
BIOLIF	5 x 2	0% (0/10)	20% (2/10)	80% (8/10)
Instrumentation	3 x 2	0% (0/6)	33.3% (2/6)	66.6% (4/6)

0: motion comparable to unfused levels; 1: reduced motion without stiffness; 2: no motion and rigid

D)

Treatment	n	RADIOGRAPHIC FUSION GRADE 0	1	2	3
BIOLIF	5 x 2	0% (0/10)	30% (3/10)	20% (2/10)	50% (5/10)
Instrumentation	3 x 2	0% (0/6)	50% (3/6)	50% (3/6)	0% (0/6)

0: no fusion; 1: bone connectivity gap >2mm; 2: bone connectivity gap < 2mm; 3: complete fusion

Figure 3. Six-month termination assessments: a) Photograph of explants (sagittal view), **b)** Termination X-ray (sagittal view), **c-d)** Summary of Manual palpation and Radiographic fusion scores: classifications are provided for each specimen, evaluated by two reviewers (n).

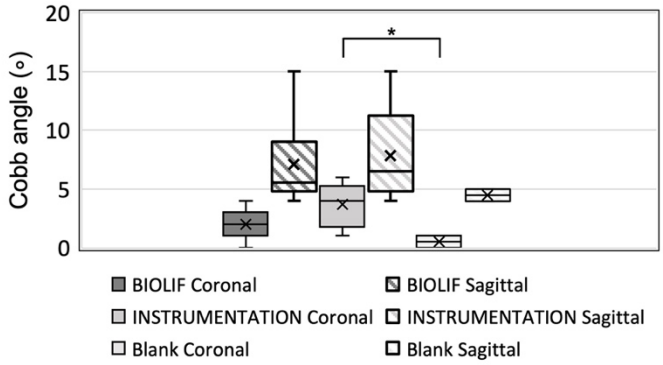

Figure 4. Sagittal and coronal alignment measured by Cobb angles (*p<0.05).

To further assess the mobility at the operated segment, range of motion (ROM) and stiffness in axial rotation (AR), flexion/extension (FE) and lateral bending (LB) were determined (Figure 5). It was observed that the ROM of segments treated by the BIOLIF approach, for the three spine movements, was to the same extent as the ROM determined for segments treated by the Instrumented approach. BIOLIF and Instrumentation treatment groups had lower ROM in AR (p<0.001), LB (p<0.001) and FE (p<0.001) when compared with the Blank group. Coherently, the stiffness (N.m/°) of BIOLIF treated segments, measured at AR, FE and LB, was equivalent to the stiffness measured for the Instrumented-treated segments. The non-treated sample (Blank) presented a lower stiffness for each of the movements tested: AR (p<0.001), LB (p<0.001) and for FE (p<0.001). AR, FE and LB results were stable across replicas.

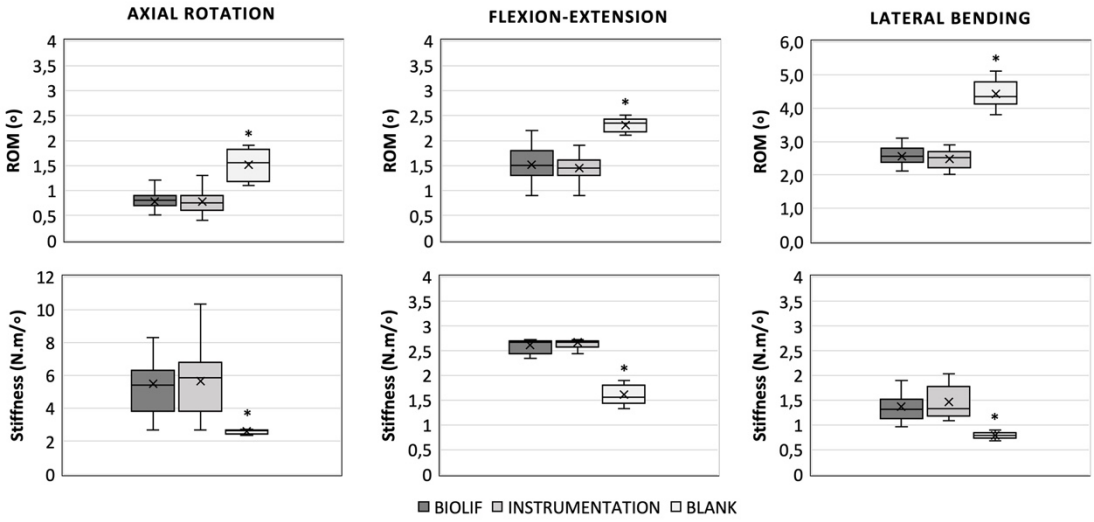

Figure 5. Biomechanical testing of spinal segments: Top row) Range of motion (ROM) and **Bottom row)** Stiffness (N.m/°) measurements, both obtained for the three main spinal movements: axial rotation (AR), flexion/extension (FE) and lateral bending (LB). Measurements acquired for BIOLIF and Instrumentation significantly different from blank (*p<0.001).

Bone fusion was further assessed by micro-computed tomography (microCT) (Figure 6) which permitted the determination of morphologic and volumetric differences between the experimental groups. As observed in Figure 6a, both sagittal and coronal sections of the BIOLIF explant reveal solid bone bridges between both endplates (indicated by *). A statistically significant higher bone volume (p<0.05), measured as the percentage bone volume to tissue volume ratio (BV/TV), was observed in BIOLIF group compared with Instrumentation group (Figure 6b, top). In the qualitative evaluation, according with modified Bridwell criteria for interbody spinal fusion (Figure 6b, bottom), BIOLIF specimens were classified predominantly in grades I and II (65% vs 50% answers in Instrumentation group).

Histological techniques for hard tissue processing were used to evaluate the bio-integration of the proposed BIOLIF material with the surrounding tissue and cells (Figure 7a). BIOLIF was found attached to native tissue (no gap at this interface), with its porous core structure populated with cells. Soft tissue histology was used to assess the microarchitecture of the developed tissue at the intervertebral space. As observed in Figure 7b, Masson's Trichrome staining distinguish a relatively well-organized newly formed osseous structure in red at BIOLIF samples, from the light green collagenous tissue present in the control group. In both groups, a continuity of tissue is observed between top and bottom vertebrae, indicative of fusion.

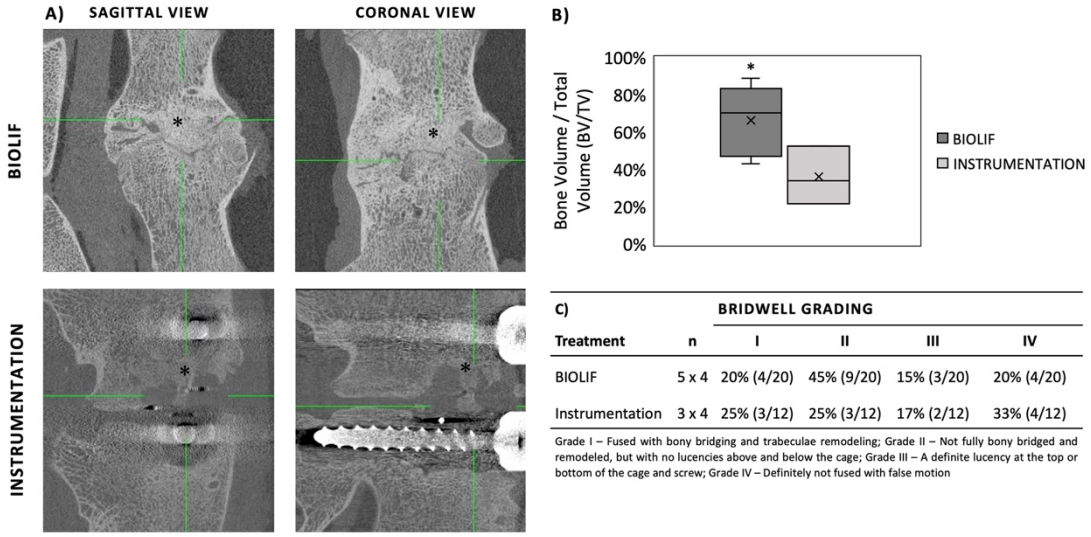

C)

Treatment	n	BRIDWELL GRADING I	II	III	IV
BIOLIF	5 x 4	20% (4/20)	45% (9/20)	15% (3/20)	20% (4/20)
Instrumentation	3 x 4	25% (3/12)	25% (3/12)	17% (2/12)	33% (4/12)

Grade I – Fused with bony bridging and trabeculae remodeling; Grade II – Not fully bony bridged and remodeled, but with no lucencies above and below the cage; Grade III – A definite lucency at the top or bottom of the cage and screw; Grade IV – Definitely not fused with false motion

Figure 6. microCT analysis of the 6-month end-point explants: a) Imaging: sagittal and coronal views of treated segment obtained by micro-computed tomography, highlighting bone growth in-between vertebrae (*); **Quantitative and qualitative evaluation: b)** significant differences in Bone Volume/Total Volume (BV/TV) between treatment groups (*p<0.05); **c):** Summary of modified Bridwell grading of the microCT images: classifications are provided for each specimen, evaluated by two reviewers (n).

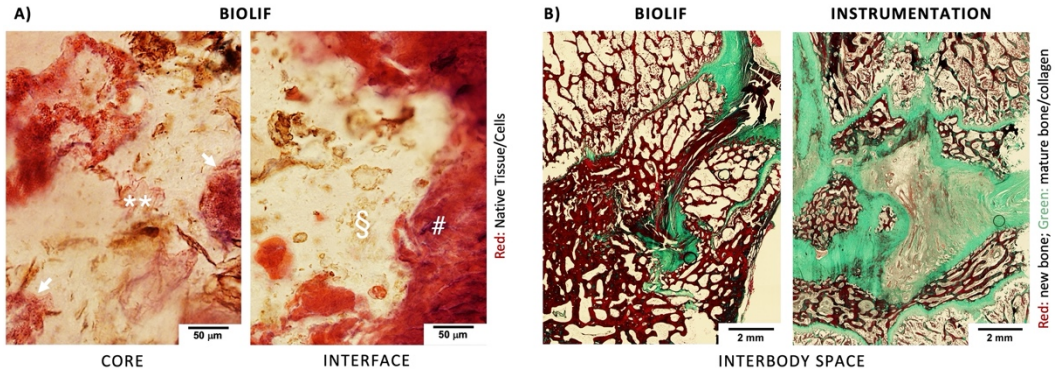

Figure 7. Bio-integration and bone fusion assessment by histological imaging at the intervertebral space: a) H&E staining of samples processed by soft-tissue histology (**: BIOLIF core; Arrowhead: BIOLIF pores populated with cells; §: BIOLIF interface; #: Native tissue; Scale bar 50 µm; **b)** Masson's trichrome staining of samples processed by hard-tissue histology - scale bar 2 mm.

4. Discussion

In the present *in vivo* study, the PCL pDA pMAA foam was successfully extruded through the portable device into the IVD space in a controlled manner without causing neurological damage to the animals, nor any other adverse effects identified by the authors. This minimally invasive approach reduced disturbances to the healthy surrounding tissues (as compared to standard instrumentation), which might

have had a positive impact on the faster post-op mobility observed in BIOLIF treated animals. It is recognized that a less aggressive surgical approach to cause less post-op pain and improved recovery of general condition [25]. By avoiding screw fixation and autograft harvesting in the BIOLIF group, surgery time was expressively inferior and post-op mobility was significantly higher, factors of considerable relevance when assessing the cost and ultimately cost-effectiveness of a surgical treatment [26,27]. From a surgical procedure perspective, the risk of neurological lesions related with cage insertion is well recognized in posterior lumbar interbody fusion approaches [28], given the narrow neural corridor available to access the IVD. With an *in situ* foaming approach, which uses a thin cannula for material extrusion, we could considerably minimize nerve route and dural sac retraction. In current interbody fusion practice, cage positioning is crucial for a successful lumbar arthrodesis [29,30], and the risks of non-union and cage migration are very well recognized, when the cage is undersized and posteriorly located [29,30]. Some of these risks may be overcome by the controlled extrusion and positioning of BIOLIF in the IVD.

During the interbody bone growth process, the mismatch between the cage size and intervertebral disc gap, which leads to the risk of cage subsidence and collapse of the intervertebral disc space, is one of the documented risk factors for IF-associated spinal deformity [31,32]. Herein, sagittal and coronal Cobb angles measured at termination confirmed segmental spinal alignment similar to the Instrumentation control group, although a slight kyphosis compared with the Blank reference was observed in both groups. Segmental spinal deformity is not commonly addressed in other spinal fusion studies in animal models (which typically benefit from instrumentation [33,34]), however in humans, loss of lordosis in lumbar interbody fusion is frequently reported [35,36].

In this proposed approach, adhesivity of the foam is fundamental to achieve immediate spinal stability, which is essential to yield a solid spinal fusion [37]. PCL pDA pMAA adhesivity to spinal plugs was confirmed and reported in our previous *ex vivo* study [9]. Also in that study, an hydroxyapatite layer was shown to be formed when immersed for 2 weeks in simulated body fluid [9], providing an attractive ground for bone ingrowth and integration of the foam with adjacent vertebral bodies [18,38]. Herein, microCT analysis of the explants collected at termination revealed a BV/TV ratio superior to the control Instrumentation group (average 70.1% BIOLIF vs 33.9% instrumentation, $p<0.05$). These results are in line with BV/TV ratios reported by Abbah et al, in porcine spinal fusion studies at a 6-month time-point reference, where PCL-tricalcium phosphate formulations were prepared with bone morphogenetic protein-2 (BMP-2) [34] or bone marrow stromal cells [13].

Biomechanical studies showed comparable bending and rotational stiffness between both groups. The limited mobility of the treated segment (reduced range of motion and increased stiffness) is supportive of spinal fusion, and coherent with other IF studies in the porcine [34] and ovine models [21]. A long-term consequence of segmental stiffness is the stress generated in adjacent intervertebral discs, associated with the extent of hardware used [39], leading to the development of adjacent segmental degeneration. Future studies could evaluate the potential of the proposed approach in minimizing this drawback. The histological findings collected in this work provided positive insights about the behavior of BIOLIF in relation with surrounding tissue and cells. BIOLIF foam was found attached to surrounding tissue, indicative of its integration, while for standard PEEK cages, it is well described in the literature that its inherent hydrophobic properties impede cell attachment and osteogenesis [40]. In our previous *ex vivo* study, we described the morphological characteristics (porosity, interconnectivity, degree of anisotropy) of the extruded PCL pDA pMAA foam, which revealed equivalent to those found in trabecular bone [9]. An interconnected porous network is essential for bone in-growth, by facilitating cell supply, vascularization, and integration with the native tissue. Histological sections of this *in vivo* study reveal that a porous foam was achieved *in situ*, with pores of different dimensions found populated with cells. Future advancements could include the *in situ* enrichment of the BIOLIF foam with exogenous cell sources, as for instance, autologous or allogeneic mesenchymal stem cells have generated high fusion rates in pre-clinical studies and clinical trials [41]. In a previous work, we have successfully incorporated dexamethasone and TCP via carbon dioxide foaming of PCL, which could be added to the formulation to further improve osteogenesis [42]. For the time being, results obtained through the diverse quantitative and qualitative assessments conducted in the present work, seem to support the hypothesis that spinal fusion can be achieved by BIOLIF in the described model, and that the selected porcine model and surgical approach was deemed adequate to test both the surgical feasibility and spinal fusion capacity. These outcomes open the possibility of a non-instrumented spinal fusion in the future.

Acknowledgements

This work has been funded by National funds, through the Foundation for Science and Technology (FCT) - project UIDB/50026/2020 and UIDP/50026/2020, and contract under the Transitional Rule DL 57/2016 (CTTI-57/18-I3BS(5)).

References

[1] D.J. Miller, M.G. Vitale, Dr. Russell A. Hibbs: Pioneer of Spinal Fusion, Spine (Phila. Pa. 1976). (2015). https://doi.org/10.1097/BRS.0000000000001001.

[2] R. Roy-Camille, G. Saillant, C. Mazel, Internal fixation of the lumbar spine with pedicle screw plating, Clin. Orthop. Relat. Res. (1986). https://doi.org/10.1097/00003086-198602000-00003.

[3] S.D. Kuslich, C.L. Ulstrom, S.L. Griffith, J.W. Ahern, J.D. Dowdle, G. Tipton, The Bagby and Kuslich method of lumbar interbody fusion: History, techniques, and 2-year follow-up results of a United States prospective, multicenter trial, Spine (Phila. Pa. 1976). (1998). https://doi.org/10.1097/00007632-199806010-00019.

[4] J.J. Enders, D. Coughlin, T.E. Mroz, S. Vira, Surface Technologies in Spinal Fusion, Neurosurg. Clin. N. Am. (2020). https://doi.org/10.1016/j.nec.2019.08.007.

[5] P. Park, M. Wang, K.D. Than, J. Uribe, Emerging Technologies in Spinal Surgery, Oper. Neurosurg. (Hagerstown, Md.). (2021). https://doi.org/10.1093/ons/opab064.

[6] A. V. Patel, C.A. White, J.T. Schwartz, N.L. Pitaro, K.C. Shah, S. Singh, V. Arvind, J.S. Kim, S.K. Cho, Emerging Technologies in the Treatment of Adult Spinal Deformity, Neurospine. (2021). https://doi.org/10.14245/ns.2142412.206.

[7] J.N. Shillingford, J.L. Laratta, N.O. Sarpong, R.G. Alrabaa, M.K. Cerpa, R.A. Lehman, L.G. Lenke, C.R. Fischer, Instrumentation complication rates following spine surgery: a report from the Scoliosis Research Society (SRS) morbidity and mortality database, J. Spine Surg. (2019). https://doi.org/10.21037/jss.2018.12.09.

[8] A.K. Allouni, W. Davis, K. Mankad, J. Rankine, I. Davagnanam, Modern spinal instrumentation. Part 2: Multimodality imaging approach for assessment of complications, Clin. Radiol. (2013) P75-81. https://doi.org/10.1016/j.crad.2012.05.002.

[9] R.M. Duarte, J. Correia-Pinto, R.L. Reis, A.R.C. Duarte, Advancing spinal fusion: Interbody stabilization by in situ foaming of a chemically modified polycaprolactone, J. Tissue Eng. Regen. Med. (2020). https://doi.org/10.1002/term.3111.

[10] D. Mondal, M. Griffith, S.S. Venkatraman, Polycaprolactone-based biomaterials for tissue engineering and drug delivery: Current scenario and challenges, Int. J. Polym. Mater. Polym. Biomater. 65 (2016) 255–265. https://doi.org/10.1080/00914037.2015.1103241.

[11] S.A. Abbah, C.X.L. Lam, D.W. Hutmacher, J.C.H. Goh, H.K. Wong, Biological performance of a polycaprolactone-based scaffold used as fusion cage device in a large animal model of spinal

reconstructive surgery, Biomaterials. 30 (2009) 5086–5093. https://doi.org/10.1016/j.biomaterials.2009.05.067.

[12] S.A. Abbah, C.X.F. Lam, A.K. Ramruttun, J.C.H. Goh, H.K. Wong, Fusion performance of low-dose recombinant human bone morphogenetic protein 2 and bone marrow-derived multipotent stromal cells in biodegradable scaffolds: A comparative study in a large animal model of anterior lumbar interbody fusion, Spine (Phila. Pa. 1976). 36 (2011) 1752–1759. https://doi.org/10.1097/BRS.0b013e31822576a4.

[13] S.A. Abbah, C.X.F. Lam, K.A. Ramruttun, J.C.H. Goh, H.-K. Wong, Autogenous Bone Marrow Stromal Cell Sheets-Loaded mPCL/TCP Scaffolds Induced Osteogenesis in a Porcine Model of Spinal Interbody Fusion, Tissue Eng. Part A. 17 (2011) 809–817. https://doi.org/10.1089/ten.tea.2010.0255.

[14] Y. Li, Z. gang Wu, X. kang Li, Z. Guo, S. hua Wu, Y. quan Zhang, L. Shi, S. hin Teoh, Y. chun Liu, Z. yong Zhang, A polycaprolactone-tricalcium phosphate composite scaffold as an autograft-free spinal fusion cage in a sheep model, Biomaterials. 35 (2014) 5647–5659. https://doi.org/10.1016/j.biomaterials.2014.03.075.

[15] M.R.N.O. Yong, S. Saifzadeh, G.N. Askin, R.D. Labrom, D.W. Hutmacher, C.J. Adam, Biological performance of a polycaprolactone-based scaffold plus recombinant human morphogenetic protein-2 (rhBMP-2) in an ovine thoracic interbody fusion model, Eur. Spine J. 23 (2014) 650–657. https://doi.org/10.1007/s00586-013-3085-x.

[16] I. Busscher, J.J.W. Ploegmakers, G.J. Verkerke, A.G. Veldhuizen, Comparative anatomical dimensions of the complete human and porcine spine, Eur. Spine J. (2010). https://doi.org/10.1007/s00586-010-1326-9.

[17] I. Busscher, A.J. Van Der Veen, J.H. Van Dieen, I. Kingma, G.J. Verkerke, A.G. Veldhuizen, In Vitro biomechanical characteristics of the spine: A comparison between human and porcine spinal segments, Spine (Phila. Pa. 1976). (2010). https://doi.org/10.1097/BRS.0b013e3181b21885.

[18] R.M. Duarte, P. Varanda, R.L. Reis, A.R.C. Duarte, J. Correia-Pinto, Biomaterials and Bioactive Agents in Spinal Fusion, Tissue Eng. Part B Rev. (2017) ten.teb.2017.0072. https://doi.org/10.1089/ten.teb.2017.0072.

[19] C.B. Chan, M. Spierenburg, S.L. Ihle, C. Tudor-Locke, Use of pedometers to measure physical activity in dogs, J. Am. Vet. Med. Assoc. (2005). https://doi.org/10.2460/javma.2005.226.2010.

[20] D.L. Wheeler, D.C. Fredericks, R.F. Dryer, H.W. Bae, Allogeneic mesenchymal precursor cells

(MPCs) combined with an osteoconductive scaffold to promote lumbar interbody spine fusion in an ovine model, Spine J. (2016). https://doi.org/10.1016/j.spinee.2015.08.019.

[21] K.C. McGilvray, E.I. Waldorff, J. Easley, H.B. Seim, N. Zhang, R.J. Linovitz, J.T. Ryaby, C.M. Puttlitz, Evaluation of a polyetheretherketone (PEEK) titanium composite interbody spacer in an ovine lumbar interbody fusion model: biomechanical, microcomputed tomographic, and histologic analyses, Spine J. (2017). https://doi.org/10.1016/j.spinee.2017.06.034.

[22] K.H. Bridwell, L.G. Lenke, K.W. McEnery, C. Baldus, K. Blanke, Anterior fresh frozen structural allografts in the thoracic and lumbar spine: Do they work if combined with posterior fusion and instrumentation in adult patients with kyphosis or anterior column defects?, Spine (Phila. Pa. 1976). (1995). https://doi.org/10.1097/00007632-199506020-00014.

[23] A. Bisschop, R.M. Holewijn, I. Kingma, A. Stadhouder, P.P.A. Vergroesen, A.J. Van Der Veen, J.H. Van Dieën, B.J. Van Royen, The effects of single-level instrumented lumbar laminectomy on adjacent spinal biomechanics, Glob. Spine J. (2014). https://doi.org/10.1055/s-0034-1395783.

[24] H. Abbasi, A. Abbasi, Using Porcine Cadavers as an Alternative to Human Cadavers for Teaching Minimally Invasive Spinal Fusion: Proof of Concept and Anatomical Comparison, Cureus. (2019). https://doi.org/10.7759/cureus.6158.

[25] C.L. Goldstein, F.M. Phillips, Y.R. Rampersaud, Comparative Effectiveness and Economic Evaluations of Open Versus Minimally Invasive Posterior or Transforaminal Lumbar Interbody Fusion, Spine (Phila. Pa. 1976). (2016). https://doi.org/10.1097/BRS.0000000000001462.

[26] M.D. Alvin, J.A. Miller, D. Lubelski, B.P. Rosenbaum, K.G. Abdullah, R.G. Whitmore, E.C. Benzel, T.E. Mroz, Variations in cost calculations in spine surgery cost-effectiveness research, Neurosurg. Focus. (2014). https://doi.org/10.3171/2014.3.FOCUS1447.

[27] Y. Lu, S.A. Qureshi, Cost-effective studies in spine surgeries: A narrative review, Spine J. (2014). https://doi.org/10.1016/j.spinee.2014.04.026.

[28] J. Boktor, R. Pockett, N. Verghese, The expandable transforaminal lumbar interbody fusion - Two years follow-up, J. Craniovertebr. Junction Spine. (2018). https://doi.org/10.4103/jcvjs.JCVJS_21_18.

[29] Y.H. Hu, C.C. Niu, M.K. Hsieh, T.T. Tsai, W.J. Chen, P.L. Lai, Cage positioning as a risk factor for posterior cage migration following transforaminal lumbar interbody fusion - An analysis of 953 cases, BMC Musculoskelet. Disord. (2019). https://doi.org/10.1186/s12891-019-2630-0.

[30] M.K. Park, K.T. Kim, W.S. Bang, D.C. Cho, J.K. Sung, Y.S. Lee, C.K. Lee, C.H. Kim, B.K. Kwon,

W.K. Lee, I. Han, Risk factors for cage migration and cage retropulsion following transforaminal lumbar interbody fusion, Spine J. (2019). https://doi.org/10.1016/j.spinee.2018.08.007.

[31] T. Amorim-Barbosa, C. Pereira, D. Catelas, C. Rodrigues, P. Costa, R. Rodrigues-Pinto, P. Neves, Risk factors for cage subsidence and clinical outcomes after transforaminal and posterior lumbar interbody fusion, Eur. J. Orthop. Surg. Traumatol. (2021). https://doi.org/10.1007/s00590-021-03103-z.

[32] Y.C. Yao, P.H. Chou, H.H. Lin, S.T. Wang, C.L. Liu, M.C. Chang, Risk Factors of Cage Subsidence in Patients Received Minimally Invasive Transforaminal Lumbar Interbody Fusion, Spine (Phila. Pa. 1976). (2020). https://doi.org/10.1097/BRS.0000000000003557.

[33] M. Wang, S.A. Abbah, T. Hu, R.W.M. Lam, S.Y. Toh, T. Liu, S.M. Cool, K. Bhakoo, J. Li, J.C.H. Goh, H.K. Wong, Polyelectrolyte complex carrier enhances therapeutic efficiency and safety profile of bone morphogenetic protein-2 in porcine lumbar interbody fusion model, Spine (Phila. Pa. 1976). (2015). https://doi.org/10.1097/BRS.0000000000000935.

[34] S.A. Abbah, W.M.R. Lam, T. Hu, J. Goh, H.K. Wong, Sequestration of rhBMP-2 into self-assembled polyelectrolyte complexes promotes anatomic localization of new bone in a porcine model of spinal reconstructive surgery, Tissue Eng. - Part A. (2014). https://doi.org/10.1089/ten.tea.2013.0593.

[35] J. Liu, P. Duan, P. V. Mummaneni, R. Xie, B. Li, Y. Dong, S. Berven, D. Chou, Does transforaminal lumbar interbody fusion induce lordosis or kyphosis? Radiographic evaluation with a minimum 2-year follow-up, J. Neurosurg. Spine. (2021). https://doi.org/10.3171/2020.12.SPINE201665.

[36] S. Ohyama, Y. Aoki, M. Inoue, G. Kubota, A. Watanabe, T. Nakajima, Y. Sato, H. Takahashi, A. Nakajima, J. Saito, Y. Eguchi, S. Orita, K. Inage, Y. Shiga, K. Nakagawa, S. Ohtori, Influence of Preoperative Difference in Lumbar Lordosis Between the Standing and Supine Positions on Clinical Outcomes After Single-level Transforaminal Lumbar Interbody Fusion: Minimum 2-year Follow-up, Spine (Phila. Pa. 1976). (2021). https://doi.org/10.1097/BRS.0000000000003955.

[37] J. Li, W. Wang, R. Zuo, Y. Zhou, Biomechanical Stability Before and After Graft Fusion with Unilateral and Bilateral Pedicle Screw Fixation: Finite Element Study, World Neurosurg. (2019). https://doi.org/10.1016/j.wneu.2018.11.141.

[38] A. El-Ghannam, P. Ducheyne, 1.109 – Bioactive Ceramics, in: Compr. Biomater., 2011: pp. 157–179. https://doi.org/10.1016/B978-0-08-055294-1.00021-0.

[39] P. Wangsawatwong, A.G.U. Sawa, B. de A. Pereira, J.N. Lehrman, J.D. Turner, J.S. Uribe, B.P.

Kelly, Does the Choice of Spinal Interbody Fusion Approach Significantly Affect Adjacent Segment Mobility?, Spine (Phila. Pa. 1976). (2021). https://doi.org/10.1097/brs.0000000000004058.

[40] B.J.V. Yoon, F. Xavier, B.R. Walker, S. Grinberg, F.P. Cammisa, C. Abjornson, Optimizing surface characteristics for cell adhesion and proliferation on titanium plasma spray coatings on polyetheretherketone, Spine J. (2016). https://doi.org/10.1016/j.spinee.2016.05.017.

[41] M.A. Robbins, D.R. Haudenschild, A.M. Wegner, E.O. Klineberg, Stem Cells in Spinal Fusion, Glob. Spine J. (2017). https://doi.org/10.1177/2192568217701102.

[42] R.M. Duarte, J. Correia-Pinto, R.L. Reis, A.R.C. Duarte, Subcritical carbon dioxide foaming of polycaprolactone for bone tissue regeneration, J. Supercrit. Fluids. 140 (2018) 1–10.

CHAPTER VI

Injectable and expandable composition, devices, kits, methods and uses thereof

This chapter is based on the following patent application: **Duarte RM**, Correia-Pinto J, Reis RL and Duarte ARC, Injectable and expandable composition, devices, kits, methods and uses thereof. International Application Number PCT/IB2018/057985, Publication number WO/2019/073463

(12) INTERNATIONAL APPLICATION PUBLISHED UNDER THE PATENT COOPERATION TREATY (PCT)

(19) World Intellectual Property Organization
International Bureau

(43) International Publication Date
18 April 2019 (18.04.2019)

WIPO | PCT

(10) International Publication Number
WO 2019/073463 A1

(51) International Patent Classification:
A61L 27/18 (2006.01) *A61L 27/54* (2006.01)
A61L 27/34 (2006.01)

(21) International Application Number:
PCT/IB2018/057985

(22) International Filing Date:
15 October 2018 (15.10.2018)

(25) Filing Language: English

(26) Publication Language: English

(30) Priority Data:
110348 13 October 2017 (13.10.2017) PT
18152785.4 22 January 2018 (22.01.2018) EP

(71) Applicants: **UNIVERSIDADE DO MINHO** [PT/PT]; Largo Do Paço, 4700-320 Braga (PT). **ASSOCIATION FOR THE ADVANCEMENT OF TISSUE ENGINEERING AND CELL BASED TECHNOLOGIES & THERAPIES - A4TEC** [PT/PT]; Univ. Do Minho Dep-3b S Research Group Campos De Gualtar, 4710-057 Braga (PT).

(72) Inventors: **CRUZ DUARTE, Ana Rita**; Rua Helena Felix, Nº 20, 2º Recuado, 2820-266 Charneca Da Caparica (PT). **REIS, Rui L.**; Rua Arquitecto João Anderson, 101, Habitação 2.3, 4250-242 Porto (PT). **NUNES CORREIA PINTO, Jorge Manuel**; Rua São João De Brito 512, 5ºe, 4100-453 Porto (PT). **FERNANDES DUARTE, Rui Miguel**; Rua Peixoto N.3 2O Trás, 4715-318 Braga (PT).

(74) Agent: **TEIXEIRA DE CARVALHO, Anabela**; Patentree, Edifício Net, Rua de Salazares 842, 4149-002 Porto (PT).

(81) Designated States *(unless otherwise indicated, for every kind of national protection available)*: AE, AG, AL, AM, AO, AT, AU, AZ, BA, BB, BG, BH, BN, BR, BW, BY, BZ, CA, CH, CL, CN, CO, CR, CU, CZ, DE, DJ, DK, DM, DO, DZ, EC, EE, EG, ES, FI, GB, GD, GE, GH, GM, GT, HN, HR, HU, ID, IL, IN, IR, IS, JO, JP, KE, KG, KH, KN, KP, KR, KW, KZ, LA, LC, LK, LR, LS, LU, LY, MA, MD, ME, MG, MK, MN, MW, MX, MY, MZ, NA, NG, NI, NO, NZ, OM, PA, PE, PG, PH, PL, PT, QA, RO, RS, RU, RW, SA, SC, SD, SE, SG, SK, SL, SM, ST, SV, SY, TH, TJ, TM, TN, TR, TT, TZ, UA, UG, US, UZ, VC, VN, ZA, ZM, ZW.

(84) Designated States *(unless otherwise indicated, for every kind of regional protection available)*: ARIPO (BW, GH, GM, KE, LR, LS, MW, MZ, NA, RW, SD, SL, ST, SZ, TZ, UG, ZM, ZW), Eurasian (AM, AZ, BY, KG, KZ, RU, TJ, TM), European (AL, AT, BE, BG, CH, CY, CZ, DE, DK, EE, ES, FI, FR, GB, GR, HR, HU, IE, IS, IT, LT, LU, LV, MC, MK, MT, NL, NO, PL, PT, RO, RS, SE, SI, SK, SM, TR), OAPI (BF, BJ, CF, CG, CI, CM, GA, GN, GQ, GW, KM, ML, MR, NE, SN, TD, TG).

Published:
— *with international search report (Art. 21(3))*
— *before the expiration of the time limit for amending the claims and to be republished in the event of receipt of amendments (Rule 48.2(h))*
— *in black and white; the international application as filed contained color or greyscale and is available for download from PATENTSCOPE*

WO 2019/073463 A1

(54) **Title:** INJECTABLE AND EXPANDABLE COMPOSITION, DEVICES, KITS, METHODS AND USES THEREOF

(57) **Abstract:** The present disclosure relates to injectable and expandable compositions, devices, kits and methods for use in an approach for the in-situ foaming of polymers for bone or tissue defects, namely to fill and/or fuse a tissue defect. The present disclosure relates to compositions, devices, kits and methods for use in an approach for the in-situ foaming of polymers for bone or tissue defects, namely for bone tissue defect filling/fusion. The design of extrudable and expandable compositions for bone fusion is one of the most challenging fields in the intersection of polymer and biomedical engineering. An aspect of the present disclosure relates to an injectable expandable composition for use in medicine, veterinary or cosmetic, comprising a polycaprolactone particle filler; a polydopamine adhesive bound to said filler; a polymethacrylic acid plasticizer bound to said polydopamine adhesive.

D E S C R I P T I O N

INJECTABLE AND EXPANDABLE COMPOSITION, DEVICES, KITS, METHODS AND USES THEREOF

Technical field

[0001] The present disclosure relates to injectable and expandable compositions, devices, kits and methods for use in an approach for the in-situ foaming of polymers for bone or tissue defects, to fill and/or fuse a tissue defect.

Background Art

[0002] The adhesive technologies currently available have been extensively reviewed in the literature. Two distinct groups can be identified, synthetic adhesives and biologically inspired materials [1–3]. Among the synthetic adhesives are poly(methyl methacrylate) bone cement, which is the class of synthetic materials that has more extensively been used in bone fixing fractures; cyanoacrylates; polyurethanes; dentine and enamel, used in dental applications; calcium and phosphate bone cements and glass ionomer cements. Synthetic adhesives have high adhesion strength however they present crucial disadvantages such as poor biocompatibility and limited biodegradability.

[0003] On the other hand, biologically inspired materials raise less biocompatibility concerns and may overcome the ability of synthetic adhesives to adhere in a wet environment. Nonetheless, these are not able to provide the mechanical integrity required for bone tissue applications and are instead more suitable as soft tissue adhesives. Biologically inspired adhesives include fibrin glue, gelatin-resorcinol-formaldehyde glue, protein-aldehyde systems, mussel proteins and biomimetic castles and glues from different animal species.

[0004] These facts are disclosed in order to illustrate the technical problem addressed by the present disclosure.

General Description

[0005] The present disclosure relates to compositions, devices, kits and methods for use in an approach for the in-situ foaming of polymers for bone or tissue defects, namely filling and/or fusion.

[0006] The design of extrudable and expandable compositions for bone fusion is one of the most challenging fields in the intersection of polymer and biomedical engineering.

[0007] An aspect of the present disclosure relates to an injectable expandable composition for use in medicine, veterinary or cosmetic, comprising:

a bio-polymer or co-polymer polyester particle filler;

a polydopamine adhesive bound to said filler;

a polyacrylate plasticizer bound to said polydopamine adhesive.

[0008] An aspect of the present disclosure relates to an injectable expandable composition for use in medicine, veterinary or cosmetic, comprising a polycaprolactone particle filler; a polydopamine adhesive bound to said filler; a polymethacrylic acid plasticizer bound to said polydopamine adhesive, for treating a bone defect, in particular for treating a bone defect, for bone regeneration or for bone tissue engineering.

[0009] The injectable expandable composition of the present disclosure has surprisingly improved bioactive and adhesive properties suitable for treating a bone defect, for bone regeneration or for bone tissue engineering, namely for use in diverse trauma and pathology-driven needs in bone surgery.

[0010] In an embodiment for better results, the bio-polymer or co-polymer polyester particle filler may be selected from a list consisting of: poly (L-lactic acid), poly (D-L-lactic acid) (PLA); polyglycolic acid [Polyglycoside (PGA)], poly (glycol-co-trimethylene carbonate) (PGA/PTMC), poly (D, L-lactic-co-caprolactone) (PLA/PCL), poly (glycol-co-caprolactone) (PGA/PCL); polyethylene oxide (PEO), polydioxanone (PDS), polypropylene fumarate, poly (ethyl glutamate-co-glutamic acid), poly (tert-butyloxycarbonylmethyl glutamate), poly (carbonate ester), polycaprolactone (PCL), polycaprolactone co-butylacrylate, polyhydroxyalkanoate as polyhydroxybutyrate (PHBT) , polyhydroxybutyrate copolymers with hydroxyvalerate (PHB / HV), poly (phosphazene), poly (phosphate ester), poly (amino acid) and poly (hydroxybutyrate), polydepsipeptides, copolymers of maleic anhydride, polyphosphazenes, polyiminocarbonates, cyanoacrylate, or mixtures thereof. Preferably, the filler may be a polycaprolactone, a polycaprolactone derivate, or mixtures thereof.

[0011] In an embodiment for better results, the polyacrylate plasticizer is selected from a list consisting of:

poly(acrylates), poly(hydroxyalkylacrylates), poly(methacrylates), poly(hydroxyalkyl methacrylates), poly(alkyl acrylates),poly(alkyl methacrylates), poly(allyl methacrylates), poly(diacrylates), poly(triacrylates), poly(dimethacrylates), poly(trimethacrylates), poly(alkyl diacrylates), poly(glycerol methacrylates), poly(aminoalkyl acrylates), poly(aminoalkylmethacrylates), poly(aminoalkyldiacrylates), poly(aminoalkyl dimethacrylates),

poly(ethoxybiphenol-A dimethacrylates), poly(ethyleneglycol methacrylates), poly(ethyleneglycol dimethacrylates), poly(ethyleneglycol trimethacrylates), poly(siloxanyl acrylates), poly(siloxanylmethacrylates), poly(siloxanyl alkyl acrylates), poly(siloxanyl alkyl methacrylates), poly(siloxanyl alkyl diacrylates), poly(siloxanyl alkyl dimethacrylates), poly(sylil methylene methacrylates). Preferably, polymethacrylic acid.

[0012] In an embodiment for better results, injectable expandable composition of the present disclosure may comprise 70-89.5 % ($w/w_{composition}$) of a particle filler of bio-polymer or co-polymer, preferably 75-85 % ($w/w_{composition}$) of a particle filler of bio-polymer or co-polymer; in particular polycaprolactone.

[0013] In an embodiment for better results, injectable expandable composition of the present disclosure may comprise 0.5-5 % ($w/w_{composition}$) of polydopamine adhesive, preferably 1-4 % ($w/w_{composition}$) polydopamine adhesive.

[0014] In an embodiment for better results, injectable expandable composition of the present disclosure may comprise 10-30 % ($w/w_{composition}$) of polyacrylate plasticizer, preferably 15-25% ($w/w_{composition}$) of polyacrylate plasticizer, in particular polymethacrylic acid.

[0015] In an embodiment for better results, the particles of polycaprolactone have a size from 900-100 µm, preferably from 750-200 µm, more preferably from 600-300 µm.

[0016] In an embodiment for better results, injectable expandable composition of the present disclosure may further comprise: a bone growth stimulant, a bone growth promoter, a growth hormone, a cell attractant, a drug molecule, cells, bioactive glass, bioceramics - including: tricalcium phosphate, hydroxyapatite, calcium phosphate, calcium sulfate, calcium carbonate, aluminium oxide; or combinations thereof. These components may be added to the injectable expandable composition (before extrusion) and /or expanded foam material (after extrusion).

[0017] In an embodiment for better results, the drug molecule may be an anti-inflammatory, antipyretic, analgesic, anticancer, or mixtures thereof; in particular dexamethasone.

[0018] In an embodiment for better results, the bone growth promoter may be selected from: fibroblast growth factor, transforming growth factor beta, insulin growth factor, platelet-derived growth factor, oxysterols or mixtures thereof; in particular bone morphogenetic protein.

[0019] In an embodiment for better results, cells may be selected from: osteoblasts, osteoclasts, osteocytes, pericytes, endothelial cells, endothelial progenitor cells, bone progenitor cells, hematopoietic progenitor cells, hematopoietic stem cells, neural progenitor cells, neural stem cells, mesenchymal stromal/stem cells, induced pluripotent stem cells, embryonic stem cells, perivascular stem cells, amniotic fluid stem cells, amniotic membrane stem cells, umbilical cord stem cells,

genetically engineered cells, bone marrow aspirate, stromal vascular fraction, or combinations thereof. These components may be added to the injectable expandable composition (before extrusion) and /or expanded foam material (after extrusion).

[0020] In an embodiment for better results, cells may be mammal cells. These components may be added to the injectable expandable composition (before extrusion) and /or expanded foam material (after extrusion).

[0021] The cells can be processing in supercritical CO_2 and survive. (P. J. Ginty. *et. al,* Mammalian cell survival and processing in supercritical CO_2, 2006, in Proceedings of the National Academy of Sciences, vol. 103, no.19, page. 7426-31.)

[0022] In an embodiment for better results, injectable expandable composition of the present disclosure is an implantable composition.

[0023] In an embodiment for better results, injectable expandable composition of the present disclosure is an extrudable composition.

[0024] In an embodiment for better results, injectable expandable composition of the present disclosure for treating a bone defect, for bone regeneration or for bone tissue engineering, in particular bone fusion.

[0025] In an embodiment for better results, injectable expandable composition of the present disclosure for filling and fixing bone or tissue.

[0026] In an embodiment for better results, injectable expandable composition of the present disclosure for use in the treatment of bone defect resulting from pathologies including: post-traumatic pathologies, deformities, degenerative pathologies, infections, post-surgical or genetic pathologies, idiopathic or combinations thereof.

[0027] In an embodiment for better results, injectable expandable composition of the present disclosure for treating, inhibiting or reversing vertebral column diseases or disorders of intervertebral disc.

[0028] In an embodiment for better results, injectable expandable composition of the present disclosure in a method for prevention or treatment trauma and/or orthopaedic surgery comprising polycaprolactone, polydopamine and polymethacrylic acid,

wherein said composition is administrated as a biodegradable material,
wherein said material comprises particles of polycaprolactone, bound to polydopamine and wherein said polydopamine is bound to polymethacrylic acid.

[0029] Another aspect of the present disclosure relates to an expanded foam material for use in medicine obtainable by the method described in the present disclosure or comprising the injectable expandable composition of the present disclosure, comprising a porosity of 30-90%, preferably 40-60%.

[0030] In an embodiment for better results, the expanded foam material of the present disclosure comprises a pore size between of 100-900 µm, preferably 150-200 µm.

[0031] In an embodiment for better results, the expanded foam material of the present disclosure comprises a porous interconnectivity of 20-90%, preferably 25-70%, more preferably 30-50%.

[0032] In an embodiment, the morphological structure and the calculation of the morphometric parameters (Porosity (%), Interconnectivity (%), Mean pore size (mm), Density (mm-1) and degree of anisotropy) that characterize the 3D extruded foams can be calculated by micro-computed tomography (micro-CT) using a Skyscan 1272 equipment (Bruker, Germany) with penetrative X-rays of 50 KeV and 200 µA, in high-resolution mode with a pixel size of 21.6 µm. A CT analyser (v1.15.4.0, 2012-2015, Bruker Micro-CT) was used to calculate the parameters from the 2D images of the matrices.

[0033] Another aspect of the present disclosure relates to a spinal implant comprising the expanded foam material of the present disclosure can be obtained from the injectable expandable composition of the present disclosure.

[0034] Another aspect of the present disclosure relates to a method for obtaining an expanded foam material of the present disclosure, comprising the steps of:

loading the injectable expandable composition described in any of the previous claims in a high-pressure chamber;

sealing said high pressure chamber;

pressurizing said high pressure chamber at 20 – 150 bar, preferably at 45-120 bar, more preferably at 50-60 bar.

[0035] In an embodiment for better results, the pressurizing step is carried in the presence of a pressurizing agent.

[0036] In an embodiment for better results, the pressurizing agent is selected from a list consisting of: nitrogen, nitrous oxide, ethanol, methanol, sulfur hexafluoride, cyclohexane, methane, toluene, p-xylene, tetrafluoromethane, perfluoroethane, tetrafluoroethylene, 1,1-difluoroethylene, carbon dioxide or mixtures thereof; preferably carbon dioxide.

[0037] In an embodiment for better results, the method further comprises a step of heating the high-pressure chamber to 35-90 °C, preferably at 60 °C, for 5-60 min, preferably for 15 min.

[0038] Another aspect of the present disclosure relates to a portable syringe for obtaining an expanded foam material of the present disclosure comprising a high-pressure chamber for the injectable expandable composition of the present disclosure;

a pressurizing agent container;

an inlet for the pressurizing agent into the pressure chamber;

an outlet for the expanded foam material of the present disclosure;

heating system to heat the pressure chamber at a temperature of 35-90 °C, preferably at 60 °C, wherein the high-pressure chamber is able to work at a pressure between 20-150 bar, preferably 45-120 bar, more preferably 45-50 bar.

[0039] A kit comprising the injectable expandable composition of the present disclosure and the portable syringe for obtaining an expanded foam material of the present disclosure.

[0040] **Table 1** establishes a comparison between synthetic and biologically inspired adhesives.

[0041] **Table 1** presents the features required for bone adhesive materials and technologies to serve its purpose, wherein + represents a good level of the feature; ++ represents a very good level of the feature; - represents a negative level of the feature; and NA, no available information in the literature.

	Synthetic adhesives	Biologically inspired	PCL pDA pMAA
High level of adhesion in wet environment	+	++	+
Mechanical stability	+	-	++
Easy application (RT conditions)	+	NA	-
Adequate working time	++	++	+
Rapid setting time (1-10 min)	++	NA	+
Low exothermic reactions	-	++	++
Non-toxic and biocompatible	-	++	++
Allow healing of fracture	-	NA	++

[0042] From Table 1 it is clear that the best material should be in the intersection of a synthetic adhesive and a biomimetic approach. This was the rational for the development of a new bone adhesive

material described in the present disclosure: a polycaprolactone based adhesive modified with polydopamine and polymethacrylic acid (PCL pDA pMAA).

[0043] Polycaprolactone (PCL) is a biocompatible, bioresorbable polymer, FDA approved for several applications in the human body, and widely studied for the preparation of bone implants. The ease of processing of polycaprolactone (PCL), given by its soluble nature in organic solvents, low melting point and glass transition temperature, make it very attractive for processing either by solvent-based technologies, in particular wet-spinning or electrospinning; or melt-based technologies, in particular extrusion, gas foaming or 3D printing.

[0044] Polycaprolactone (PCL) is an inert material, which, while being an advantage by conferring it biocompatible properties is also a disadvantage in the sense that the polymer is not bioactive per se. One way to overcome this is to functionalize the polymer. For example, the enhancement of the poor bioadhesive properties of polycaprolactone can be done by coating PCL with polydopamine (pDA).

[0045] Polydopamine (pDA) is a molecule inspired in the composition of mussel adhesive properties. Its ability to self-polymerize provide a versatile and easy way to functionalize and coat a large variety of materials, from metals to ceramics and polymers.[4,5] Different studies report the functionalization of polycaprolactone substrates for biomedical applications. Kim et al. report the decoration of polycaprolactone microspheres with pDA for cell therapy approaches [6]. In another work, the same group reports the design of inter-fiber networks of electrospun polycaprolactone fibers with pDA with enhanced mechanical and adhesive properties [7]. Not only dopamine enhances the adhesive properties of the material but also may induce bioactivity of the structures. Particularly it has been reported that coating PCL with poydopamine may induce the mineralization of the structure and the formation of a bone-like hydroxyapatite layer, promoting bone-bone bonding [8–10]. Hence, this approach represents major advantages to overcome the lack of biomineralization of pure PCL matrices.

[0046] On the other hand, polymethacrylic acid (pMAA), belongs to the acrylate family of synthetic adhesives. Despite their excellent adhesive properties, the use of these materials has been hindered particularly due to their toxicity. Nonetheless, the possibility to control the its concentration in a polymeric blend may overcome biocompatibility issues, while still enhancing the adhesiveness of the matrices, as demonstrated by Kim et al [11].

[0047] In this present disclosure it was evaluated, not only the possibility to design a new bone adhesive but also the ability to create a bioactive and adhesive porous foam structure, which can be directly delivered into the site of lesion. In an embodiment, the composition described in the present subject-matter, namely the polycaprolactone-based polymeric material surprisingly confer adequate morphological, mechanical and biological properties to the implants. Rheological properties were tuned

to allow the extrusion of the material from a dedicated surgical tool for in situ foaming, using subcritical carbon dioxide as porogen, designed specifically for this application.

Brief Description of the Drawings

[0048] The following figures provide preferred embodiments for illustrating the description and should not be seen as limiting the scope of disclosure.

[0049] **Figure 1:** Represents an embodiment of the device of the present disclosure wherein;

(1) represents the mechanical piston;

(2) represents the high-pressure chamber;

(3) represents the extrusion tip;

(4) represents the pressurizing agent inlet, namely CO_2;

(5) represents the handle;

(6) represents the sealing top.

[0050] **Figure 2:** Represents an embodiment of the device of the present disclosure with the high-pressure chamber open.

[0051] **Figure 3** schematically represents the chemical modification performed and the rational for the functionalization of the material with pDA and pMAA, and it also presents the characterization of the different samples, by SEM, FTIR and XPS.

[0052] **Figure 4:** Adhesion testing on glass surface (**A**) Force versus displacement curve for the different samples studied; (**B**) Adhesion strength for the different samples studied.

[0053] **Figure 5:** Adhesion strength on spinal plugs (**A**) Force versus displacement curve and photograph of sample under testing; (**B**) Adhesion strength determined as a function of the material used; (**C-E**) macroscopic pictures of spinal plugs with different formulations after tensile testing: PCL, PCL pDA, PCL pDA pMAA respectively. Yellow line represents site of fracture.

[0054] **Figure 6:** Cell viability determined after the MTS assay

[0055] **Figure 7:** Ex vivo testing of antero-lateral surgical technique in a porcine spine and micro computed tomography cross-section images (A and B) of the samples. Top row: PCL pDA pMAA extruded through a syringe; Bottom row: PCL pDA pMAA extruded through the high-pressure device into the intervertebral disk space.

[0056] **Figure 8:** Represents an embodiment of A) SEM images of PCL pDA pMAA immersed in SBF solution at different time points (scale bar: 5 μm); B) Ca/P atomic ratio calculated from the EDS data; C) XRD spectra of PCL pDA pMAA immersed at different time points, compared with PCL as control (CTR).

[0057] **Figure 9:** In vivo evaluation of adhesion and bio-integration of the PCL pDA pMMA with native tissues: histological analysis (Masson's Trichrome).

[0058] **Figure 10:** In vivo spinal fusion performance assessment of PCL pDA pMMA as compared to PEEK cage + autograft (control) in a porcine model after 6 months: fusion was evaluated by radiological imaging (X-ray), micro-computed tomography (micro-CT) and histological analysis (Masson's Trichrome).

Detailed Description

[0059] The present disclosure relates to compositions, devices, kits and methods for use in an approach for the in situ foaming of polymers for bone tissue defect filling/fusion.

[0060] An aspect of the present disclosure relates to an injectable expandable composition for use in medicine, veterinary or cosmetic, comprising a polycaprolactone particle filler; a polydopamine adhesive bound to said filler; a polymethacrylic acid plasticizer bound to said polydopamine adhesive.

[0061] In an embodiment, the polycaprolactone doping with dopamine was carried out as follows. Poly-dopamine was grafted on the surface of PCL microparticles following the reported procedure by Kim et al [6] and Choi et al [7]. Briefly, PCL beads (Polycaprolactone average Mn 45.000, Sigma) were milled to powder using an Ultra centrifugal mill (Retsch ZM200) under liquid nitrogen. A solution of 10 x 10^{-3} M Tris-HCl (TRIZMA® hydrochloride, CAS 1185-53-1, Sigma) was prepared and the pH adjusted to 8.5, using a sodium hydroxide (CAS 1310-73-2, Fisher Chemical, UK) solution (1 M). Dopamine-hydrochloride (CAS 62-31-7, Sigma) was added to the solution (2mg.mL^{-1}) as well as the PCL microparticles and the solution was stirred overnight. The change in colour to dark brown indicates that the polymerization took place. The particles were recovered by filtration and were dialysed for three days in order to eliminate any residual monomer that did not react. The final samples of PCL-pDA were recovered and dried by freeze-drying.

[0062] In an embodiment, the polycaprolactone doped with dopamine and further grafted with polymethacrylic acid (pMAA) was performed as follows. Grafting polymethacrylic acid (pMAA) to PCL pDA samples was carried out in a subsequent step. In the formulation described in this disclosure, 20% wt/wt pMAA in respect to PCL pDA was tested. Based on the procedure reported by Kim and co-workers[11], 10 wt% of N-(3-Dimethylaminopropyl)-N'-ethylcarbodiimide polymer-bound (EDC) (EC-No 217-579-2) and N-Hydroxysuccinimide (NHS) (CAS 6066-82-6) were dissolved in poly(methacrylic acid, sodium salt) (pMAA) solution (CAS 79-41-4). The correspondent amount of PCL pDA was then added, together with 1 mL phosphate buffered solution (PBS) solution. The reaction was allowed to take place

for 4 hours, after which the samples was precipitated with ethanol for 12 hours. The monomers which did not reacted were washed with ethanol and the sample was left to dry at room temperature.

[0063] In an embodiment, the characterization was performed by scanning electron microscopy (SEM), Fourier transform infrared spectroscopy (FTIR) and/or X-ray photoelectron spectroscopy (XPS).

[0064] In an embodiment, morphological properties of the samples prepared were analyzed by scanning electron microscopy (SEM) (JSM-6010 LV, JEOL, Japan). The samples were fixed by mutual conductive adhesive tape on aluminium stubs and were sputter-coated with gold before analysis.

[0065] In an embodiment, Fourier Transform Infrared Spectroscopy - FTIR analysis was used to evaluate the chemical modifications of PCL doped with pDA and pMAA. The samples were powdered and mixed with potassium bromide, and the mixture was moulded into a transparent pellet using a press (Pike). Spectra were recorded at 32 scans with a resolution of 2 cm^{-1} (Shimadzu — IR Prestige 21).

[0066] In an embodiment, X-ray photoelectron spectroscopy (XPS) was used to evaluate the surface chemistry of the samples prepared to confirm the doping of PCL with dopamine. The chemical composition of 3 samples was examined by XPS surface measurements. The C 1s, O 1s, N 1s, Na 1s and survey spectra were recorded using a Kratos Axis-Supra instrument. Monochromatic X-ray source Al Kα (1486.6 eV) was used for all samples and experiments. The residual vacuum in the analysis chamber was maintained at around 8.5x10-9 torr. The samples were fixed to the sample holder with double sided carbon tape. Charge referencing was done by setting the binding energy of C 1s photo peak at 285.0 eV C1s hydrocarbon peak. An electron flood gun was employed to minimize surface charging i.e., charge compensation.

[0067] In an embodiment, the mechanical characterization was also carried out. Adhesion tests of the materials were performed in a first approach using a glass substrate, in particular a glass surface. All the adhesion experiments were conducted at room temperature. A contact area of 20 × 25 mm was employed. The material was melted, and the two plates were superimposed and maintained until solidification of the material. The bonded glass slides were placed on a universal testing machine with a load cell of 1kN (INSTRON 5540, Instron Int. Lda, High Wycombe, UK)) in tensile mode and a crosshead speed of 2 $mm.min^{-1}$. The load was applied until detachment, which was confirmed by the graphic. The lap shear bonding strength was determined from the maximum of the force–deformation curve obtained. The results are presented as the average of at least three samples.

[0068] In an embodiment, the adhesion spinal plugs experiments were also performed: Ex vivo porcine spinal plugs (6 x 6 x 15 mm) were prepared from adjacent vertebrae. The intervertebral disc was removed, and vertebrae surfaces debrided by the aid of a surgical curette. Application of the PCL formulations in-between spinal plugs was performed as described for the glass surface testing experiments. The shear bond strength test was performed with a crosshead speed of 2 $mm.min^{-1}$ until

complete fracture of the specimens. The maximum force (N) was recorded on a computer and divided by the bonded area (in mm^2) in order to calculate the bond strength (N/cm^2).

[0069] In an embodiment, the fractures were observed under a stereomicroscope (STEMI 1000, ZEISS)

In an embodiment, cytotoxicity studies were conducted. An immortalized mouse lung fibroblasts cell line (L929), from European Collection of Cell Cultures, UK, was maintained in basal culture medium DMEM (Dulbecco's modified Eagle's medium; Sigma–Aldrich, Germany), plus 10% FBS (heat-inactivated fetal bovine serum, Biochrom AG, Germany) and 1% A/B (antibiotic–antimycotic solution, Gibco, UK). Cells were cultured in a humidified incubator at 37 °C in a 5% CO_2 atmosphere. The cytotoxicity evaluation was performed in accordance with ISO 10993-5:2009 guidelines. Confluent L929 cells were harvested and seeded in a 96 well plate (BD Biosciences, USA). Briefly, 100 µl of cell suspension with a concentration of 1 x 10^4 cells ml^{-1} were added to the well. Cells were statically cultures for 24 hours in DMEM medium under the culture conditions previously described. The indirect contact was performed replacing the culture medium with the materials leachable. The leachables were obtained after 24 hours of extraction using a ratio 100 mg of material in 1 mL supplemented DMEM. A latex extract was used as positive control for cell death, and for negative control cell culture medium was used. The samples were cultured for 24 hours under a 5% CO_2 atmosphere at 37 °C and the cell viability was evaluated by the MTS assay. This assay is based on the bioreduction of a tetrazolium compound 3-(4,5-dimethylthiazol-2-yl)-5-(3-carboxymethoxyphenyl)-2-(4-sulphofenyl)-2H-tetrazolium) (Cell Titer 96® Aqueous Solution Cell Proliferation Assay, Promega, USA) into a water soluble brown formazan product. This was quantified by UV spectroscopy, reading the formazan absorbance at 490 nm in a microplate reader (Synergy HT, Bio-Tek Instruments, USA). The results are presented as a function of the absorbance for cells cultured in DMEM and correspond to the average of at least three measurements (± standard deviation).

[0070] In an embodiment, **Fig. 1** represents the device developed to apply, by extrusion, the PCL pDA pMAA now disclosed comprising a mechanical piston (1), a high-pressure chamber (2), a extrusion tip (3) and a CO_2 inlet (4).

[0071] In an embodiment, the *in-situ* extrusion of modified PCL into bone defect (intervertebral disc space) was conducted as follows. Briefly, the extrusion is performed after loading the polymer (PCL pDA pMAA) in the high-pressure chamber, which is then sealed and pressurized with carbon dioxide at 50 bar (Air Liquide, 99.998 mol%). The device is heated up, in particular to 60 °C, to promote the plasticization of the polymer and after, for example, 15 minutes of settling time, under these conditions it is possible to extrude the material through the tip of the device. The polymer is extruded *in situ* to the defect site and shaped to the defect geometry.

[0072] The defect site is performed in the intervertebral disc space. In an embodiment, the morphological structure and the calculation of the morphometric parameters that characterize the samples of PCL pDA pMAA were evaluated by micro-computed tomography (micro-CT) using a Skyscan 1272 equipment (Bruker, Germany) with penetrative X-rays of 50 KeV and 200 µA, in high-resolution mode with a pixel size of 21.6 µm. A CT analyser (v1.15.4.0, 2012-2015, Bruker Micro-CT) was used to calculate the parameters from the 2D images of the matrices.

[0073] In an embodiment, to evaluate the bioactivity of the samples of PCL pDA pMAA, these were soaked in 10 mL of simulated body fluid (SBF) solution during 1, 3, 7 and 14 days at 37 °C. The SBF was prepared by dissolving NaCl, $NaHCO_3$, KCl, $K_2HPO_4.3H_2O$, $MgCl_2.6H_2O$ and Na_2SO_4 in distilled water and buffered with Tris (Hydroxymethyl) Aminomethane buffer and HCl to reach a pH value of 7.4, following the protocol described by Kokubo and Takadama [T. Kokubo, H. Takadama, How useful is SBF in predicting in vivo bone bioactivity? *Biomaterials* **2006**, *27*, 2907–2915.]. Tests were carried out in sterile conditions. Upon removal from SBF, the samples were rinsed with sterile distilled water and left to air dry before further analysis. PCL samples were used as negative control.

[0074] In an embodiment, scanning electron microscopy coupled with energy dispersive X-ray spectroscopy (SEM/EDS) was carried out as follows. The morphology and composition of the calcium-phosphates deposited on the surface of the matrices was investigated with a JSM-6010 LV, JEOL microscope with an integrated energy dispersive X-ray spectroscope (EDS) (INCAx-Act, PentaFET Precision, Oxford Instruments). To perform SEM, a conductive gold coating was applied to the samples. For EDS, the analyses were conducted at low vacuum and without any coating.

[0075] In an embodiment, X-ray diffraction (XRD) was used to evaluate the crystalline planes of the calcium-phosphates precipitated on the surface of the samples. The XRD diffraction patterns were collected on a Bruker D8 Discover, at a voltage of 40 kV and a current of 40 mA in a 2θ range from 10° to 60° with a step size of 0.02°.

[0076] Polycaprolactone (PCL) has been reported to be an excellent polymer for the development of scaffolds for tissue engineering, particularly for bone tissue engineering. Its properties, particularly its biocompatibility and degradation rate make it suitable for different applications in the field of regenerative medicine. However, this polymer per se does not present any bioactivity and it presents weak adhesive properties. Different strategies have been described in the literature to overcome these drawbacks. The triangular approach on tissue engineering of combining a polymeric scaffold with bioactive agents and cells is one way to overcome the fact that polymers are usually inert but have unequalled morphological and mechanical properties. In the present disclosure, a two-step approach for the modification of PCL was followed, providing it adhesive and bioactive properties.

[0077] **Figure 2** represents the device wherein the high-pressure chamber (2) is unscrewed of the metal syringe structure (5) and the presence of both ends of the mechanical piston (1). This referred mechanical piston when pressed and closed creates an increased pressure in the high-pressure chamber (2) which forces the chemical compound leaving the chamber (2) by the extrude tip (3).

[0078] **Figure 3** schematically represents the chemical modification performed and the rational for the functionalization of the material with pDA and pMAA, and it also presents the characterization of the different samples, by SEM (scale bars 500 µm and 10 µm), FTIR and XPS.

[0079] In an embodiment, SEM images show all three types of samples, the pure PCL microparticles and the PCL microparticles modified with pDA and pDA + pMAA. At a higher magnification image, it is possible to see that addition of pDA results in a rougher surface, as compared to PCL. When adding pMAA this effect is even more noticeable. Chemical analysis of the polymers was carried out by FTIR and XPS. By FTIR it is possible to observe, as indicated by the arrows in the figure, the characteristic peak of the amine N-H stretching group in pDA at 3440 cm^{-1}. The presence of a single bands indicates that the secondary amine has reacted with PCL and a primary amine is present in the PCL pDA formulation. This is consistent with the information reported in the literature, namely on the description of the chemical reaction involved between dopamine and different substrates at pH 8.5 and Tris-solution[5,12]. When pMAA is grafted the amine group of dopamine may react with the carboxylic group of methacrylic acid and an amide is possibly formed. These observations are supported by the appearance of the characteristic bands of N-H bending of the amide II band at 1550-1510 cm^{-1} and the N-H stretch at 3500-3400 cm^{-1}.

[0080] In an embodiment, the adhesive properties of the materials of the present subject-matter were characterized by mechanical testing. Two different studies were carried out in different conditions to evaluate the adhesion strength of PCL. In a first approach the adhesive properties were tested in a glass surface. Two glass plates were glued with the different materials and were subjected to a tensile force to evaluate the maximum load at detachment. **Fig. 4A** represents the load applied versus the extension and as can be observed, both PCL pDA and PCL pDA pMAA present similar behaviour and higher adhesive properties than PCL itself. Both pDA modified samples present maximum load before detachment between 200 and 300 N, whereas highest values were observed for the PCL pDA (265 N load).

[0081] In an embodiment, the adhesion strength can be determined from the maximum load taking into consideration the surface area. **Fig. 4B** presents the differences between the samples studied. PCL presents an adhesive strength of 0.074 (±0.02) N/cm^2, PCL pDA of 16.2 (±2.4) N/cm^2 and PCL pDA pMAA of 13.7 (±0.6) N/cm^2. In the embodiments, it was shown that modifying polycaprolactone with polydopamine and polydopamine plus methacrylic acid significantly enhances the mechanical properties

of the polymer, particularly the adhesive properties of polycaprolactone ($p<0.001$). The differences in adhesion strength between PCL pDA and PCL pDA pMAA were, however not significantly different. The adhesive strength was further evaluated in spinal plugs, cut with a regular geometry. Adhesion with PCL, PCL pDA and PCL pDA pMAA was evaluated and the results are presented in **Fig. 5**.

[0082] In an embodiment, cytotoxicity of the materials prepared was assessed by the MTS assay, according to the protocol described in the ISO 10993-5:2009. Extracts of the different formulations were tested and the viability was determined as a function of the negative control. **Figure 6** presents the results of cellular viability after 24 hours of cell culture in contact with the leachables of the materials, the cells may be added to the injectable expandable composition or to the expanded foam material after extrusion.

[0083] In an embodiment, the results demonstrate that the materials produced are non-cytotoxic once viability is above 70 % in all groups. PCL pDA pMAA before and after extrusion presents distinct effect on cell viability (72 % and 85 %, respectively), whereas the final form of the biomaterial after extrusion presents a more favourable cellular response.

[0084] In an embodiment, the development of porous and interconnected structures from polycaprolactone has been explored through various different techniques. In the present disclosure, it was developed a portable high-pressure device (**Fig. 1**) for *in situ* polymer foaming based on the principles of gas foaming and extrusion. The use of supercritical carbon dioxide foaming for the preparation of porous structures for tissue engineering has been explored since 1996, when Mooney and coworkers proposed the use of CO_2 as a porogen agent for the preparation of poly-lactic acid foams [D. J. Mooney, D. F. Baldwin, N. P. Suh, J. P. Vacanti, R. Langer, *Biomaterials* **1996**, *17*, 1417]. The use of carbon dioxide as a porogen agent has significant advantages over others, namely the fact that this is a physical foaming agent. No chemical reaction takes place upon foaming, reducing the risk of production of any by-products that may be toxic. On the other hand, carbon dioxide foaming can be carried out under milder operating conditions due to the ability of carbon dioxide to act as a plasticizing agent and reduce the glass transition temperature and melting temperature of the polymer. Additionally, the polymer viscosity is also reduced improving the ease of manipulation and allowing an appropriate working time. Following the same principle, extrusion using carbon dioxide has become particularly interesting for the development of porous structures in a continuous mode, however, its potential has not been fully explored as large quantities of raw-materials are usually required in an extruder.

[0085] Curia and co-workers have demonstrated the effect of carbon dioxide on melting temperature depression and the viscosity reduction of polycaprolactone under different operating conditions [13].

Their work shows that PCL (Mw 10,000) pressurized with 50 bar suffers a decrease in melting temperature of nearly 10 °C and a reduction in viscosity of nearly 50% comparing to its value at the same temperature at ambient pressure. In an embodiment, the preferred operating conditions are 60 °C and 50 bar. In order to mimic the antero-lateral surgical approach for lumbar interbody fusion, PCL pDA pMAA was extruded through the high-pressure portable device into the site of the defect, created in the intervertebral disc space of an ex vivo porcine spine, as shown in **fig. 5 and 7**. Hardening of the foam occurred within few seconds allowing immediate stabilization of the vertebrae. Such approach is deemed compatible for application to any other bone defects that require an adhesive filler and stabilization for regeneration. As control, the samples were also injected in the defect site through a syringe at ambient pressure. The solidified structures were taken from the defect site and the morphological parameters were analysed by micro-computed tomography. **Fig. 7** presents the 3 axial cross-sections of both samples and as it can be observed the sample injected through the syringe is highly compact and presents residual porosity and interconnectivity. On the other hand, the sample extruded through the high-pressure device presents an interesting morphological profile, which is comparable to trabecular bone (**Table 2**).

[0086] **Table 2.** Morphological parameters of the samples extruded into the bone defect, determined by micro-CT at room temperature.

	PCL pDA pMAA extruded through syringe	PCL pDA pMAA extruded through high pressure device	Reference values for trabecular bone[14]
Porosity (%)	3	45	52-96
Interconnectivity (%)	-	28	-
Mean pore size (μm)	-	169	450-1310
Density (mm^{-1})	2	17	7-34
Degree of anisotropy	2	2.06	1.1-2.38

[0087] In an embodiment, the bioactivity or the ability of implants for bone regeneration to induce the formation of a bone-like hydroxyapatite layer has been reported to be a factor that strongly enhances the integration of the scaffold with the tissue, and therefore, the success of healing and tissue regeneration. The bioactive properties of PCL pDA pMAA were evaluated in a simulated body fluid, and

as a control PCL samples were used. The samples were extruded through the device in the conditions described above (60 °C and 50 bar). **Fig. 8** presents the SEM images of the materials after immersion as well as the chemical characterization of the calcium-phosphates precipitated on the surface.

[0088] In an embodiment, the adhesive and bioactive properties of PCL pDA pMAA were assessed in a porcine spinal interbody fusion model for 6 months. The intervertebral disk was surgically removed and PCL pDA pMAA was extruded by the device to fill the void site. Immediate hardening of the material and adhesion to surrounding tissues occurred and no spinal instrumentation was used for stabilisation. **Fig. 9A** reveals integration of the PCL pDA pMAA with native tissues while **Fig. 9B** highlights the migration of surrounding cells to the porous core of the PCL pDA pMAA structure, becoming populated by cells to support new tissue formation. In vivo spinal fusion performance, as compared to PEEK cage + autograft (control), was further evaluated by radiological imaging (X-ray), micro-computed tomography (micro-CT) and histological analysis (Masson's Trichrome) (**Fig. 10**). Interbody fusion is seen in the intervertebral space treated by PCL pDA pMAA, evidenced by a continuous bone mass between upper and lower vertebral bodies which indicate osseous development within the previously void site.

[0089] A new PCL-based biopolymer was synthesized to achieve improved bioactive and adhesive properties aiming application as bone adhesive for diverse trauma and pathology-driven needs in bone surgery. Such biopolymer, composed of PCL pDA and pMAA was produced into a foam through a dedicated portable high-pressure device, towards direct application in bone defects. Such in situ foaming resulted in immediate stabilization of osseous components, while resulting in a 3D structure with morphological properties similar to those found in trabecular bone.

[0090] The term "comprising" whenever used in this document is intended to indicate the presence of stated features, integers, steps, components, but not to preclude the presence or addition of one or more other features, integers, steps, components or groups thereof.

[0091] It will be appreciated by those of ordinary skill in the art that unless otherwise indicated herein, the particular sequence of steps described is illustrative only and can be varied without departing from the disclosure. Thus, unless otherwise stated the steps described are so unordered meaning that, when possible, the steps can be performed in any convenient or desirable order.

[0092] Flow diagrams of particular embodiments of the presently disclosed methods are depicted in figures. The flow diagrams do not depict any particular means, rather the flow diagrams illustrate the functional information one of ordinary skill in the art requires to perform said methods required in accordance with the present disclosure.

[0093] The disclosure should not be seen in any way restricted to the embodiments described and a person with ordinary skill in the art will foresee many possibilities to modifications thereof.

[0094] The above described embodiments are combinable.

[0095] The following claims further set out particular embodiments of the disclosure.

[0096] The following documents are herewith expressly incorporated by reference.

[1] D. F. Farrar, Bone adhesives for trauma surgery: A review of challenges and developments. *Int. J. Adhes. Adhes.* **2012**, *33*, 89–97.

[2] N. V Shah, R. Meislin, *Orthopedics* **2013**, *36*, 945.

[3] A. P. Duarte, J. F. Coelho, J. C. Bordado, M. T. Cidade, M. H. Gil, Surgical adhesives: Systematic review of the main types and development forecast. *Prog. Polym. Sci.* **2012**, *37*, 1031–1050.

[4] H. Lee, S. M. Dellatore, W. M. Miller, P. B. Messersmith, *Science* **2007**, *318*, 426.

[5] Y. Liu, K. Ai, L. Lu, Polydopamine and its derivative materials: Synthesis and promising applications in energy, environmental, and biomedical fields. *Chem. Rev.* **2014**, *114*, 5057–5115.

[6] M. Kim, J. S. Kim, H. Lee, J. H. Jang, *Macromol. Biosci.* **2016**, *16*, 738.

[7] W. Choi, S. Lee, S. H. Kim, J. H. Jang, *Macromol. Biosci.* **2016**, 824.

[8] D. Zhang, O. J. George, K. M. Petersen, A. C. Jimenez-Vergara, M. S. Hahn, M. A. Grunlan, *Acta Biomater.* **2014**, *10*, 4597.

[9] J. Xie, S. Zhong, B. Ma, F. D. Shuler, C. T. Lim, *Acta Biomater.* **2013**, *9*, 5698.

[10] M. Mabrouk, D. Bijukumar, J. A. S. Mulla, D. R. Chejara, R. V. Badhe, Y. E. Choonara, P. Kumar, L. C. Du Toit, V. Pillay, *Mater. Lett.* **2015**, *161*, 503.

[11] J. H. Kim, J. I. Lim, H. K. Park, *J. Porous Mater.* **2013**, *20*, 177.

[12] B. H. Kim, D. H. Lee, J. Y. Kim, D. O. Shin, H. Y. Jeong, S. Hong, J. M. Yun, C. M. Koo, H. Lee, S. O. Kim, *Adv. Mater.* **2011**, *23*, 5618.

[13] S. Curia, D. S. A. De Focatiis, S. M. Howdle, *Polym. (United Kingdom)* **2015**, *69*, 17.

[14] L. M. Mathieu, T. L. Mueller, P. Bourban, D. P. Pioletti, R. Müller, J.-A. E. Månson, *Biomaterials* **2006**, *27*, 905.

[15] P. **J. Ginty**. *et. al,* Mammalian cell survival and processing in supercritical CO_2 **2006,** in Proceedings of the National Academy of Sciences, vol. 103, no.19, pag. 7426-31.

C L A I M S

1. An injectable expandable composition comprising:
   a polycaprolactone particle filler;
   a polydopamine adhesive bound to said polycaprolactone particle filler;
   a polymethacrylic acid plasticizer bound to said polydopamine adhesive.

2. The injectable expandable composition according to the previous claim comprising 70-89.5 % (w/$w_{composition}$) of polycaprolactone particle filler.

3. The injectable expandable composition according to the previous claim comprising 75-85 % (w/$w_{composition}$) of polycaprolactone particle filler.

4. The injectable expandable composition according to any one of the previous claims comprising 0.5-5 % (w/$w_{composition}$) of polydopamine adhesive.

5. The injectable expandable composition according to the previous claim comprising 1-4 % (w/$w_{composition}$) polydopamine adhesive.

6. The injectable expandable composition according to any one of the previous claims comprising 10-30 % (w/$w_{composition}$) of polymethacrylic acid plasticizer.

7. The injectable expandable composition according to the previous claim comprising 15-25% (w/$w_{composition}$) polymethacrylic acid plasticizer.

8. The injectable expandable composition according to any one of the previous claims, wherein the particles of polycaprolactone have a size from 900-100 μm.

9. The injectable expandable composition according to any one of the previous claims, wherein the particles of polycaprolactone have a size 750-200 μm, preferably from 600-300 μm.

10. The injectable expandable composition according to any one of the previous claims further comprising a compound selected from: a bone growth stimulant, a bone growth promoter, a growth hormone, a cell attractant, a drug molecule, cells, bioactive glass, bioceramics, or combinations thereof,

    wherein the drug molecule is an anti-inflammatory, antibiotic, antipyretic, analgesic, anticancer, or mixtures thereof; in particular dexamethasone;
    wherein the bone growth promoter is selected from: fibroblast growth factor, transforming growth factor beta, insulin growth factor, platelet-derived growth factor, bone morphogenetic protein, oxysterols, or combinations thereof;
    wherein cells are selected from: osteoblasts, osteoclasts, osteocytes, pericytes, endothelial cells, endothelial progenitor cells, bone progenitor cells, hematopoietic progenitor cells, hematopoietic stem cells, neural progenitor cells, neural stem cells, mesenchymal stromal/stem cells, induced pluripotent stem cells, embryonic stem cells, perivascular stem cells, amniotic fluid stem cells, amniotic membrane stem cells, umbilical cord stem cells, genetically engineered cells, bone marrow aspirate, stromal vascular fraction, or combinations thereof.

11. The composition for use in medicine comprising polycaprolactone; polydopamine; a polymethacrylic acid;

    wherein said composition is administrated in the form of an injectable expandable composition;
    wherein said injectable expandable composition comprises a polycaprolactone particle filler; a polydopamine adhesive bound to said filler; a polymethacrylic acid plasticizer bound to said polydopamine adhesive.

12. The composition for use according to the previous claim, wherein the composition is an implantable composition and/or an extrudable composition.

13. The composition for use according to any one of the claims 11-12 for treating a bone defect, for bone regeneration or for bone tissue engineering.

14. The composition for use according to any one of the claims 11-13 for bone fusion or for filling and fixing bone or tissue.

15. The composition for use according to any one of the claims 11-14, for treating, inhibiting or reversing vertebral column diseases or lesions.

16. The composition for use according to any one of the claims 11-15, for treating, inhibiting or reversing disorders of intervertebral disc.

17. An expanded foam material comprising the injectable expandable composition according to any one of the previous claims.

18. The expanded foam material according to the previous claims further comprising a compound selected from: a bone growth stimulant, a bone growth promoter, a growth hormone, a cell attractant, a drug molecule, cells, bioactive glass, bioceramics, or combinations thereof,
wherein the drug molecule is an anti-inflammatory, antibiotic, antipyretic, analgesic, anticancer, or mixtures thereof; in particular dexamethasone;
wherein the bone growth promoter is selected from: fibroblast growth factor, transforming growth factor beta, insulin growth factor, platelet-derived growth factor, bone morphogenetic protein, oxysterols, or combinations thereof;
wherein cells are selected from: osteoblasts, osteoclasts, osteocytes, pericytes, endothelial cells, endothelial progenitor cells, bone progenitor cells, hematopoietic progenitor cells, hematopoietic stem cells, neural progenitor cells, neural stem cells, mesenchymal stromal/stem cells, induced pluripotent stem cells, embryonic stem cells, perivascular stem cells, amniotic fluid stem cells, amniotic membrane stem cells, umbilical cord stem cells, genetically engineered cells, bone marrow aspirate, stromal vascular fraction, or combinations thereof.

19. A method for obtaining an expanded foam material according to the previous claims 17-18, comprising the steps of:
loading the injectable expandable composition described in any of the previous claims 1-16 in a high-pressure chamber;
sealing said high pressure chamber;
pressurizing said high pressure chamber at 20 – 150 bar, preferably at 50-60 bar;
heating the high-pressure chamber to 35-90 °C, preferably at 60 °C, for 5-60 min, preferably for 15 min.

20. A portable syringe for obtaining an expanded foam material described in the previous claims 1-16 comprising a high-pressure chamber for containing the composition described in any one of the previous claims 1-16;
a pressurizing agent chamber;
an inlet for the pressurizing agent in the pressure container;
an outlet for the expanded foam material;
heating system to heat the pressure chamber at a temperature of 35-90 °C, preferably at 60 °C,
wherein the high-pressure chamber is able to work at a pressure between 40-120 bar, preferably 45-120 bar, more preferably 50-60 bar.

21. A kit comprising the injectable expandable composition of any one of the claims 1-16, or the material described in any one of the previous claims and the portable syringe of the previous claim.

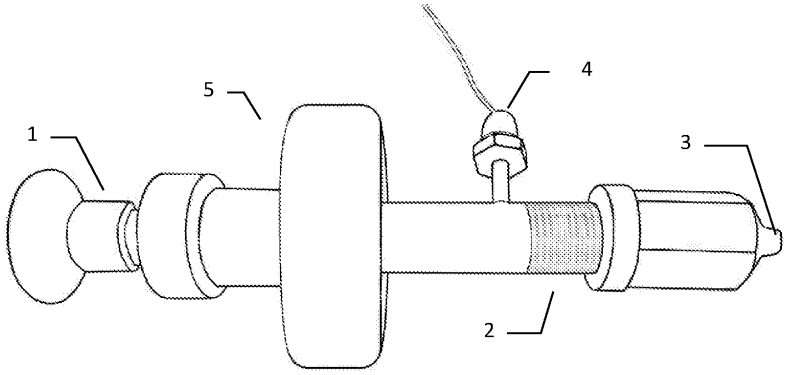

Fig. 1

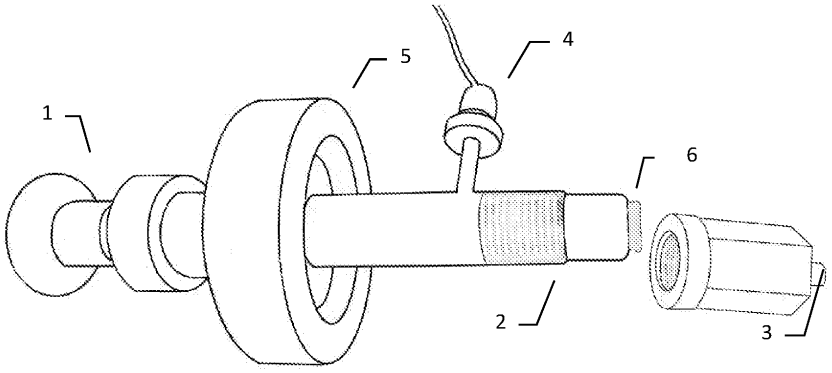

Fig. 2

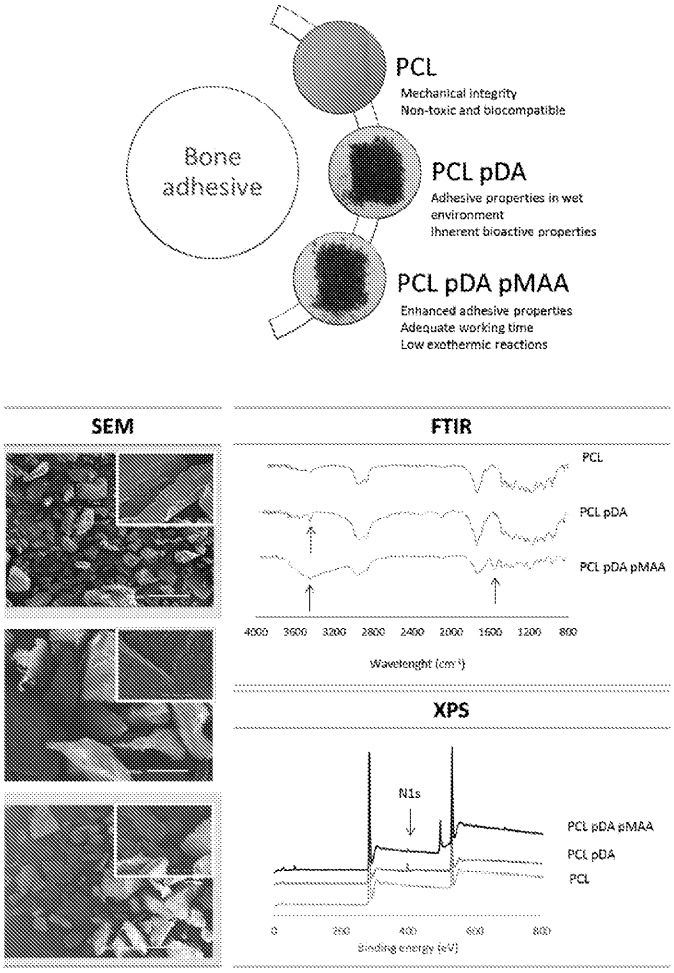
Bone adhesive
PCL
Mechanical integrity
Non-toxic and biocompatible
PCL pDA
Adhesive properties in wet environment
Inherent bioactive properties
PCL pDA pMAA
Enhanced adhesive properties
Adequate working time
Low exothermic reactions
SEM
FTIR
PCL
PCL pDA
PCL pDA pMAA
4000 3600 3200 2800 2400 2000 1600 1200 800
Wavelenght (cm⁻¹)
XPS
N1s
PCL pDA pMAA
PCL pDA
PCL
0 200 400 600 800
Binding energy (eV)

Fig. 3

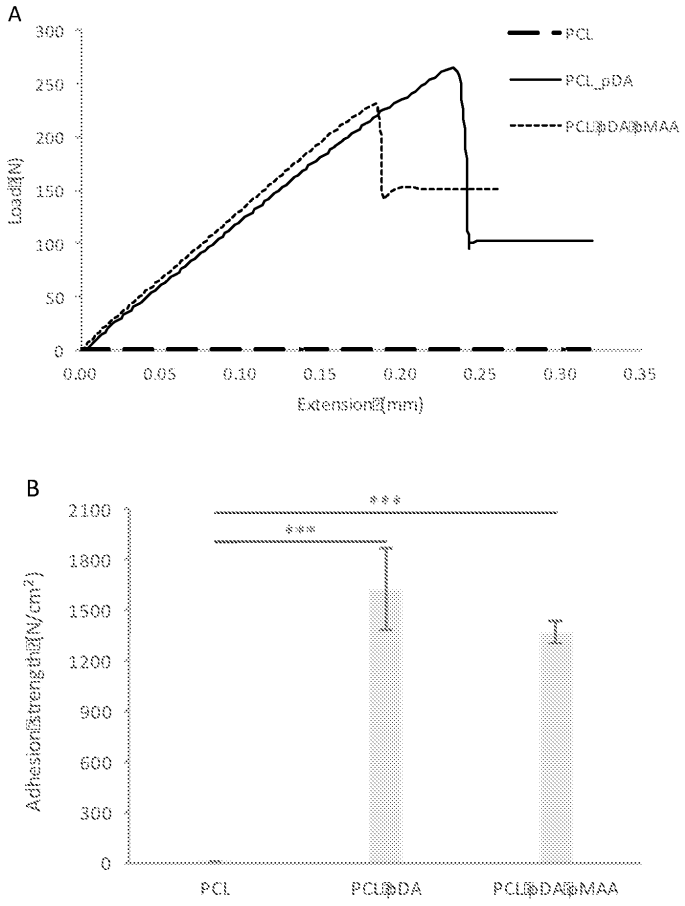
A
300
250
200
150
100
50
0
Load (N)
0.00
0.05
0.10
0.15
0.20
0.25
0.30
0.35
Extension (mm)
PCL
PCL_pDA
PCL@DA@MAA
B
2100
1800
1500
1200
900
600
300
0
Adhesion strength (N/cm²)
***
***
PCL
PCL@DA
PCL@DA@MAA

Fig. 4

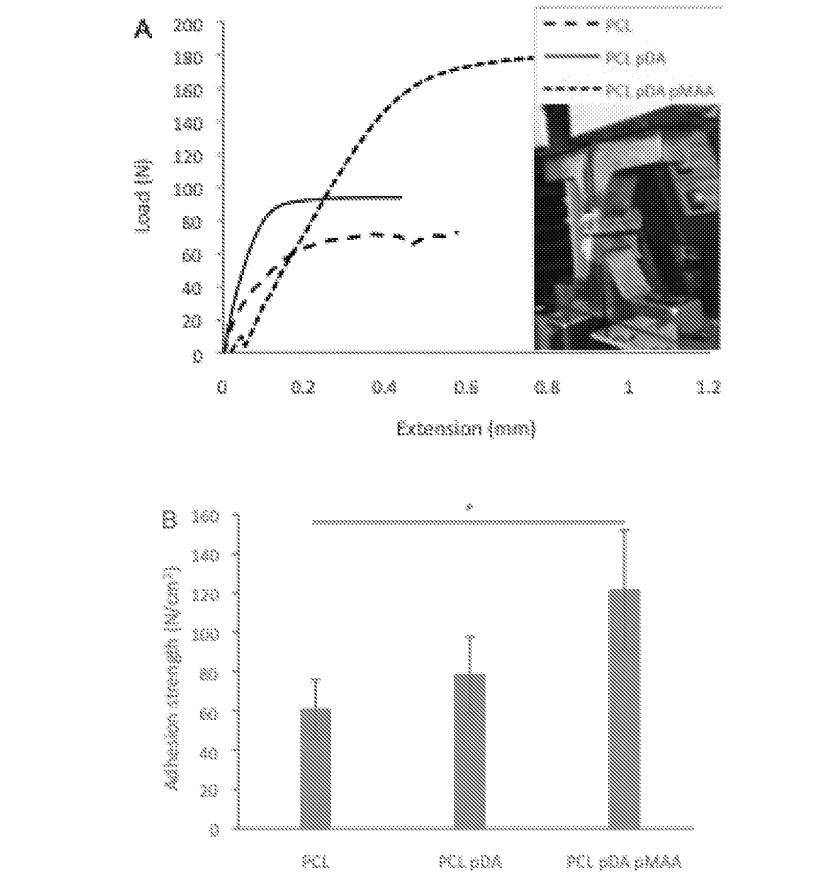
A
Load (N)
Extension (mm)
PCL
PCL pDA
PCL pDA pMAA
B
Adhesion strength (N/cm²)
PCL
PCL pDA
PCL pDA pMAA
C
D
E

Fig. 5

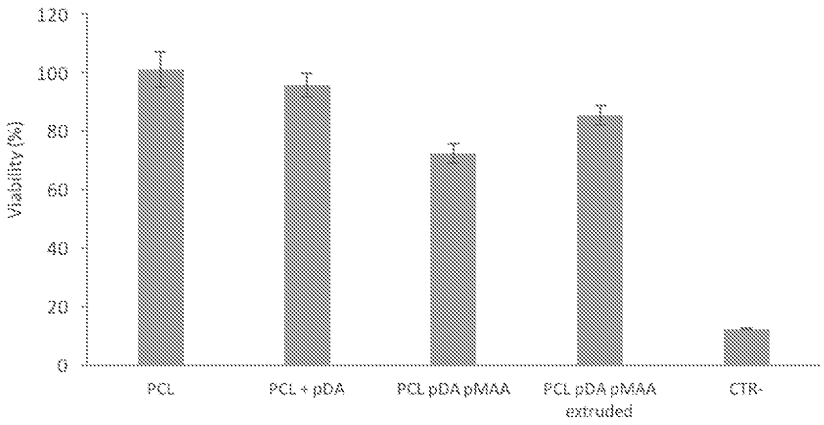
120
100
80
60
40
20
0
Viability (%)
PCL
PCL + pDA
PCL pDA pMAA
PCL pDA pMAA extruded
CTR-

Fig. 6

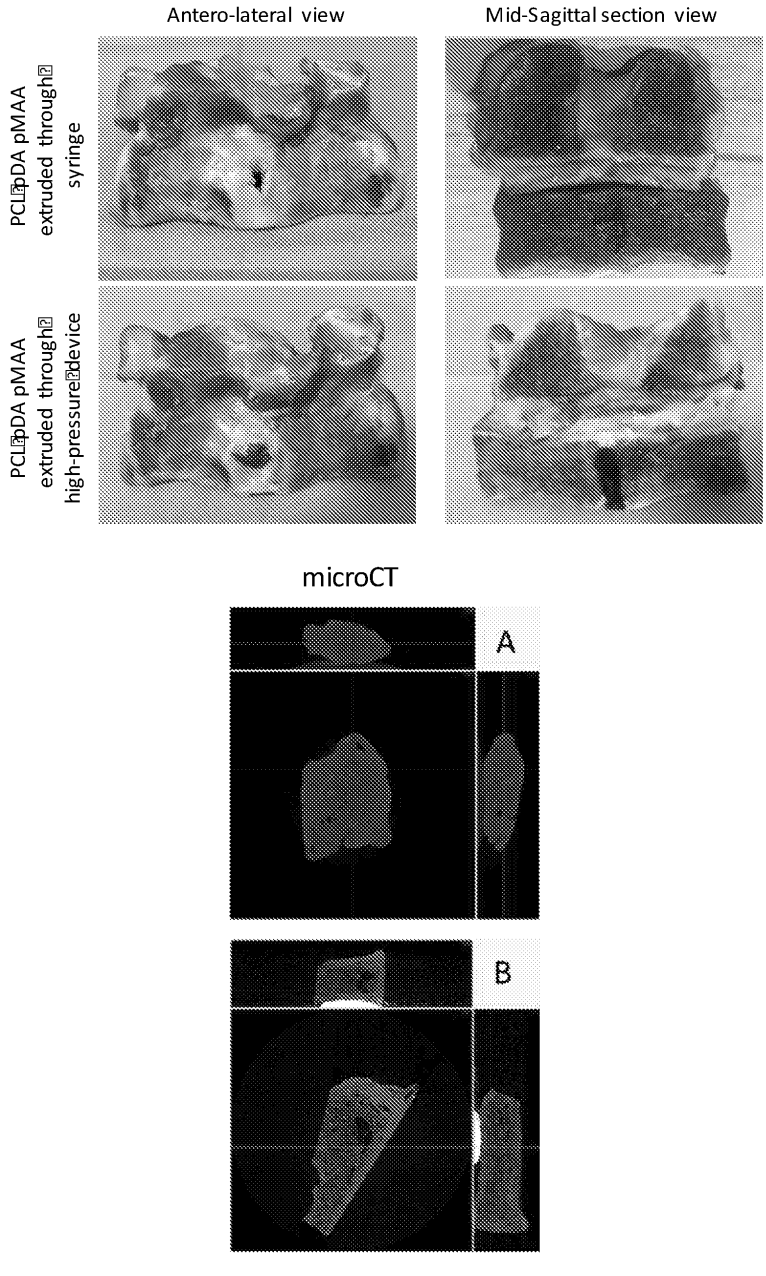
Antero-lateral view
Mid-Sagittal section view
PCL-pDA pMAA extruded through syringe
PCL-pDA pMAA extruded through high-pressure device
microCT
A
B

Fig. 7

A

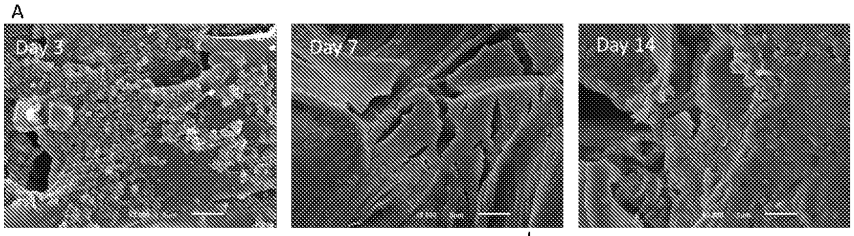

B

Immersion days	Ca/P ratio
1	1.58
3	1.83
7	1.61
14	2.18

C

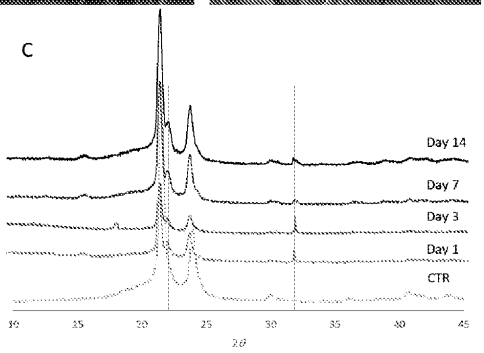

Fig. 8

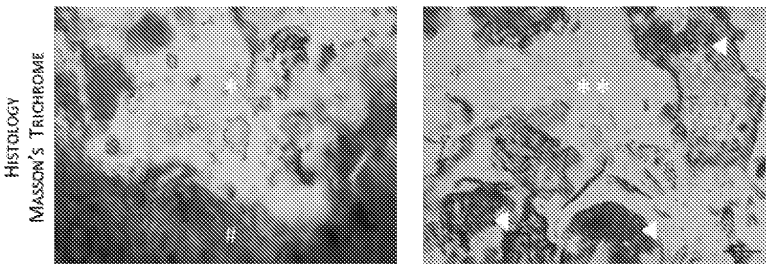
HISTOLOGY
MASSON'S TRICHROME
A. PCL pDA pMAA interface (*) with native tissue (#)
B. PCL pDA pMAA porous core (**) populated with cells (arrow head)

Fig.9

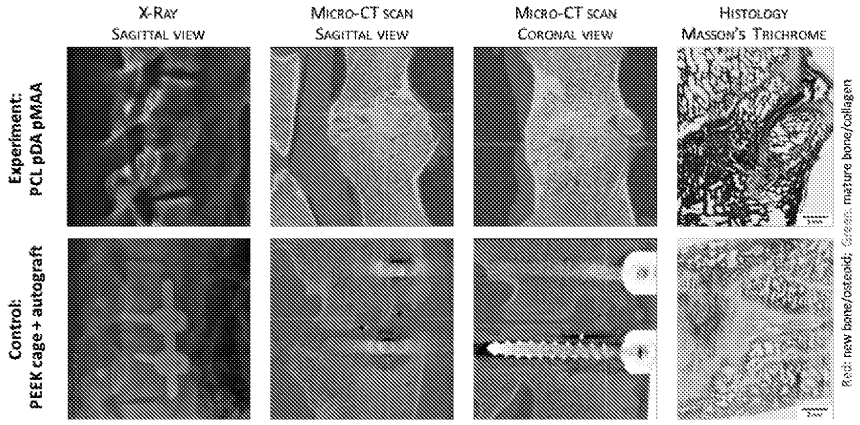
X-Ray
Sagittal view
Micro-CT scan
Sagittal view
Micro-CT scan
Coronal view
Histology
Masson's Trichrome
Experiment:
PCL pDA pMAA
Control:
PEEK cage + autograft
Red: new bone/osteoid; Green: mature bone/collagen

Fig.10

SECTION 3.

CHAPTER VII

Discussion, Future Perspectives and Conclusions

Discussion

Spinal fusion remains the standard of care for a wide range of spinal pathologies such as deformity, instability, degenerative disc disease or spinal fractures. The procedure aims to provide the mechanical stability and adequate osteoconductive environment required for bone fusion to occur between vertebral segments. Mechanical stability is ensured using implanted spinal hardware, while bone ingrowth is promoted by bone graft and/or bone substitute.

Despite its recognized effectiveness [1], important concerns persist about non-fusion rates [2], and instrumentation-related complications (IRC) [3] such as nerve damage, blood vessel damage, infection [4] or hardware failure [3,5]. These concerns have driven innovation and research in diversified fields, ranging from:

- Improving characteristics of the medical hardware, such as mechanical properties, surface properties, material porosity [6]
- Computer-assisted technologies such as neuronavigation and robotics, is becoming widespread to increase pedicle screw insertion accuracy [7]
- Development of bone graft substitutes, to replace autograft and/ or improve bone fusion rates [8]
- Advanced tissue engineering and regenerative approaches, based on biomaterials, cells and growth factors, to repair or replace damaged tissue [9]

For each approach, instrumentation remains as a fundamental element of the surgical procedure. Here lies the hypothesis of the present thesis – the development of a biological approach for an instrumentation-free spinal fusion. To achieve such functionality, the new biomaterial would require a set of specific characteristics:

1. Adhesive to vertebrae whilst structurally robust, to provide immediate stabilization of the vertebrae and intervertebral spacing, therefore avoiding instrumentation;
2. Injectable into the intervertebral disc space, for application through Minimally Invasive Spine Surgery techniques;
3. Osteoconductive properties, to induce bone formation and effective interbody fusion;
4. Biodegradable, to be replaced by new bone during the natural bone ingrowth process.

With the advent of the field of Tissue Engineering (TE) in 1993 by Professor Robert Langer and JP Vacanti [10], new biomaterials are proposed year on year, with extraordinary advancements in processing technologies, creation of sophisticated chemical modifications to fulfill the most demanding

biological requirements, with the ambition of providing solutions to unmet clinical needs. Perhaps the core challenge in Tissue Engineering is achieving the appropriate balance between i) the biomaterials' mechanical properties and structural architecture, to fit the tissue's requirements; and ii) a suitable chemical environment to promote tissue growth, which involves a suite of specific cell types, cellular interactions and cocktail of growth factors.

For Spinal Fusion, some of these building blocks have already reached clinical practice, in isolation or combination, and their application as well as clinical outcomes were reviewed in the initial stage of this thesis (Chapter I) [9]. Sub-optimal fusion rates and/ or complications continue to drive an intense body of research involving new biomaterials and/or biologics, which was also analyzed in this initial chapter. Tricalcium Phosphate (TCP), Hydroxyapatite (HA) and Calcium Phosphate (CaP) have been important mineral components of an osteoconductive structure, while growth factors such as Bone Morphogenetic Protein-2 (BMP-2) or Platelet Rich Plasma (PRP) are regularly employed to accelerate bone formation in Spinal Fusion [9,11–13]. Most recent publications have explored ways to reduce dosages of growth factors (particularly BMP-2 due to its undesired side effects), either through controlled release delivery systems and/ or combination with other bioactive agents such as NELL-1 [14,15]. Demineralized bone and collagen-based matrices are found as scaffolding systems to support delivery of bioactive agents [11–13,16], and from a structural perspective, synthetic biodegradable polyesters, such as polylactic acid (PLA) or polycaprolactone (PCL) [9,17] remain expressive in spinal fusion research. Polycaprolactone in particular, an FDA-approved polymer used for several biomedical applications [18], has been extensively explored in bone TE, and particularly spinal fusion as a platform for development of composites [19–22]. This is possible because polyesters act as biologically inert materials, with tunable physical and mechanical properties that are suitable for scaffolding purposes and/ or drug delivery [23,24]. Such polyesters are easily modified to tackle issues such as cell adhesion, hydrophobicity, and inflammatory side effects, and PCL particularly has attracted attention for its biocompatibility, bioabsorbability, and mechanical properties [23,24].

In this context, we further explored – in Chapter III – novel processing conditions which could create an injectable PCL porous foam, compatible with physiological conditions. The goal was to develop a "whipped-cream" approach, where the PCL material is delivered into the lesion site, where it would expand and solidify into a 3D porous structure. This *in situ* foaming would allow the biomaterial to structurally adapt to the anatomy of the lesion site, while the adhesive properties of the foam would provide an immediate fixation and stabilization of the vertebral segment. A processing technique that

has been well-established for polymer processing is the use of gas and/ or supercritical foaming, which produces highly porous and interconnected structures for tissue engineering and regenerative medicine [25]. Carbon dioxide is the supercritical fluid used per excellence, particularly due to its low critical properties (Pc = 7.4 MPa and Tc = 31 °C), but also due to its innocuity. Little has been reported in the literature in what concerns the use of carbon dioxide at lower P, T conditions (Chapter II, Table I) [26]. In this work, we have evaluated the possibility to foam polycaprolactone under subcritical carbon dioxide atmosphere, by working with several parameters in a benchtop reactor: pressure, temperature, polycaprolactone molecular weight, contact time for plasticization, and CO_2 density. Gas foaming is highly dependent on the molecular weight of the polymers, and indeed in our study we verified that, at the processing conditions aimed for this application, i.e., below 5.0 MPa and 50 °C, polycaprolactone with a molecular weight of 80 000 Da did not foam. On the other hand, PCL 45 000 Da could be foamed and was, for this reason, selected to proceed the optimization process. The lowest P, T conditions which resulted in a stable three-dimensional foam were 5.0 MPa and 45 °C respectively, and therefore, PCL foaming at subcritical conditions was demonstrated, and as such, enabling further development of our hypothesis: *in situ* interbody PCL foaming at physiologically compatible conditions. To provide bioactive traits to this PCL structure, it was further ambitioned to incorporate, during the same processing step, two osteoinductive agents: β-tricalcium phosphate (β-TCP, 10 wt%) and dexamethasone (5 and 10 wt%) [9,27–29], which was conducted effectively. The produced foams were subject to a comprehensive and advanced set of characterization tests, to verify the appropriateness of its architecture to support bone development: foams revealed a pore size range of 164–882 μm, 73–99% porosity and 79–99% interconnectivity, assessed by micro-computed tomography, which revealed to be in very good agreement with data reported in the literature for trabecular bone (Table 3) [47]. It was found that addition of β-TCP did not result in augmented young modulus upon compression as compared to non-supplemented PCL, possibly due to the higher porosity and pore size. Nevertheless, its morphology and bioactivity shall offer a more osteoinductive and osteoconductive environment aimed towards improved osteointegration. Pore size and porosity are intimately related with surface area, whereas structures with higher surface area, are more exposed to water molecules which shall lead to faster hydrolytic degradation of the PCL component [30]. These can be fine-tuned in order to reach the best performing structure on what regards matching new bone formation and scaffold degradation rates, as well as controlled release of bioactive agents such as the dexamethasone, which in this study was sustainably released from the scaffolds within one month.

The achievement of PCL foaming at subcritical conditions, obtaining a three-dimensional structure with suitable mechanical and morphological properties, supported the next stage of BIOLIF development: interbody stabilization by *in situ* foaming (Chapter IV).

At this point, the processing conditions optimized at the benchtop reactor, were mimicked into a portable reactor, designed as a surgical tool, to deliver the biomaterial safely and effectively into the intervertebral disc space. The tool was designed to: i) withstand the required pressure and temperature to generate the foam, ii) have a size and format equivalent to a 20 cc syringe, built in stainless-steel (316SS), iii) be manageable within the very narrow surgical site and comprising a tip optimized (length and diameter) for delivery of the foam directly into the intervertebral space. The tool comprises a mechanical piston used to ensure complete extrusion of the material and controlled application of the foam *in situ*.

While appropriate morphological and bioactive properties were obtained with the initial PCL formulation, the adhesive capacity of the foam was further improved. The design of bone adhesives is one of the most challenging fields in the intersection of polymer and biomedical engineering [31,32]. Multiple routes are under investigation with great attention being given to bioadhesives produced by marine organisms such as O-phospho-L-serine, found in the sandcastle worm [33] and 3,4-dihydroxy-L-phenylalanine (DOPA) amino acid found in mussels [34], for their extraordinary bonding capacity in wet environments and at ambient temperature. Its analogue dopamine has the ability to self- polymerize, which provides a versatile and easy way to functionalize and coat a large variety of materials, from metals to ceramics and polymers [35,36]. Not only polydopamine (pDA) enhances the adhesive properties of the material but also may induce bioactivity of the structures, particularly by inducing mineralization of the structure and the formation of a bone-like hydroxyapatite (HA) layer, promoting bone–bone bonding [37–39]. PCL pDA adhesiveness was further improved through additional modification with polymethacrylic acid (pMAA), a synthetic adhesive belonging to the acrylate family. The possibility to control its concentration in a polymeric blend may overcome biocompatibility issues, while still enhancing the adhesiveness of the matrices, as demonstrated by J. H. Kim, Lim, and Park (2013) [40]. The functionalization of PCL with pDA and pMAA was confirmed by SEM images, FTIR and XPS analysis and the adhesive properties of the novel materials were characterized by mechanical testing, in a first approach, using glass surface. Two glass plates were glued with the different formulations (PCL; PCL pDA; PCL pDA pMAA) and were subjected to a tensile force to evaluate the maximum load at detachment. PCL presented an adhesive strength of 0.074 (±0.02) N/cm^2, PCL pDA of 16.2 (±2.4) N/cm^2 and PCL pDA pMAA of 13.7 (±0.6) N/cm^2. These results provided evidence that

modifying PCL with pDA and pDA plus methacrylic acid significantly enhances the mechanical properties of the polymer, particularly the adhesive properties of PCL ($p < 0.001$). Adhesion properties were further evaluated using *ex vivo* spinal plugs and extruded polymer foam. PCL pDA pMAA presented higher adhesive properties (121.53 N/cm^2) than nonmodified PCL ($p < 0.05$). After tensile testing, PCL and PCL pDA materials detached from one of the bone interfaces, whereas the PCL pDA pMAA maintained fully adhered: the material–bone interface remained intact at both ends with breaking site occurring at the vertebral trabecular bone. In order to mimic the anterolateral surgical approach for lumbar interbody fusion, PCL pDA pMAA was extruded through the portable device into a defect created in the IVD space of an *ex vivo* porcine spine. Extrusion of the polymer within the lesion boundaries happened in a controlled manner, and hardening of the foam occurred within few seconds allowing immediate stabilization of the vertebrae. A similar behaviour was observed for PCL pDA pMAA extruded via standard syringe (control group); however, the solidification is not immediate. The solidified structures were taken from the defect site, and the morphological parameters were analysed by micro-CT. The sample injected through the syringe is highly compact and presents residual porosity and no interconnectivity. On the other hand, the sample extruded through the high-pressure device presented morphological properties (porosity 45%, mean pore size 169 μm, degree of anisotropy 2.06) within the range described for trabecular bone [41]. It is herein described a successful approach for the *in situ* foaming of polymers for intervertebral disc space filling.

The bioactive properties of PCL pDA pMAA were evaluated in a SBF, and PCL samples were used as a control. SEM images demonstrate the presence of precipitated CaPs on the surface of the materials as early as day 1 and a layer-like structure at days 7 and 14. PCL samples, used as control, did not show presence of any crystals as reported in the literature [42]. This confirms the hypothesis that pDA not only provides adhesive properties to PCL but also seems to induce some degree of mineralization of the structures.

As opposed to the implantation of a premanufactured 3D scaffold, *in situ* foaming of the proposed PCL pDA pMAA allows foam impregnation and adherence to bone before hardening, resulting in immediate stabilization of vertebral segments. Such approach could open the possibility of avoiding additional instrumentation for bone stabilization. In addition, while the foam is injected at the interbody space, it adapts to defect geometry and volume, resulting in optimal filling of the defect. Typical functionalization of PCL for bone applications include reinforcement with a mineral component such as β-TCP [19,43], or CaP with or without further addition with BMP-2 [22,43], yet herein, the combination of pDA and pMAA provided the adhesive properties to PCL, while simultaneously inducing mineralization of the

structure. In a previous work, the authors have successfully incorporated dexamethasone and TCP via carbon dioxide foaming of PCL, which could be added to the formulation to further improve osteogenesis [26].

Once validated the morphological, mechanical, adhesive, bioactive and cytocompatibility characteristics of the new foam, an *in vivo* study was designed to test the surgical feasibility and biologic performance for a successful spinal fusion. Standard interbody fusion with instrumentation using screws, rods and cage filled with autologous iliac crest bone graft (ICBG) was used as control. The porcine model, well established in the literature for spinal fusion studies [9,20,43], was selected to conduct the anterolateral lumbar approach. The similarity of the spinal anatomy with humans [44], in shape and size, was considered key for an adequate feasibility evaluation of the BIOLIF approach. In this *in vivo* study, the PCL pDA pMAA foam was successfully extruded through the portable device into the IVD space in a controlled manner without causing neurological damage to the animals, nor any other adverse effects identified by the authors. This minimally invasive approach reduced disturbances to the healthy surrounding tissues (as compared to standard instrumentation), which might have had a positive impact on the faster post-op mobility observed in BIOLIF treated animals.

By avoiding screw fixation and autograft harvesting in the BIOLIF group, surgery time was expressively inferior and post-op mobility was significantly higher, factors of considerable relevance when assessing the cost and ultimately cost-effectiveness of a surgical treatment [45,46]. From a surgical procedure perspective, the risk of neurological lesions related with cage insertion (in posterior approaches) [47], can be minimized by the use of the thin cannula for BIOLIF extrusion directly into the IVD space, and post-op risks associated with non-union and cage migration [48,49] can possibly be overcome by the controlled positioning of BIOLIF in the IVD. At the 6-month termination time-point, all treated animals revealed segmental spinal alignment, measured by sagittal and coronal Cobb angles a result indicative of spinal stability achieved by both BIOLIF and Instrumentation. microCT analysis of the BIOLIF explants collected at termination revealed a BV/TV ratio superior to the positive control Instrumentation group (average 70.1% BIOLIF vs 33.9% instrumentation). These results are in line with BV/TV ratios reported by Abbah *et al*, in porcine spinal fusion studies at a 6-month time-point reference, where PCL-tricalcium phosphate formulations were prepared with bone morphogenetic protein-2 (BMP-2) [50] or bone marrow stromal cells [20].

The limited mobility of the treated segment (reduced range of motion and increased stiffness) observed in both groups are supportive of spinal fusion, and coherent with other the IF studies in the porcine [50]

and ovine models [51]. The histological findings collected in this work provided positive insights about the behavior of BIOLIF in relation with surrounding tissue and cells. BIOLIF foam was found attached to surrounding tissue, indicative of its integration, while for standard PEEK cages, it is well described in the literature that its inherent hydrophobic properties impede cell attachment and osteogenesis [52]. An interconnected porous network is essential for bone in-growth, by facilitating cell supply, vascularization, and integration with the native tissue. Histological sections of this *in vivo* study reveal that a porous foam was achieved *in situ*, with pores of different dimensions found populated with cells. Future advancements could include the *in situ* enrichment of the BIOLIF foam with exogenous cell sources, as for instance, autologous or allogeneic mesenchymal stem cells have generated high fusion rates in pre-clinical studies and clinical trials [53].

For the time being, results obtained through the diverse quantitative and qualitative assessments conducted in the present work, seem to support the hypothesis that spinal fusion can be achieved by BIOLIF in the described model, and that the selected porcine model and surgical approach was deemed adequate to test both the surgical feasibility and spinal fusion capacity. Based on these initial encouraging outcomes, further systematic assessments are required, particularly regarding safety and material degradation, both based on based on ISO 10993, and optimization of the delivery device design.

Future perspectives

The future of spinal pathology treatment will likely be based on a multidisciplinary approach, which may include conservative strategies, centered on active and healthy aging, new approaches based on regenerative medicine, crucial in preventing the progression of degenerative disease, and a multiplicity of surgical treatments as solution for the most complex pathologies.

With the increase in life expectancy, the percentage of the population over 65 years old has been raising consistently in developed countries. Literature data confirm that the need for spinal fusion is significantly higher in the elderly population. This reality will force the convergence of fusion-related technology in two fundamental areas: reduction of surgical aggressiveness using minimally invasive surgery (MIS) techniques and improvement of fusion quality using biomaterials and additives with osteo-inductive properties.

Annually, in Europe, more than 62,000 transforaminal lumbar interbody fusion (TLIF) surgeries are performed, and minimally invasive surgery techniques for spinal fusion is growing due to its recognized lower morbidity. Although MIS TLIF is a common procedure, it requires multiple instruments and multiple steps, which depending on each case, might lead to high variability in surgery duration and complexity. Future developments in this space will likely address simplification of the procedure.

Older patients are more likely to have suboptimal bone quality compromising the quality of the fusion. Innovative and sophisticated solutions based on new biomaterials and osteogenic/ osteoinductive/ osteoconductive compositions are being proposed at a rapid pace [54], demonstrating strong evidence of fusion with no donor morbidity, with the additional benefit of unlimited supply.

The biomaterial and approach proposed in this thesis could respond in the 2 domains described: be applied by a minimally invasive route leading to a decrease in surgical aggressiveness, as well as promoting an improvement in the quality and rate of fusion. In addition to the entire path of development, optimization and validation, the concept presented may evolve from interbody fusion into other uses, namely for the treatment of vertebral fractures as a filling solution for the vertebral body.

Therapies and procedures that improve patient safety, reduce surgical time, and provide optimized outcomes are expected to increase and innovative technologies will continue to shape the space.

Conclusions

The work produced in this thesis led to the development of new methodologies and materials, applicable to spinal fusion, that are beyond the present state of the art, namely:

i. Supercritical technology was explored and validated as processing technique to produce a polycaprolactone (PCL)-based foam. Processing parameters such as pressure and temperature, were optimized to yield a 3D porous structure, morphologically and mechanically adequate for bone development, at subcritical and physiological compatible conditions (45°C, 5 MPa).

ii. The PCL processing conditions achieved at the benchtop reactor were replicated into a portable reactor, optimized as a surgical tool, capable of effectively and safely deliver the PCL foam into the intervertebral disc.

iii. A new PCL composition was developed with advanced adhesive and bioactive properties, by functionalization with polydopamine and polymethacrylic acid (PCL pDA pMAA) – *ex vivo* intervertebral *in situ* foaming and spine stabilization was achieved.

iv. PCL pDA pMAA *in situ* foaming by the portable device was surgically feasible in an anterolateral interbody fusion porcine model, leading to reduced surgical time and faster recovery as compared to treatment by standard instrumentation.

v. Spinal fusion was observed 6 months post-op, equivalent in both experimental groups - BIOLIF and Instrumentation, as evaluated by bone volume/ tissue volume through micro computed tomography, reduced range of motion and increased stiffness, by mechanical testing and bone-biomaterial integration observed by histological analysis.

These outcomes open the possibility of a non-instrumented spinal fusion approach for the future, aiming for reduced complications associated with hardware, and improved fusion rates.

References

[1] B.I. Martin, S.K. Mirza, N. Spina, W.R. Spiker, B. Lawrence, D.S. Brodke, Trends in Lumbar Fusion Procedure Rates and Associated Hospital Costs for Degenerative Spinal Diseases in the United States, 2004 to 2015, Spine (Phila. Pa. 1976). (2019). https://doi.org/10.1097/BRS.0000000000002822.

[2] K.L. Ong, J.D. Auerbach, E. Lau, J. Schmier, J.A. Ochoa, Perioperative outcomes, complications, and costs associated with lumbar spinal fusion in older patients with spinal stenosis and spondylolisthesis, Neurosurg. Focus. (2014). https://doi.org/10.3171/2014.4.FOCUS1440.

[3] J.N. Shillingford, J.L. Laratta, N.O. Sarpong, R.G. Alrabaa, M.K. Cerpa, R.A. Lehman, L.G. Lenke, C.R. Fischer, Instrumentation complication rates following spine surgery: a report from the Scoliosis Research Society (SRS) morbidity and mortality database, J. Spine Surg. (2019). https://doi.org/10.21037/jss.2018.12.09.

[4] J. Guimarães Consciência, R. Pinto, T. Saldanha, European Surgical Orthopaedics and Traumatology, in: G. Bentley (Ed.), Eur. Surg. Orthop. Traumatol., Springer, Berlin, Heidelberg, 2014. https://doi.org/10.1007/978-3-642-34746-7.

[5] A.K. Allouni, W. Davis, K. Mankad, J. Rankine, I. Davagnanam, Modern spinal instrumentation. Part 2: Multimodality imaging approach for assessment of complications, Clin. Radiol. (2013) P75-81. https://doi.org/10.1016/j.crad.2012.05.002.

[6] J.J. Enders, D. Coughlin, T.E. Mroz, S. Vira, Surface Technologies in Spinal Fusion, Neurosurg. Clin. N. Am. (2020). https://doi.org/10.1016/j.nec.2019.08.007.

[7] P. Park, M. Wang, K.D. Than, J. Uribe, Emerging Technologies in Spinal Surgery, Oper. Neurosurg. (Hagerstown, Md.). (2021). https://doi.org/10.1093/ons/opab064.

[8] J.C. Wang, Future of Biologics for Spinal Fusion, Glob. Spine J. (2016). https://doi.org/10.1055/s-0036-1582582.

[9] R.M. Duarte, P. Varanda, R.L. Reis, A.R.C. Duarte, J. Correia-Pinto, Biomaterials and Bioactive Agents in Spinal Fusion, Tissue Eng. Part B Rev. (2017) ten.teb.2017.0072. https://doi.org/10.1089/ten.teb.2017.0072.

[10] R. Langer, J.P. Vacanti, Tissue engineering, Science (80-.). (1993). https://doi.org/10.1126/science.8493529.

[11] J.C. Liao, Positive effect on spinal fusion by the combination of platelet-rich plasma and collagen-mineral scaffold using lumbar posterolateral fusion model in rats, J. Orthop. Surg. Res. (2019). https://doi.org/10.1186/s13018-019-1076-2.

[12] J.L. Van Eps, J.S. Fernandez-Moure, F.J. Cabrera, F. Taraballi, F. Paradiso, S. Minardi, X. Wang, B. Aghdasi, E. Tasciotti, B.K. Weiner, Improved Posterolateral Lumbar Spinal Fusion Using a Biomimetic, Nanocomposite Scaffold Augmented by Autologous Platelet-Rich Plasma, Front. Bioeng. Biotechnol.

(2021). https://doi.org/10.3389/fbioe.2021.622099.

[13] M. Plantz, J. Lyons, J.T. Yamaguchi, A.C. Greene, D.J. Ellenbogen, M.J. Hallman, V. Shah, C. Yun, A.E. Jakus, D. Procissi, S. Minardi, R.N. Shah, W.K. Hsu, E.L. Hsu, Preclinical Safety of a 3D-Printed Hydroxyapatite-Demineralized Bone Matrix Scaffold for Spinal Fusion, Spine (Phila. Pa. 1976). (2021). https://doi.org/10.1097/brs.0000000000004142.

[14] L. Liu, W.M.R. Lam, M. Naidu, Z. Yang, M. Wang, X. Ren, T. Hu, R. Kumarsing, K. Ting, J.C.H. Goh, H.K. Wong, Synergistic Effect of NELL-1 and an Ultra-Low Dose of BMP-2 on Spinal Fusion, Tissue Eng. - Part A. (2019). https://doi.org/10.1089/ten.tea.2019.0124.

[15] T. Hu, L. Liu, R.W.M. Lam, S.Y. Toh, S.A. Abbah, M. Wang, A.K. Ramruttun, K. Bhakoo, S. Cool, J. Li, J. Cho-Hong Goh, H. Wong, Bone marrow mesenchymal stem cells with low dose bone morphogenetic protein 2 enhances scaffold-based spinal fusion in a porcine model, J. Tissue Eng. Regen. Med. (2021). https://doi.org/10.1002/term.3260.

[16] M. Krticka, L. Planka, L. Vojtova, V. Nekuda, P. Stastny, R. Sedlacek, A. Brinek, M. Kavkova, E. Gopfert, V. Hedvicakova, M. Rampichova, L. Kren, K. Liskova, D. Ira, J. Dorazilová, T. Suchy, T. Zikmund, J. Kaiser, D. Stary, M. Faldyna, M. Trunec, Lumbar interbody fusion conducted on a porcine model with a bioresorbable ceramic/biopolymer hybrid implant enriched with hyperstable fibroblast growth factor 2, Biomedicines. (2021). https://doi.org/10.3390/biomedicines9070733.

[17] G. Bhakta, A.K. Ekaputra, B. Rai, S.A. Abbah, T.C. Tan, B.Q. Le, A. Chatterjea, T. Hu, T. Lin, M.T. Arafat, A.J. van Wijnen, J. Goh, V. Nurcombe, K. Bhakoo, W. Birch, L. Xu, I. Gibson, H.K. Wong, S.M. Cool, Fabrication of polycaprolactone-silanated β-tricalcium phosphate-heparan sulfate scaffolds for spinal fusion applications, Spine J. (2018). https://doi.org/10.1016/j.spinee.2017.12.002.

[18] D. Mondal, M. Griffith, S.S. Venkatraman, Polycaprolactone-based biomaterials for tissue engineering and drug delivery: Current scenario and challenges, Int. J. Polym. Mater. Polym. Biomater. 65 (2016) 255–265. https://doi.org/10.1080/00914037.2015.1103241.

[19] S.A. Abbah, C.X.L. Lam, D.W. Hutmacher, J.C.H. Goh, H.K. Wong, Biological performance of a polycaprolactone-based scaffold used as fusion cage device in a large animal model of spinal reconstructive surgery, Biomaterials. 30 (2009) 5086–5093. https://doi.org/10.1016/j.biomaterials.2009.05.067.

[20] S.A. Abbah, C.X.F. Lam, K.A. Ramruttun, J.C.H. Goh, H.-K. Wong, Autogenous Bone Marrow Stromal Cell Sheets-Loaded mPCL/TCP Scaffolds Induced Osteogenesis in a Porcine Model of Spinal Interbody Fusion, Tissue Eng. Part A. 17 (2011) 809–817. https://doi.org/10.1089/ten.tea.2010.0255.

[21] Y. Li, Z. gang Wu, X. kang Li, Z. Guo, S. hua Wu, Y. quan Zhang, L. Shi, S. hin Teoh, Y. chun Liu, Z. yong Zhang, A polycaprolactone-tricalcium phosphate composite scaffold as an autograft-free spinal fusion cage in a sheep model, Biomaterials. 35 (2014) 5647–5659. https://doi.org/10.1016/j.biomaterials.2014.03.075.

[22] M.R.N.O. Yong, S. Saifzadeh, G.N. Askin, R.D. Labrom, D.W. Hutmacher, C.J. Adam, Biological performance of a polycaprolactone-based scaffold plus recombinant human morphogenetic protein-2 (rhBMP-2) in an ovine thoracic interbody fusion model, Eur. Spine J. 23 (2014) 650–657. https://doi.org/10.1007/s00586-013-3085-x.

[23] I. Manavitehrani, A. Fathi, H. Badr, S. Daly, A.N. Shirazi, F. Dehghani, Biomedical applications of biodegradable polyesters, Polymers (Basel). 8 (2016). https://doi.org/10.3390/polym8010020.

[24] D. Mogosanu, E. Giol, M. Vandenhaute, D. Dragusin, S. Samal, P. Dubruel, Polyester Biomaterials for Regenerative Medicine, in: S. Cao, H. Zhu (Eds.), Front. Biomater. Des. Synth. Strateg. Biocompat. Polym. Scaffolds Biomed. Appl., Bentham Science Publishers Ltd., 2014: p. 155.

[25] D.J. Mooney, D.F. Baldwin, N.P. Suh, J.P. Vacanti, R. Langer, Novel approach to fabricate porous sponges of poly(D,L-lactic-co-glycolic acid) without the use of organic solvents, Biomaterials. 17 (1996) 1417–1422. https://doi.org/10.1016/0142-9612(96)87284-X.

[26] R.M. Duarte, J. Correia-Pinto, R.L. Reis, A.R.C. Duarte, Subcritical carbon dioxide foaming of polycaprolactone for bone tissue regeneration, J. Supercrit. Fluids. 140 (2018) 1–10.

[27] A. Martins, A.R.C. Duarte, S. Faria, A.P. Marques, R.L. Reis, N.M. Neves, Osteogenic induction of hBMSCs by electrospun scaffolds with dexamethasone release functionality, Biomaterials. 31 (2010) 5875–5885. https://doi.org/10.1016/j.biomaterials.2010.04.010.

[28] A.R.C. Duarte, J.F. Mano, R.L. Reis, Dexamethasone-loaded scaffolds prepared by supercritical-assisted phase inversion, Acta Biomater. 5 (2009) 2054–2062. https://doi.org/10.1016/j.actbio.2009.01.047.

[29] Y. Zhou, D.W. Hutmacher, S.L. Varawan, T.M. Lim, In vitro bone engineering based on polycaprolactone and polycaprolactone-tricalcium phosphate composites, Polym. Int. 56 (2007) 333–342. https://doi.org/10.1002/pi.2138.

[30] Q. Zhang, Y. Jiang, Y. Zhang, Z. Ye, W. Tan, M. Lang, Effect of porosity on long-term degradation of poly (ε-caprolactone) scaffolds and their cellular response, Polym. Degrad. Stab. (2013). https://doi.org/10.1016/j.polymdegradstab.2012.10.008.

[31] K.O. Böker, K. Richter, K. Jäckle, S. Taheri, I. Grunwald, K. Borcherding, J. von Byern, A. Hartwig, B. Wildemann, A.F. Schilling, W. Lehmann, Current state of bone adhesives-Necessities and hurdles, Materials (Basel). (2019). https://doi.org/10.3390/ma12233975.

[32] M.R. Norton, G.W. Kay, M.C. Brown, D.L. Cochran, Bone glue - The final frontier for fracture repair and implantable device stabilization, Int. J. Adhes. Adhes. (2020). https://doi.org/10.1016/j.ijadhadh.2020.102647.

[33] A. Kirillova, C. Kelly, N. von Windheim, K. Gall, Bioinspired Mineral-Organic Bioresorbable Bone Adhesive, Adv. Healthc. Mater. (2018). https://doi.org/10.1002/adhm.201800467.

[34] A.I. Neto, A.C. Cibrão, C.R. Correia, R.R. Carvalho, G.M. Luz, G.G. Ferrer, G. Botelho, C. Picart, N.M. Alves, J.F. Mano, Nanostructured polymeric coatings based on chitosan and dopamine-modified

hyaluronic acid for biomedical applications, Small. (2014). https://doi.org/10.1002/smll.201303568.

[35] H. Lee, S.M. Dellatore, W.M. Miller, P.B. Messersmith, Mussel-Inspired Surface Chemistry for Multifunctional Coatings, Science (80-.). 318 (2007) 426–430. https://doi.org/10.1126/science.1147241.

[36] Y. Liu, K. Ai, L. Lu, Polydopamine and its derivative materials: Synthesis and promising applications in energy, environmental, and biomedical fields, Chem. Rev. 114 (2014) 5057–5115. https://doi.org/10.1021/cr400407a.

[37] M. Mabrouk, D. Bijukumar, J.A.S. Mulla, D.R. Chejara, R. V. Badhe, Y.E. Choonara, P. Kumar, L.C. Du Toit, V. Pillay, Enhancement of the biomineralization and cellular adhesivity of polycaprolactone-based hollow porous microspheres via dopamine bio-activation for tissue engineering applications, Mater. Lett. 161 (2015) 503–507. https://doi.org/10.1016/j.matlet.2015.08.146.

[38] J. Xie, S. Zhong, B. Ma, F.D. Shuler, C.T. Lim, Controlled biomineralization of electrospun poly(ε-caprolactone) fibers to enhance their mechanical properties, Acta Biomater. 9 (2013) 5698–5707. https://doi.org/10.1016/j.actbio.2012.10.042.

[39] D. Zhang, O.J. George, K.M. Petersen, A.C. Jimenez-Vergara, M.S. Hahn, M.A. Grunlan, A bioactive "self-fitting" shape memory polymer scaffold with potential to treat cranio-maxillo facial bone defects, Acta Biomater. 10 (2014) 4597–4605. https://doi.org/10.1016/j.actbio.2014.07.020.

[40] J.H. Kim, J.I. Lim, H.K. Park, Porous chitosan-based adhesive patch filled with poly(l-3,4-dihydroxyphenylalanine) as a transdermal drug-delivery system, J. Porous Mater. 20 (2013) 177–182. https://doi.org/10.1007/s10934-012-9587-9.

[41] L.M. Mathieu, T.L. Mueller, P. Bourban, D.P. Pioletti, R. Müller, J.-A.E. Månson, Architecture and properties of anisotropic polymer composite scaffolds for bone tissue engineering., Biomaterials. 27 (2006) 905–16. https://doi.org/10.1016/j.biomaterials.2005.07.015.

[42] P.S.P. Poh, D.W. Hutmacher, B.M. Holzapfel, A.K. Solanki, M.M. Stevens, M.A. Woodruff, In vitro and in vivo bone formation potential of surface calcium phosphate-coated polycaprolactone and polycaprolactone/bioactive glass composite scaffolds, Acta Biomater. 30 (2016) 319–333. https://doi.org/10.1016/j.actbio.2015.11.012.

[43] S.A. Abbah, C.X.F. Lam, A.K. Ramruttun, J.C.H. Goh, H.K. Wong, Fusion performance of low-dose recombinant human bone morphogenetic protein 2 and bone marrow-derived multipotent stromal cells in biodegradable scaffolds: A comparative study in a large animal model of anterior lumbar interbody fusion, Spine (Phila. Pa. 1976). 36 (2011) 1752–1759. https://doi.org/10.1097/BRS.0b013e31822576a4.

[44] I. Busscher, A.J. Van Der Veen, J.H. Van Dieen, I. Kingma, G.J. Verkerke, A.G. Veldhuizen, In Vitro biomechanical characteristics of the spine: A comparison between human and porcine spinal segments, Spine (Phila. Pa. 1976). (2010). https://doi.org/10.1097/BRS.0b013e3181b21885.

[45] M.D. Alvin, J.A. Miller, D. Lubelski, B.P. Rosenbaum, K.G. Abdullah, R.G. Whitmore, E.C. Benzel, T.E. Mroz, Variations in cost calculations in spine surgery cost-effectiveness research, Neurosurg. Focus. (2014). https://doi.org/10.3171/2014.3.FOCUS1447.

[46] Y. Lu, S.A. Qureshi, Cost-effective studies in spine surgeries: A narrative review, Spine J. (2014). https://doi.org/10.1016/j.spinee.2014.04.026.

[47] J. Boktor, R. Pockett, N. Verghese, The expandable transforaminal lumbar interbody fusion - Two years follow-up, J. Craniovertebr. Junction Spine. (2018). https://doi.org/10.4103/jcvjs.JCVJS_21_18.

[48] Y.H. Hu, C.C. Niu, M.K. Hsieh, T.T. Tsai, W.J. Chen, P.L. Lai, Cage positioning as a risk factor for posterior cage migration following transforaminal lumbar interbody fusion - An analysis of 953 cases, BMC Musculoskelet. Disord. (2019). https://doi.org/10.1186/s12891-019-2630-0.

[49] M.K. Park, K.T. Kim, W.S. Bang, D.C. Cho, J.K. Sung, Y.S. Lee, C.K. Lee, C.H. Kim, B.K. Kwon, W.K. Lee, I. Han, Risk factors for cage migration and cage retropulsion following transforaminal lumbar interbody fusion, Spine J. (2019). https://doi.org/10.1016/j.spinee.2018.08.007.

[50] S.A. Abbah, W.M.R. Lam, T. Hu, J. Goh, H.K. Wong, Sequestration of rhBMP-2 into self-assembled polyelectrolyte complexes promotes anatomic localization of new bone in a porcine model of spinal reconstructive surgery, Tissue Eng. - Part A. (2014). https://doi.org/10.1089/ten.tea.2013.0593.

[51] K.C. McGilvray, E.I. Waldorff, J. Easley, H.B. Seim, N. Zhang, R.J. Linovitz, J.T. Ryaby, C.M. Puttlitz, Evaluation of a polyetheretherketone (PEEK) titanium composite interbody spacer in an ovine lumbar interbody fusion model: biomechanical, microcomputed tomographic, and histologic analyses, Spine J. (2017). https://doi.org/10.1016/j.spinee.2017.06.034.

[52] B.J.V. Yoon, F. Xavier, B.R. Walker, S. Grinberg, F.P. Cammisa, C. Abjornson, Optimizing surface characteristics for cell adhesion and proliferation on titanium plasma spray coatings on polyetheretherketone, Spine J. (2016). https://doi.org/10.1016/j.spinee.2016.05.017.

[53] M.A. Robbins, D.R. Haudenschild, A.M. Wegner, E.O. Klineberg, Stem Cells in Spinal Fusion, Glob. Spine J. (2017). https://doi.org/10.1177/2192568217701102.

[54] N. Neves, B.B. Campos, I.F. Almeida, P.C. Costa, A.T. Cabral, M.A. Barbosa, C.C. Ribeiro, Strontium-rich injectable hybrid system for bone regeneration, Mater. Sci. Eng. C. (2016). https://doi.org/10.1016/j.msec.2015.10.038.